



VTEM™ Plus

REPORT ON A HELICOPTER-BORNE VERSATILE TIME DOMAIN
ELECTROMAGNETIC (VTEM™ Plus) AND HORIZONTAL MAGNETIC
GRADIOMETER GEOPHYSICAL SURVEY

PROJECT: LIVINGSTONE CREEK
LOCATION: SOUTH OF YUKON
FOR: GOVERNMENT OF YUKON
SURVEY FLOWN: MARCH – JUNE, 2016
PROJECT: GL160031

Geotech Ltd.
245 Industrial Parkway North
Aurora, ON Canada L4G 4C4

Tel: +1 905 841 5004
Web: www.geotech.ca
Email: info@geotech.ca



TABLE OF CONTENTS

EXECUTIVE SUMMARY	3
1. INTRODUCTION	4
1.1 General Considerations	4
1.2 Survey and System Specifications	5
1.3 Topographic Relief and Cultural Features	6
2. DATA ACQUISITION	7
2.1 Survey Area	7
2.2 Survey Operations	7
2.3 Flight Specifications	10
2.4 Aircraft and Equipment	10
2.4.1 Survey Aircraft.....	10
2.4.2 Electromagnetic System	10
2.4.3 Full waveform vtem™ sensor calibration.....	14
2.4.4 Horizontal Magnetic Gradiometer	14
2.4.5 Radar Altimeter.....	14
2.4.6 Laser Altimeter	14
2.4.7 Barometric Altimeter	14
2.4.8 GPS Navigation System	14
2.4.9 Digital Navigation System	14
2.4.10 Digital Acquisition System.....	15
2.5 Base Station	15
3. QUALITY ASSURANCE AND QUALITY CONTROL	16
3.1 Preproduction calibration and testing	16
3.2 Daily Calibrations and Pre-flight precautions.....	16
3.3 Daily field quality control	17
3.3.1 General	17
3.3.2 Electromagnetic data.....	17
3.3.3 Magnetic data and Magnetic Base Station	17
3.3.4 Altitude	17
3.4 Quality Control in the Office	17
4. PERSONNEL	19
5. DATA PROCESSING AND PRESENTATION	20
5.1 Flight Path.....	20
5.2 Electromagnetic Data	20
5.2.1 EM Anomaly selection.....	22
5.2.2 Conductivity Depth Imaging (CDI)	23
5.3 Magnetic Data	24
5.3.1 Horizontal magnetic gradiometer data	24
5.3.2 Total magnetic field data levelling	24
6. DELIVERABLES	26
6.1 Survey Report	26
6.2 Maps.....	26
6.3 Digital Data	26
7. CONCLUSIONS AND RECOMMENDATIONS	32

LIST OF FIGURES

Figure 1: Survey location	4
Figure 2: Survey area location on Goggle Earth™	5
Figure 3: Flight path of the Livingstone Creek survey over a Google Eath™ image	6
Figure 4: VTEM™ Transmitter Current Waveform	11
Figure 5: VTEM™Plus System Configuration.....	13
Figure 6: Data acquisition, data processing and interpretation workflow	18
Figure 7: Z, X and Fraser filtered X (FFx) components for “thin” target.....	21
Figure 8: EM Anomaly Symbols.....	22

LIST OF TABLES

Table 1: Survey Specifications.....	7
Table 2: Survey schedule	7
Table 3: Off-Time Decay Sampling Scheme	11
Table 4: VTEM™ system specifications	13
Table 5: Acquisition Sampling Rates.....	15
Table 6: Magnetic base stations location	15
Table 7: Geosoft GDB Data Format	27
Table 8: Geosoft Conductivity Depth Image GDB Data Format	29
Table 9: Geosoft database for the VTEM waveform	30
Table 10: Geosoft database describing the VTEM anomalies	30

APPENDICES

A. Survey location maps.....	33
B. Survey area Coordinates	34
C. Geophysical Maps	35
D. Generalized Modelling Results of the VTEM System.....	51
E. TAU Analysis	56
F. TEM Resistivity Depth Imaging (RDI)	60
G. Test and Calibrations	71
H. EM Anomalies.....	77

EXECUTIVE SUMMARY

LIVINGSTONE CREEK YUKON TERRITORIES

During March 17th to June 21st 2016 Geotech Ltd. carried out a helicopter-borne geophysical survey over the Livingstone Creek project situated in the south of the Yukon Territories.

Principal geophysical sensors included a versatile time domain electromagnetic (VTEMplus) system and horizontal magnetic gradiometer with two caesium sensors. Ancillary equipment included a GPS navigation system and a radar altimeter. A total of 4227 line-kilometres of geophysical data were acquired during the survey.

In-field data quality assurance and preliminary processing were carried out on a daily basis during the acquisition phase. Preliminary and final data processing, including generation of final digital data and map products were undertaken from the office of Geotech Ltd. in Aurora, Ontario.

The processed survey results are presented as the following maps:

- Sheet 1: Time Decay Constant (Tau Z) - Early channels 4 – 14 (0.018 – 0.103 ms)
- Sheet 2: Time Decay Constant (Tau Z) - Middle channels 15 – 30 (0.103 – 0.945 ms)
- Sheet 3: Time Decay Constant (Tau Z) - Late channels 31 – 46 (0.945 – 8.685 ms)
- Sheet 4: Apparent Conductivity - Early channels 4 – 14 (0.018 – 0.103 ms)
- Sheet 5: Apparent Conductivity - Middle channels 15 – 30 (0.103 – 0.945 ms)
- Sheet 6: Apparent Conductivity - Middle channels 31 – 46 (0.945 – 8.685 ms)
- Sheet 7: Residual Total Magnetic Field
- Sheet 8: First Vertical Derivative of the Magnetic Field
- Sheet 9: Electromagnetic Interpretation

Digital data includes all electromagnetic and magnetic products, plus ancillary data including the waveform.

This survey report describes the procedures for data acquisition, processing, final image presentation and the specifications for the digital data set.

1. INTRODUCTION

1.1 GENERAL CONSIDERATIONS

Geotech Ltd. performed a helicopter-borne geophysical survey over the Livingstone Creek project situated in the south of the Yukon Territories. (Figure 1)

Carolyn Relf represented the Yukon Geological Survey during the data acquisition and data processing phases of this project.

The geophysical surveys consisted of helicopter borne EM using the versatile time-domain electromagnetic (VTEMplus) system with Full-Waveform processing. Measurements consisted of Vertical (Z), In-line Horizontal (X) and cross-line Horizontal (Y) components of the EM fields using induction coils and the aeromagnetic total field using a magnetic gradiometer. A total of 4227 line-km of geophysical data were acquired during the survey.

The crew was based out of Whitehorse (Figure 2) in the Yukon Territories for the acquisition phase of the survey. Survey flying started on March 17th 2016 and was completed on June 21st, 2016.

Data quality control and quality assurance, and preliminary data processing were carried out on a daily basis during the acquisition phase of the project. Final data processing followed immediately after the end of the survey. Final reporting, data presentation and archiving were completed from the Aurora office of Geotech Ltd. in July, 2016.



Figure 1: Survey location

1.2 SURVEY AND SYSTEM SPECIFICATIONS

The survey area is located approximately 65 kilometres northeast of Whitehorse, Yukon Territories (Figure 2).



Figure 2: Survey area location on Goggle Earth™

The survey area, Livingstone Creek, was flown in an east-west ($N 90^{\circ} E$ azimuth) direction, with traverse line spacing of 200 metres as depicted in Figure 2 and Figure 3. Tie lines were flown perpendicular to the traverse lines at a spacing of 1200 metres. For more detailed information on the flight spacing and direction see Table 1.

The survey area is covered by NTS (National Topographic Survey) of Canada sheet 105E08.

1.3 TOPOGRAPHIC RELIEF AND CULTURAL FEATURES

Topographically, the survey area exhibits a rugged relief with an elevation ranging from 720 to 2069 metres above mean sea level over an area of 711 square kilometres (Figure 3).

There are visible signs of culture such as roads and settlements, including the Livingstone airport, along the survey area (Figure 3).

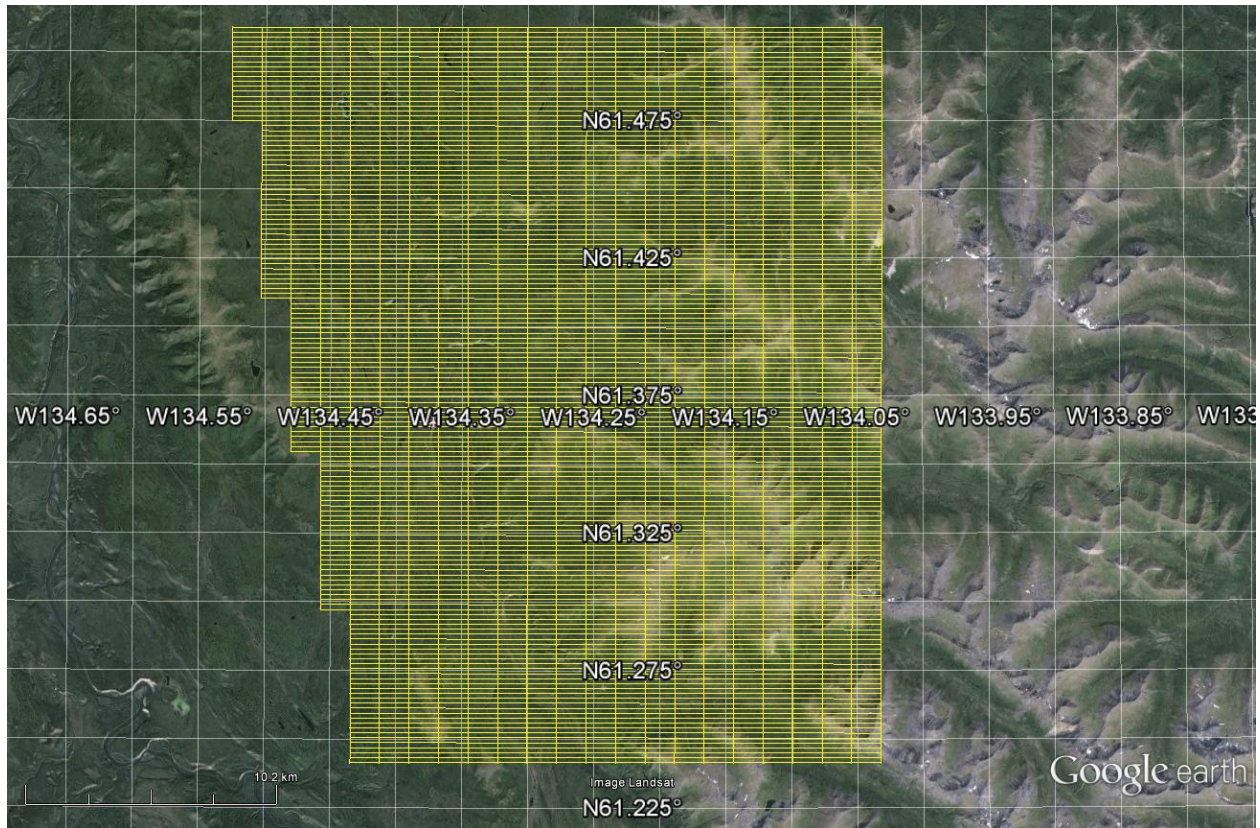


Figure 3: Flight path of the Livingstone Creek survey over a Google Earth™ image

2. DATA ACQUISITION

2.1 SURVEY AREA

The survey area (see Figure 3 and Appendix A) and general flight specifications are as follows:

Table 1: Survey Specifications

Survey block	Line spacing (m)	Area (Km ²)	Planned ¹ Line-km	Actual Line-km	Flight direction	Line numbers
Livingstone Creek	Traverse: 200	711	4201.6	3600.6	N 90° E / N 270° E	L1000 - L2491
	Tie: 1200			626.4	N 0° E / N 180° E	T3000 - L3220
TOTAL		711	4201.6	4227		

Survey area boundaries co-ordinates are provided in Appendix B.

2.2 SURVEY OPERATIONS

Survey operations were based out of Whitehorse in Yukon Territories from March 17th until June 21st 2016. The following table shows the timing of the flying.

Table 2: Survey schedule

Date	Flight #	Flown km	Block	Crew location	Comments
17-Mar-2016				Whitehorse, Yukon	Crew arrives
18-Mar-2016				Whitehorse, Yukon	Local logistics & system assembly
19-Mar-2016				Whitehorse, Yukon	System assembly
20-Mar-2016				Whitehorse, Yukon	Heli install & Test flight
21-Mar-2016				Whitehorse, Yukon	Testing
22-Mar-2016				Whitehorse, Yukon	Testing
23-Mar-2016				Whitehorse, Yukon	Test flights
24-Mar-2016				Whitehorse, Yukon	No production due to weather
25-Mar-2016				Whitehorse, Yukon	No production due to weather
26-Mar-2016				Whitehorse, Yukon	No production due to weather
28-Mar-2016				Whitehorse, Yukon	No production due to weather
29-Mar-2016				Whitehorse, Yukon	No production due to weather
30-Mar-2016				Whitehorse, Yukon	No production due to weather
31-Mar-2016	2	48	LC	Whitehorse, Yukon	48km flown limited due to technical issues
1-Apr-2016				Whitehorse, Yukon	Flight aborted due to weather
2-Apr-2016				Whitehorse, Yukon	No production due to weather
3-Apr-2016				Whitehorse, Yukon	Flight aborted due to weather
4-Apr-2016	3	86	LC	Whitehorse, Yukon	86km flown
5-Apr-2016				Whitehorse, Yukon	No production due to weather
6-Apr-2016				Whitehorse, Yukon	No production due to weather
7-Apr-2016				Whitehorse, Yukon	No production due to weather

¹ Note: Actual Line kilometres represent the total line kilometres in the final database. These line-km normally exceed the Planned Line-km, as indicated in the survey NAV files. However, the survey was stopped early as per the client's request.

Date	Flight #	Flown km	Block	Crew location	Comments
8-Apr-2016				Whitehorse, Yukon	No production due to weather
9-Apr-2016	4,5,6	240	LC	Whitehorse, Yukon	240km flown
10-Apr-2016	7	96	LC	Whitehorse, Yukon	96km flown limited due to weather
11-Apr-2016				Whitehorse, Yukon	Flight aborted due to weather
12-Apr-2016	8,9,10	288	LC	Whitehorse, Yukon	288km flown
13-Apr-2016				Whitehorse, Yukon	No production due to weather
14-Apr-2016				Whitehorse, Yukon	No production due to weather
15-Apr-2016				Whitehorse, Yukon	No production due to weather
16-Apr-2016				Whitehorse, Yukon	No production due to weather
17-Apr-2016	11	47	LC	Whitehorse, Yukon	47km flown limited due to weather
18-Apr-2016	12	92	LC	Whitehorse, Yukon	92km flown limited due to weather
19-Apr-2016	13,14,15	273	LC	Whitehorse, Yukon	273km flown
20-Apr-2016	16	91	LC	Whitehorse, Yukon	91km flown limited due to weather
21-Apr-2016	17	46	LC	Whitehorse, Yukon	46km flown limited due to weather
22-Apr-2016				Whitehorse, Yukon	No production due to weather
23-Apr-2016				Whitehorse, Yukon	No production due to weather
24-Apr-2016	18,19,20	270	LC	Whitehorse, Yukon	270km flown
25-Apr-2016				Whitehorse, Yukon	No production due to weather
26-Apr-2016	21,22	129	LC	Whitehorse, Yukon	129km flown
27-Apr-2016				Whitehorse, Yukon	No production due to weather
28-Apr-2016				Whitehorse, Yukon	No production due to weather
29-Apr-2016				Whitehorse, Yukon	No production due to weather
30-Apr-2016				Whitehorse, Yukon	No production due to weather
1-May-2016				Whitehorse, Yukon	No production due to weather
2-May-2016				Whitehorse, Yukon	No production due to weather
3-May-2016	23,24,25	259	LC	Whitehorse, Yukon	259km flown
4-May-2016	26,27	129	LC	Whitehorse, Yukon	129km flown
5-May-2016				Whitehorse, Yukon	No production due to weather
6-May-2016				Whitehorse, Yukon	No production due to weather
7-May-2016	28,29	202	LC	Whitehorse, Yukon	202km flown
8-May-2016				Whitehorse, Yukon	No production due to weather
9-May-2016				Whitehorse, Yukon	No production due to weather
10-May-2016				Whitehorse, Yukon	No production due to weather
11-May-2016	30,31	202	LC	Whitehorse, Yukon	202km flown
12-May-2016	32,33	126	LC	Whitehorse, Yukon	126km flown
13-May-2016	34,35	151	LC	Whitehorse, Yukon	151km flown
14-May-2016	36	101	LC	Whitehorse, Yukon	101km flown
15-May-2016	37,38	127	LC	Whitehorse, Yukon	127km flown
16-May-2016				Whitehorse, Yukon	No production due to weather
17-May-2016				Whitehorse, Yukon	No production due to weather
18-May-2016				Whitehorse, Yukon	No production due to weather
19-May-2016				Whitehorse, Yukon	No production due to weather
20-May-2016				Whitehorse, Yukon	No production due to weather
21-May-2016	39	105	LC	Whitehorse, Yukon	105km flown
22-May-2016	40	105	LC	Whitehorse, Yukon	105km flown
23-May-2016				Whitehorse, Yukon	No production due to weather
24-May-2016				Whitehorse, Yukon	No production due to weather

Date	Flight #	Flown km	Block	Crew location	Comments
25-May-2016				Whitehorse, Yukon	No production due to weather
26-May-2016	41	79	LC	Whitehorse, Yukon	79km flown limited due to weather
27-May-2016				Whitehorse, Yukon	No production due to weather
28-May-2016				Whitehorse, Yukon	No production due to weather
29-May-2016	42	105		Whitehorse, Yukon	105km flown
30-May-2016				Whitehorse, Yukon	No production due to weather
31-May-2016				Whitehorse, Yukon	No production due to weather
1-Jun-2016				Whitehorse, Yukon	No production due to weather
2-Jun-2016				Whitehorse, Yukon	No production due to weather
3-Jun-2016	43,44	221	LC	Whitehorse, Yukon	221km flown
4-Jun-2016				Whitehorse, Yukon	No production due to weather
5-Jun-2016				Whitehorse, Yukon	No production due to weather
6-Jun-2016				Whitehorse, Yukon	No production due to weather
7-Jun-2016				Whitehorse, Yukon	No production due to weather
8-Jun-2016	45,46	299	LC	Whitehorse, Yukon	299km flown
9-Jun-2016	47,48	134	LC	Whitehorse, Yukon	134km flown
10-Jun-2016	49	60	LC	Whitehorse, Yukon	60km flown
11-Jun-2016				Whitehorse, Yukon	No production due to weather
12-Jun-2016	50	89	LC	Whitehorse, Yukon	89km flown
13-Jun-2016				Whitehorse, Yukon	No production due to weather
14-Jun-2016				Whitehorse, Yukon	No production due to weather
15-Jun-2016				Whitehorse, Yukon	No production due to weather
16-Jun-2016	51	45	LC	Whitehorse, Yukon	45km flown limited due to weather
17-Jun-2016	52	17	LC	Whitehorse, Yukon	17km flown limited to weather
18-Jun-2016	53,54,55	94	LC	Whitehorse, Yukon	94km flown limited due to weather
19-Jun-2016	56,57,58	157	LC	Whitehorse, Yukon	157km flown
20-Jun-2016				Whitehorse, Yukon	No production due to weather
21-Jun-2016	59	15	LC	Whitehorse, Yukon	Remaining kms were flown – flying complete

2.3 FLIGHT SPECIFICATIONS

Before the survey, a drape surface was computed using an algorithm developed by the Geological Survey of Canada (GSC Open File Report 4937). The drape surface was computed based on the 30m Aster topography data, the capability of the aircraft, and a nominal terrain clearance of 85 metres. However, rugged terrain and local weather conditions resulted in pilot safety concerns and the drape surface could not be followed in all areas.

During the survey the helicopter was maintained at a mean altitude of 132 metres above the ground with an average survey speed of 95 km/hour considering only the traverse line. This allowed for an actual average Transmitter-Receiver loop terrain clearance of 101 metres and a magnetic sensor clearance of 108 metres.

The on board operator was responsible for monitoring the system integrity. He also maintained a detailed flight log during the survey, tracking the times of the flight as well as any unusual geophysical or topographic features.

On return of the aircrew to the base camp the survey data was transferred from a compact flash card (PCMCIA) to the data processing computer. The data were then uploaded via ftp to the Geotech office in Aurora for daily quality assurance and quality control by qualified personnel.

2.4 AIRCRAFT AND EQUIPMENT

2.4.1 SURVEY AIRCRAFT

The survey was flown using a Eurocopter Aerospatiale (Astar) 350 B3 helicopter, registration C-FVTM. The helicopter is owned and operated by Geotech Aviation. Installation of the geophysical and ancillary equipment was carried out by a Geotech Ltd crew.

2.4.2 ELECTROMAGNETIC SYSTEM

The electromagnetic system was a Geotech Time Domain EM (VTEM™Plus) full receiver-waveform streamed data recorded system. The “full waveform VTEM system” uses the streamed half-cycle recording of transmitter and receiver waveforms to obtain a complete system response calibration throughout the entire survey flight. The VTEM™ transmitter current waveform is shown diagrammatically in Figure 4. VTEM with the Serial number 31 had been used for the survey.

The VTEM™ Receiver and transmitter coils were in concentric-coplanar and Z-direction oriented configuration. The receiver system for the project also included a coincident-coaxial X-direction and Y-direction coils to measure the in-line and across-line dB/dt respectively, and calculate B-Field responses. The Transmitter-receiver loop was towed at a mean distance of 31 metres below the aircraft as shown in Figure 5.

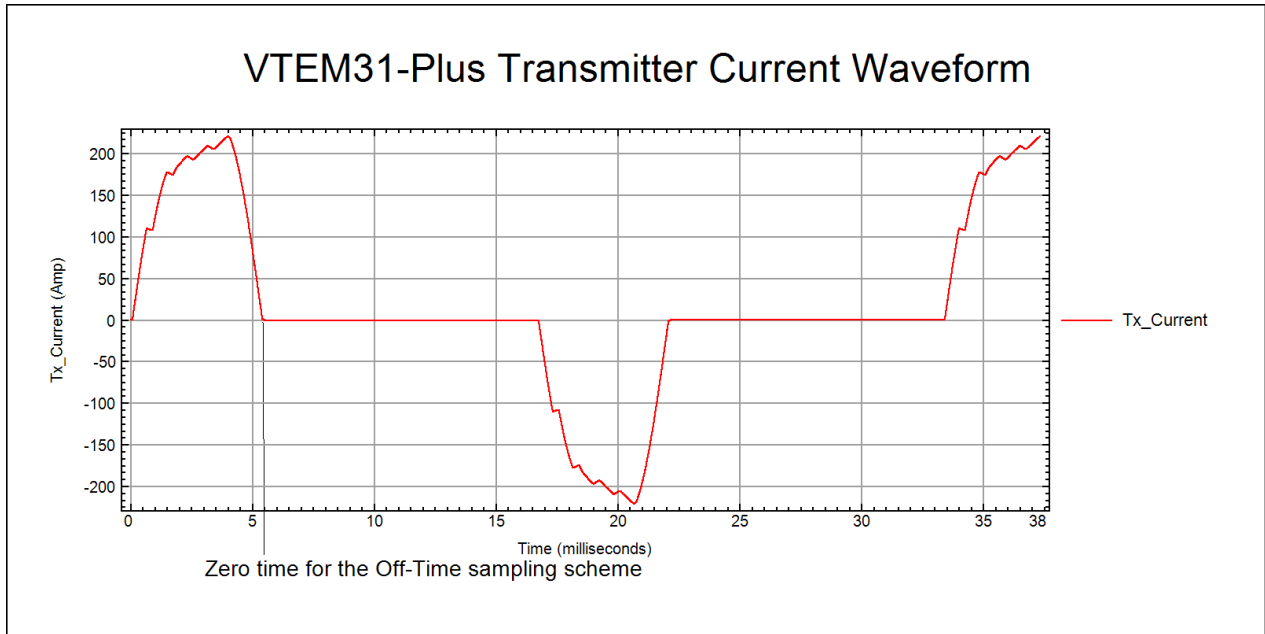


Figure 4: VTEM™ Transmitter Current Waveform

The VTEM™ decay sampling scheme is shown in [Table 3](#) below. Forty-three time measurement gates were used for the final data processing in the range from 0.021 to 8.083 msec. Zero time for the off-time sampling scheme is equal to the current pulse width and is defined as the time near the end of the turn-off ramp where the dI/dt waveform falls to 1/2 of its peak value.

Table 3: Off-Time Decay Sampling Scheme

VTEM™ Decay Sampling Scheme				
Index	Start	End	Middle	Width
Milliseconds				
4	0.018	0.023	0.021	0.005
5	0.023	0.029	0.026	0.005
6	0.029	0.034	0.031	0.005
7	0.034	0.039	0.036	0.005
8	0.039	0.045	0.042	0.006
9	0.045	0.051	0.048	0.007
10	0.051	0.059	0.055	0.008
11	0.059	0.068	0.063	0.009
12	0.068	0.078	0.073	0.010
13	0.078	0.090	0.083	0.012
14	0.090	0.103	0.096	0.013
15	0.103	0.118	0.110	0.015
16	0.118	0.136	0.126	0.018
17	0.136	0.156	0.145	0.020
18	0.156	0.179	0.167	0.023

VTEM™ Decay Sampling Scheme				
Index	Start	End	Middle	Width
Milliseconds				
19	0.179	0.206	0.192	0.027
20	0.206	0.236	0.220	0.030
21	0.236	0.271	0.253	0.035
22	0.271	0.312	0.290	0.040
23	0.312	0.358	0.333	0.046
24	0.358	0.411	0.383	0.053
25	0.411	0.472	0.440	0.061
26	0.472	0.543	0.505	0.070
27	0.543	0.623	0.580	0.081
28	0.623	0.716	0.667	0.093
29	0.716	0.823	0.766	0.107
30	0.823	0.945	0.880	0.122
31	0.945	1.086	1.010	0.141
32	1.086	1.247	1.161	0.161
33	1.247	1.432	1.333	0.185
34	1.432	1.646	1.531	0.214
35	1.646	1.891	1.760	0.245
36	1.891	2.172	2.021	0.281
37	2.172	2.495	2.323	0.323
38	2.495	2.865	2.667	0.370
39	2.865	3.292	3.063	0.427
40	3.292	3.781	3.521	0.490
41	3.781	4.341	4.042	0.560
42	4.341	4.987	4.641	0.646
43	4.987	5.729	5.333	0.742
44	5.729	6.581	6.125	0.852
45	6.581	7.560	7.036	0.979
46	7.560	8.685	8.083	1.125

Z Component: 4 - 46 time gates

X and Y Components: 20 - 46 time gates

Table 4: VTEM™ system specifications

Transmitter	Receiver
<ul style="list-style-type: none"> • Transmitter loop diameter: 26 m • Number of turns: 4 • Effective Transmitter loop area: 2123.7 m² • Transmitter base frequency: 30 Hz • Peak current: 221 A • Pulse width: 5.41 ms • Waveform shape: Bi-polar trapezoid • Peak dipole moment: 469,341 nIA • Actual average Transmitter-receiver loop terrain clearance: 101 metres above the ground 	<ul style="list-style-type: none"> • X and Y Coil diameter: 0.32 m • Number of turns: 245 • Effective coil area: 19.69 m² • Z-Coil diameter: 1.2 m • Number of turns: 100 • Effective coil area: 113.04 m²

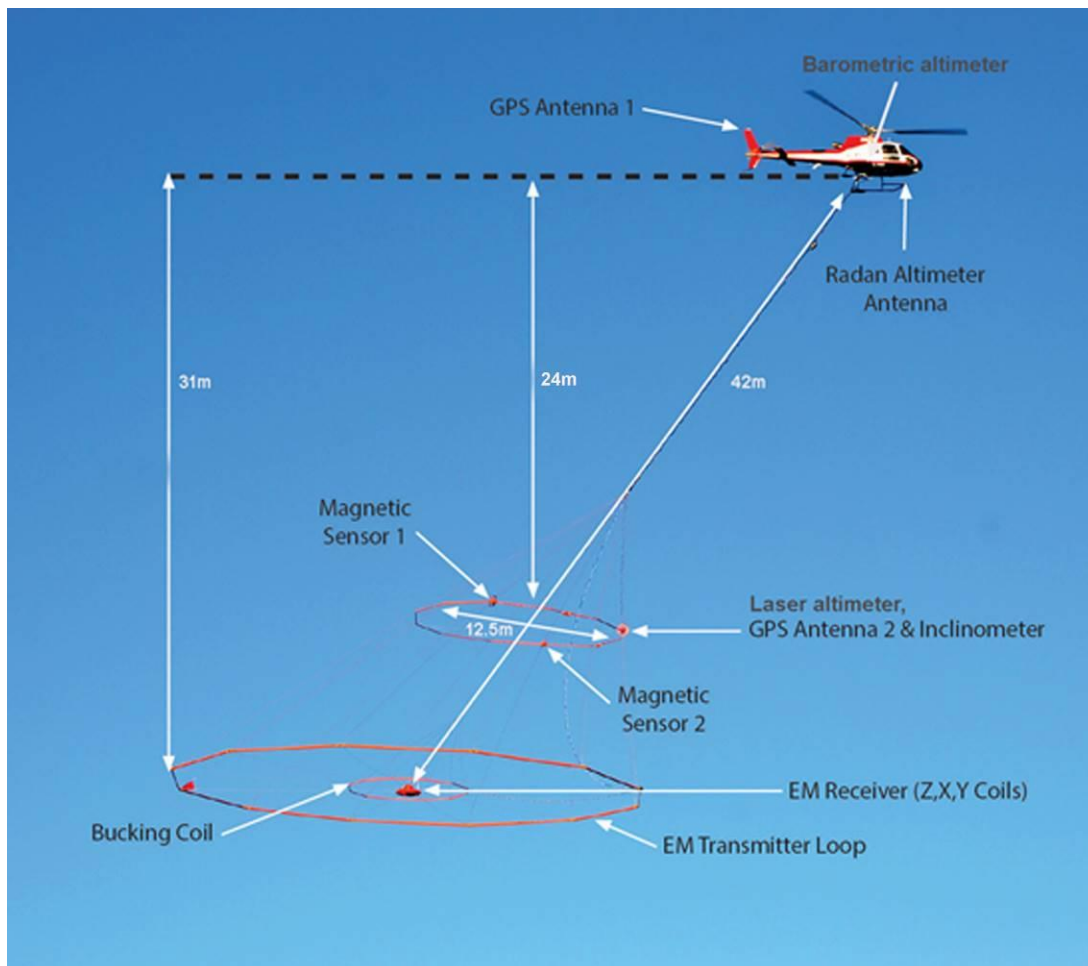


Figure 5: VTEM™ Plus System Configuration.

2.4.3 FULL WAVEFORM VTEM™ SENSOR CALIBRATION

The calibration is performed on the complete VTEM™ system installed in and connected to the helicopter, using special calibration equipment.

The procedure takes half-cycle files acquired and calculates a calibration file consisting of a single stacked half-cycle waveform. The purpose of the stacking is to attenuate natural and man-made magnetic signals, leaving only the response to the calibration signal.

2.4.4 HORIZONTAL MAGNETIC GRADIOMETER

The horizontal magnetic gradiometer consists of two Geometrics split-beam field magnetic sensors with a sampling interval of 0.1 seconds. These sensors are mounted 12.5 metres apart on a separate loop, 10 metres above the Transmitter-receiver loop. A GPS antenna and Gyro Inclinator is installed on the separate loop to accurately record the tilt and position of the magnetic gradiometer.

2.4.5 RADAR ALTIMETER

A Terra TRA 3000/TRI 40 radar altimeter was used to record terrain clearance. The antenna was mounted beneath the bubble of the helicopter cockpit (Figure 5).

2.4.6 LASER ALTIMETER

An Acuity AR3000 laser altimeter was used which has an altitude range 0.5 to 300m and accuracy ± 5 cm. The laser altimeter was located at the front of the horizontal magnetic gradient loop with a GPS antenna and inclinometer and the data was sampled at an interval of 0.2 seconds.

2.4.7 BAROMETRIC ALTIMETER

A Honeywell precision pressure transducer PPT0020AWN2VB-B was used as a barometric altimeter. It provides a high accuracy of $\pm 0.05\%$ full scale and an operating temperature range from -40 to 85°C . The barometric altimeter was located inside the helicopter cabin at about 1.5m behind and 0.5m above the radar altimeter. The data was sampled at an interval of 0.2 seconds.

2.4.8 GPS NAVIGATION SYSTEM

A dedicated Novatel® ProPak™V3 TR20 GPS receiver and ground-based GPS antenna was used with a 10 Hz raw GPS data recording. Post-flight differential GPS data processing utilizing Novatel® GrafNav 8.3 software was used to produce sub-meter accuracy of the airborne system location at 10 Hz sampling interval. The GPS ground base station was positioned at the survey base of operations at Whitehorse ($135^{\circ} 04.4780'$ W, $060^{\circ} 42.2871'$ N, 714 m ASL) and setup on March 21st, 2016 in the same vicinity of the base station magnetometer.

2.4.9 DIGITAL NAVIGATION SYSTEM

The navigation system used was a Geotech PC104 based navigation system utilizing a NovAtel's WAAS (Wide Area Augmentation System) enabled GPS receiver, Geotech navigate software, a full screen display with controls in front of the pilot to direct the flight and a NovAtel GPS antenna mounted on the helicopter tail (Figure 5). As many as 11 GPS and two WAAS satellites may be monitored at any one time. The positional accuracy or circular error probability (CEP) is 1.8 m, with WAAS active, it is 1.0 m. The co-ordinates of the survey area were set-up prior to the survey and the information was fed into the airborne navigation system. The second GPS antenna is installed on the additional magnetic loop together with Gyro Inclinometer.

2.4.10 DIGITAL ACQUISITION SYSTEM

A Geotech data acquisition system recorded the digital survey data on an internal compact flash card. Data is displayed on an LCD screen as traces to allow the operator to monitor the integrity of the system. The data type and sampling interval as provided in **Error! Reference source not found.**

Table 5: Acquisition Sampling Rates

Data Type	Sampling
TDEM	0.1 sec
Magnetometer	0.1 sec
GPS Position	0.2 sec
Radar Altimeter	0.2 sec
Inclinometer	0.1 sec
Laser Altimeter	0.2 sec
Barometric Altimeter	0.2 sec

2.5 BASE STATION

Two magnetometer base stations were employed on this project. A Geometrics Caesium vapour magnetometer was used as a magnetic sensor with a sensitivity of 0.01 nT. Each base station was recording the magnetic field at 1 Hz on a base station computer.

The two base station magnetometer sensors (Table 6), were installed away from electric transmission lines and moving ferrous objects such as motor vehicles. The base station data were backed-up to the data processing computer at the end of each survey day. The magnetic base station located at the Livingstone airstrip was recorded at all times during the survey; the diurnal correction was applied using this dataset.

Table 6: Magnetic base stations location

Base station location	Longitude	Latitude
Whitehorse airport	135° 04.4780' W	060° 42.2871' N

Base station location	Longitude	Latitude
Livingstone airstrip	134° 22.1299' W	061° 22.1754' N

3. QUALITY ASSURANCE AND QUALITY CONTROL

Quality assurance and quality control (QA/QC) were undertaken by the survey contractor, Geotech Ltd., and designated personal of the Geological Survey of Canada (GSC) and the Yukon Geological Survey (YGS). Stringent QA/QC was emphasized throughout the project so that the optimal geological signal was measured, archived and presented. The quality control procedures are summarized below.

3.1 PREPRODUCTION CALIBRATION AND TESTING

The following tests were carried out on the survey site:

1. Aluminium Plate Test – performed prior to the survey commencing. The test checked the sensitivity of the system during the survey period and ensured that the system was calibrated properly at all times.
2. Radar Altimeter Test – performed prior to survey commencing or if a new radar altimeter was installed. The test was performed to ensure the accuracy of the radar altimeter.
3. Full Waveform VTEM Calibration – performed prior to the survey commencing. This calibration is performed on the complete VTEM system installed in and connected to the helicopter, using special calibration equipment. The procedure takes half-cycle files acquired and calculates a calibration file consisting of a single stacked half-cycle waveform. The purpose of the stacking is to attenuate natural and man-made magnetic signals, leaving only the response to the calibration signal.
4. Test Flight – two test lines of a minimum of 5 km long, with a variety of conductive responses, are flown at survey height and in opposite direction.
5. Magnetic base station location test – performed to verify that the base station is located away from electric transmission lines and moving ferrous objects such as motor vehicles.

Details about preproduction calibration and tests are presented in Appendix G.

3.2 DAILY CALIBRATIONS AND PRE-FLIGHT PRECAUTIONS

The TDEM system and magnetometer were sufficiently warmed up before each survey day to minimize temperature-related system drifting.

- Timing and synchronization of all recording instruments was checked for correct operation.
- Each flight included two background pre-flight and post-flight measurements for background and assessment of noise levels, and collection of the reference waveform. The aircraft climbed to 500 m above ground level (AGL) and maintained straight and level flight for one (1) minute or five (5) km. A 'background check' was conducted at the beginning of each flight and repeated approximately every hour and after completing the last survey line of the flight. Details about this calibration are presented in Appendix G.

3.3 DAILY FIELD QUALITY CONTROL

3.3.1 GENERAL

- Check that all the files are on the server as expected.
- Download and unzip the files. Make sure they were complete and not corrupted.
- Check the header of the airborne raw data files to ensure the system was configured properly.
- Preprocess and then import the data into the Geosoft® software.
- Plot the flight path in Google Earth and Geosoft to verify that the data are complete and properly located and that those lines, as described in the flight logs, were flown.
- Check the flight path for crossing lines or lines that did not maintain proper separation.
- Plot the final flight path and look for problems, such as gaps and GPS busts.

3.3.2 ELECTROMAGNETIC DATA

- Visual check for shifts, excessive spiking, drift, etc.
- Correct/Compensate the EM data.
- Identify the backgrounds and measure/log the EM noise levels including original and compensated channels. Ensure they are within specification
- Filter the EM data and check for drift or offsets
- After splitting the GDB into lines, check again

3.3.3 MAGNETIC DATA AND MAGNETIC BASE STATION

- Check the start and end time of base station record and ensure that it covers the full survey data.
- Check the base station for cultural noise and diurnal activity. Ensure the diurnal is within specifications.
- Check the airborne magnetic data for gaps, dropouts, or excessive noise

3.3.4 ALTITUDE

- Visually check the altitude particularly at the start and ends of lines.
- Calculate the average helicopter altitude and ensure that it meets specifications.

3.4 QUALITY CONTROL IN THE OFFICE

Data verification was performed by experienced geophysicists in the processing centre or on-site using a work station that is capable of reading, analysing and duplicating the data on a daily basis. This system was available to GSC and YGS (QA/QC geophysicist) to monitor data acquisition and verification.

The work flow diagram provided below (Figure 6) shows the tests and checks applied during the course of the survey and subsequent processing. The red lines represent feedback loops that will send data back to be reprocessed or even re-flown so as to correct for any deficiencies detected either in the field during QA/QC or at the Data Processing centre where senior staff review incoming data sets.

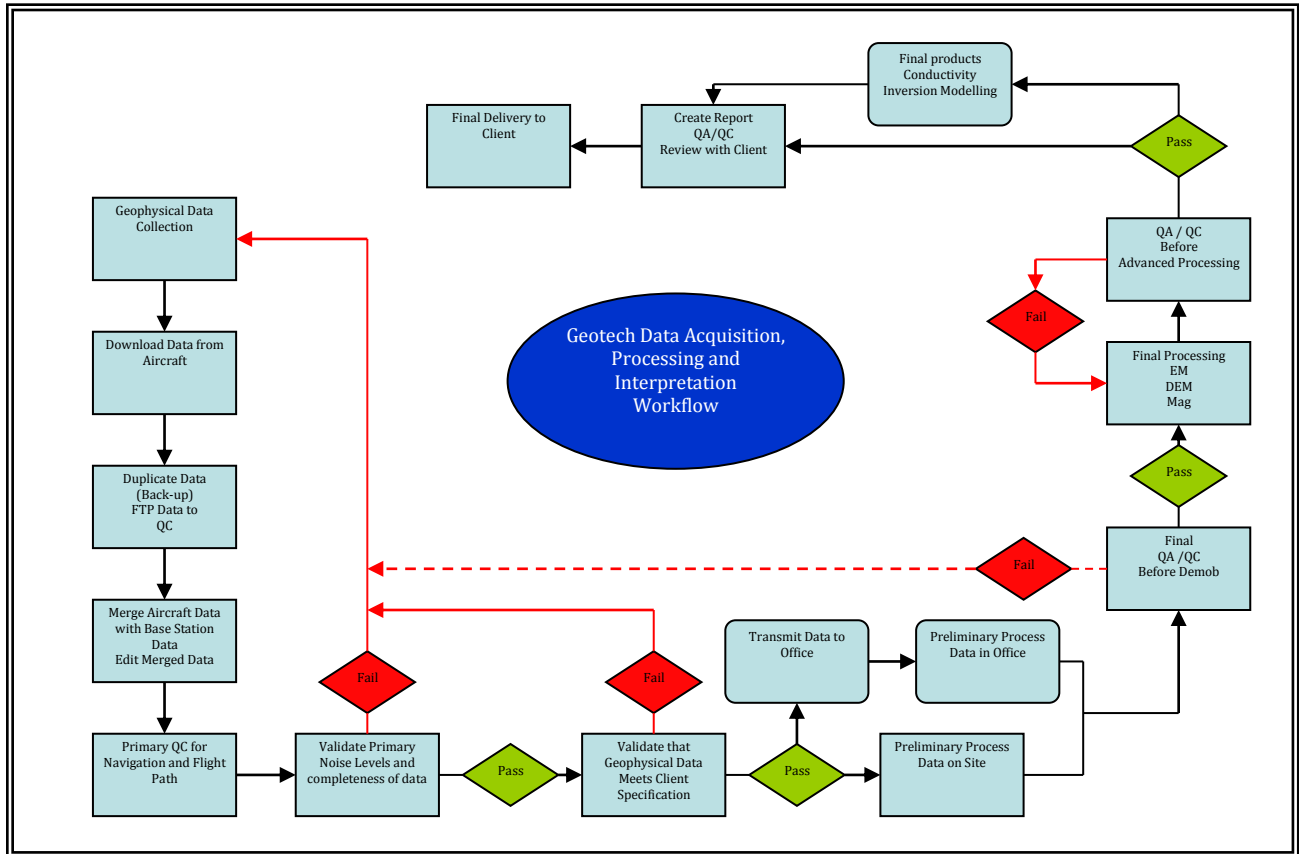


Figure 6: Data acquisition, data processing and interpretation workflow

4. PERSONNEL

The following Geotech Ltd. personnel were involved in the project.

FIELD:

Project Manager:	Darren Tuck (Office)
Data QC:	Neil Fiset (Office)
Crew chief:	Gavin Boege
Operator:	Victor Shevchenko Terry Lacey

The survey pilot and the mechanical engineer were employed directly by the helicopter operator – Geotech Aviation.

Pilot:	Pierre Forand Rob Girard
Mechanical Engineer:	Halil Buberoglu

OFFICE:

Preliminary Data Processing:	Neil Fiset Thomas Wade
Final Data Processing:	Marta Orta
Final Data QA/QC:	Geoffrey Plastow
Reporting/Mapping:	Wendy Acorn

Data acquisition phase was carried out under the supervision of Andrei Bagrianski, P. Geo, and Chief Operating Officer. Data processing phases were carried out under the supervision of Geoffrey Plastow, P. Geo, and Data Processing Manager. The customer relations were looked after by David Hitz.

5. DATA PROCESSING AND PRESENTATION

Data compilation and processing were carried out by the application of Geosoft OASIS Montaj and programs proprietary to Geotech Ltd.

5.1 FLIGHT PATH

The flight path, recorded by the acquisition program as WGS 84 latitude/longitude, was converted into the NAD83 Datum, UTM Zone 8 North coordinate system in Oasis Montaj.

The flight path was drawn using linear interpolation between x, y positions from the navigation system. Positions are updated every second and expressed as UTM easting's (x) and UTM northing's (y).

5.2 ELECTROMAGNETIC DATA

As the data are acquired by the data acquisition system on the helicopter, it goes through a digital filter to reject major spheric events and is stacked to further reduce system noise. Afterward, the streamed data is processed by applying a system response correction, B-field integration, time window binning, compensation, filtering, and leveling.

The Full Waveform EM specific data processing operations included:

- Half cycle stacking (performed at time of acquisition);
- System response correction;
- Parasitic current and drift removal by deconvolution.

The digital filtering process is a three stage filter used to reject major spheric events and to reduce noise levels. Local spheric activity can produce sharp, large amplitude events that cannot be removed by conventional filtering procedures. Smoothing or stacking will reduce their amplitude but leave a broader residual response that can be confused with geological phenomena. To avoid this possibility, a computer algorithm searches out and rejects the major spheric events. The data was then stacked using 15 half cycles, 0.3 seconds, to create a stacked half-cycle waveform at 0.1 second intervals. The stacking coefficients are tapered with a shape that approximates a Gaussian function.

During post-flight processing, the streamed data have a sensor response correction applied which corrects the receiver channels and current monitor to a common impulse response based on the Full Waveform Calibration. The B-field data are calculated by integrating the dB/dt cycles from the 192 kHz streamed data. Then, the streamed data are converted into a set of time window channels to reduce noise levels further.

The data have noise levels reduced further by the use of an EM compensation procedure which removes characteristic noise from each fiducial determined by the difference between the transmitter and bucking loop fields at the receiver during the flight. This is achieved by a statistical correlation between each time window channel and primary field measurement taken during the on-time.

Next, filtering of the electromagnetic data was performed in two steps. The first is a 4 fiducial wide non-linear filter to eliminate any large spikes remaining in the dataset. The second filter is a low pass symmetric linear digital filter that has zero phase shift which prevents any lag or peak displacement from occurring, and it suppresses only variations with a wavelength less than about 1 second or 25 metres.

The VTEM system has three receiver coil orientations: X, Y and Z. Generalized modelling results of the VTEM system are shown in Appendix D.

The Z-axis receiver coil was oriented parallel to the transmitter coil axis and both were horizontal to the ground. Z-component data produce double peak type anomalies for “thin” sub vertical targets and single peak anomalies for “thick” targets. The limits and changeover of “thin-thick” depends on dimensions of the TEM system (Appendix D, Figure D-17).

The X-axis coil is oriented parallel to the ground and along the line-of-flight. The Y-axis coil is oriented parallel to the ground and perpendicular to the line-of-flight. The combination of the X and Z coils configuration provides information on the position, depth, dip and thickness of a conductor.

The X-component data produce cross-over type anomalies: from “+ to -” in flight direction of flight for “thin” sub vertical targets and from “- to +” in direction of flight for “thick” targets.

Because of X component polarity is under line-of-flight, convolution Fraser Filter (FF, middle panel in Figure 7) is applied to X component data to represent axes of conductors in the form of grid map. In this case positive FF anomalies always correspond to “plus-to-minus” X data crossovers independent of the flight direction.

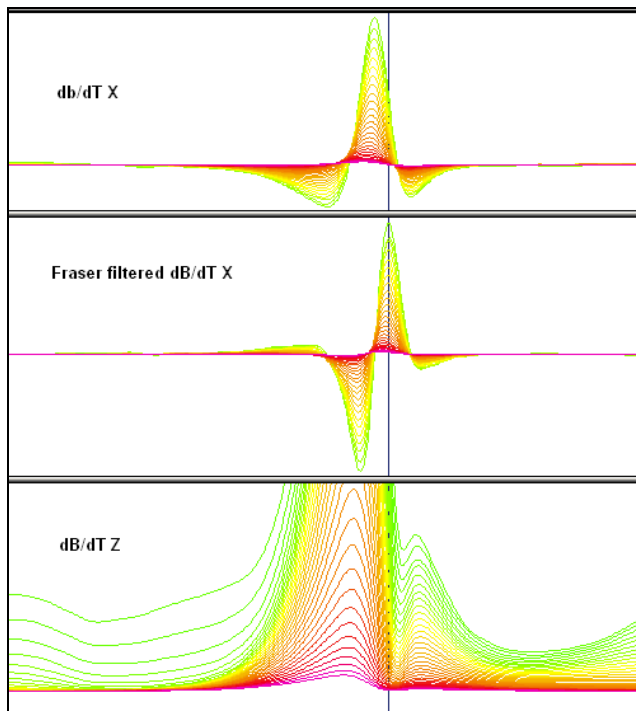


Figure 7: Z, X and Fraser filtered X (FFx) components for “thin” target.

5.2.1 EM ANOMALY SELECTION

The EM data were subjected to an anomaly recognition process using all the channels of the dBz/dt and B-field profiles. The resulting EM anomaly picks are presented as overlays on the maps and correspond to the approximate position of the conductors' centres projected to surface.

Each individual conductor pick is represented by an anomaly symbol classified according to the last channel where the anomaly is identified. Anomalies were classified into one of six categories, as presented in Figure 8. The anomaly symbol is accompanied by postings denoting the calculated dBz/dt apparent conductivity² (upper-right), time-constant (Tau)³ calculated from dBz/dt data (lower-right) and the apparent depth (lower-left). Each symbol is also given an identification letter label (upper-left), unique to each flight line.

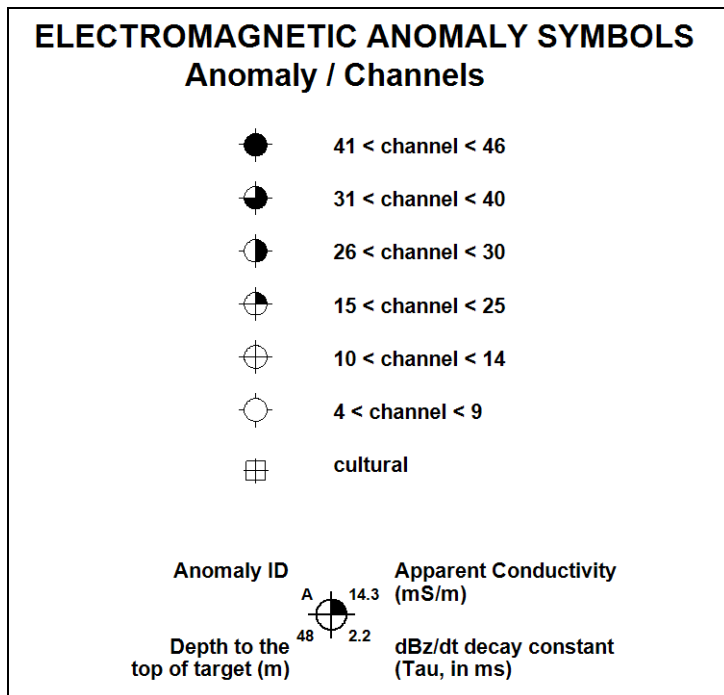


Figure 8: EM Anomaly Symbols

The anomalous responses have been picked, reviewed and edited by an interpreter on a line-by-line basis to discriminate between bedrock, overburden and conductors affected by culture⁴. The accepted channels are shown in appendix H and provided in a Geosoft database and an Excel file.

² The Geotech proprietary algorithm is based on the scheme of the apparent resistivity transform of Maxwell A. Meju (1998), the TEM response from the conductive half-space, and depth calibrated based on the forward plate modelling for the VTEM system configuration.

³ An explanation of the EM time constant (Tau) approach to VTEM data is provided in Appendix E.

⁴ Cultural components are classified according to the power line monitor (PLM) response and man-made artifacts visible on Google Earth™.

5.2.2 CONDUCTIVITY DEPTH IMAGING (CDI)

A set of Conductivity Depth Images (CDI) were generated using an in-house CDI algorithm, developed by Geotech Ltd. A total of forty-three (43) dB/dt Z component channels, starting from channel 4 (0.018 ms) to channel 46 (8.685 ms), were used for the CDI calculation of the data.

The employed CDI algorithm is based on the scheme of the apparent resistivity transform of Maxwell A. Meju (1998)⁵ and TEM response from conductive half-space. The software was developed by Geotech Ltd. and depth calibrated based on forward plate modelling for the VTEM system configuration. For more information on the CDI algorithm please refer to Appendix F.

Grids of apparent conductivity (in mS/m) were computed from the EM decays using the early channels 4-14 (0.018 – 0.103 ms), the middle channels 15-30 (0.103 – 0.945 ms) and the late channels 31-46 (0.945 – 8.685 ms) to present the response of the off-time signal.

⁵ Meju, M.A. 1998. Short Note: A simple method of transient electromagnetic data analysis, *Geophysics*, **63**, 405–410.

5.3 MAGNETIC DATA

5.3.1 HORIZONTAL MAGNETIC GRADIOMETER DATA

The horizontal gradients data from the VTEM™Plus are measured by two magnetometers 12.5 m apart on an independent bird mounted 10m above the VTEM™ loop. A GPS and a Gyro Inclinator help to determine the positions and orientations of the magnetometers. The data from the two magnetometers are corrected for position and orientation variations, as well as for the diurnal variations using the base station data.

The position of the centre of the horizontal magnetic gradiometer bird is calculated from the GPS utilizing in-house processing tool in Geosoft. Following that, data is lagged to the nose of the gradiometer loop, where the GPS antenna is located. Advanced processing is performed to calculate the in-line and cross-line (or lateral) horizontal gradient which enhance the understanding of magnetic targets. The in-line (longitudinal) horizontal gradient is calculated from the difference of two consecutive total magnetic field readings divided by the distance along the flight line direction, while the cross-line (lateral) horizontal magnetic gradient is calculated from the difference in the magnetic readings from both magnetic sensors divided by their horizontal separation.

Two advanced magnetic derivative products, the total horizontal derivative (THDR), and tilt angle derivative are created. The total horizontal derivative or gradient is defined as:

$THDR = \sqrt{H_x^2 + H_y^2}$, where H_x and H_y are cross-line and in-line horizontal gradients.

The tilt angle derivative (TDR) is defined as:

$TDR = \arctan(V_z/THDR)$, where THDR is the total horizontal derivative, and V_z is the vertical derivative.

Measured cross-line gradients can help to enhance cross-line linear features during gridding.

Note: The proposed THDR and TDR grids were calculated by the Geological Survey of Canada from the levelled total magnetic field (SRVMGLEV) to minimize the line to line effects and to obtain a better continuity for the geological contacts. Therefore H_x and H_y gradients were calculated in the spatial domain with Geosoft.

5.3.2 TOTAL MAGNETIC FIELD DATA LEVELLING

Magnetic data were levelled in the field for quality control purposes. In the office after the completion of the survey, the lagged, compensated total field magnetic data were examined and edited for spurious noise and relevelled more precisely.

As a first step in the levelling process, a filtering algorithm to remove undesirable high frequency noise (< 1.5 seconds) components was applied to the edited' lagged data. This filter did not affect the real anomalous features. The resulting noise channel has a mean of zero and values from a minimum to maximum range of +/- 0.2 nT and a Standard deviation of 0.008 nT.

Since the reference base station was located within the survey area at the Livinstone Creek airstrip the diurnal activity in the block and at the reference base station correlated very well. Therefore the edited ground reference data correction (DIURNCOR) was used and applied to the raw, edited and lagged airborne magnetometer data.

In addition, differences in the magnetic field values caused by flight altitude differences between traverse and control lines need to be reduced. To bring the levelling intersections to the same altitude, the magnetic data along the traverse lines and control lines are continued to the intended pre-planned surface height (SURFACE). The continuation is applied to the edited magnetic data profile (MAGRAW) relative to the drape surface as the datum with a Taylor series expansion consisting of the first and second vertical derivative of the total magnetic field as the first and second term of the series.

The levelling of the total field magnetic data, corrected to the height drape surface, typically begins with the calculation of all traverse and control total field magnetic value differences at their intersection points. This process was executed and the differences which were observed were statistically insignificant since the actual magnetic diurnal was subtracted from the raw edited and height corrected magnetic data. However, isolated cases exhibiting very large differences at intersections were noted. These large differences were over steep magnetic gradients coinciding with areas where there were large deviations from the intended drape surface, despite the best effort of the survey pilots. The Taylor series expansion corrections were insufficient to correct this deficiency. Akima splined level adjustments were introduced manually into the MAGTLCOR channel at these locations

In summary, the final levelled survey magnetic total field data (SRVMGLEV) consisted of a correction which removed high frequency noise (MAGHFCOR), magnetic diurnal correction (DIURNCOR), altitude correction (ALTCOR) and a tie-line levelled correction (MAGTLCOR) to the raw, edited and lagged magnetic data (MAGRAW):

$$\text{SRVMGLEV} = \text{MAGRAW} - \text{MAGHFCOR} - \text{DIURNCOR} + \text{ALTCOR} - \text{MAGTLCOR}$$

After levelling, the airborne magnetometer data were corrected for the IGRF using the location of each point, the average altitude of the drape surface, and a fixed date of 11th May, 2016. IGRF values were calculated (IGRF channel) using the year 2015 IGRF model. The altitude data used for the IGRF corrections are DGPS height average of 1375 metres. This data is presented in the SRVMGRES channel.

6. DELIVERABLES

6.1 SURVEY REPORT

The survey report describes the data acquisition, processing, and final presentation of the survey results. The survey report is provided digitally in PDF format.

6.2 MAPS

Final maps were produced at scale of 1:20,000 for best representation of the survey size and line spacing. The coordinate/projection system used was NAD83 Datum, UTM Zone 8 North. All maps show the flight path trace and topographic data; latitude and longitude are also noted on maps.

- Maps at 1:20,000 in Geosoft MAP format, as follows:

Sheet 1: Time Decay Constant (Tau Z) - Early channels 4 – 14 (0.018 – 0.103 ms)
Sheet 2: Time Decay Constant (Tau Z) - Middle channels 15 – 30 (0.103 – 0.945 ms)
Sheet 3: Time Decay Constant (Tau Z) - Late channels 31 – 46 (0.945 – 8.685 ms)
Sheet 4: Apparent Conductivity - Early channels 4 – 14 (0.018 – 0.103 ms)
Sheet 5: Apparent Conductivity - Middle channels 15 – 30 (0.103 – 0.945 ms)
Sheet 6: Apparent Conductivity - Middle channels 31 – 46 (0.945 – 8.685 ms)
Sheet 7: Residual Total Magnetic Field
Sheet 8: First Vertical Derivative of the Magnetic Field
Sheet 9: Electromagnetic Interpretation

- Maps are also presented in PDF format.
- The topographic data base was derived from 1:50000 NRC (Natural Resources Canada) NTDB dataset, www.geogratis.ca
- A Google Earth file *GL160031_FP.kml* showing the flight path of the block is included. Free versions of Google Earth software from: <http://earth.google.com/download-earth.html>

6.3 DIGITAL DATA

Copies of the data and maps on a hard drive were prepared to accompany the report. The hard drive contains a digital file of the line data in GDB Geosoft Montaj format as well as the maps in Geosoft Montaj Map and PDF format.

- DVD structure.

Data contains databases, grids and maps, as described below.
Report contains a copy of the report and appendices in PDF format.

- Database in Geosoft GDB format containing the survey data; channels listed in Table 7.

Table 7: Geosoft GDB Data Format

Contractor Channel Name	GSC Channel Name	Description	Format	Units	Sample Rate
LINE	LINE	Line number	I6	-	0.1
TIME	TIME	GPS Time (seconds of the day after midnight)	F8.1	sec	0.1
FIDUCIAL	FIDCOUNT	Acquisition system Time Increment, incrementing at 10 Hz	F8.1	-	0.1
LONG	LONG	Longitude (nose of gradiometer loop)	F12.6	deg	0.1
LAT	LAT	Latitude (nose of gradiometer loop)	F10.6	deg	0.1
EASTING	EASTING	Easting (NAD83, UTM Z8N - nose of gradiometer loop)	F10.2	m	0.1
NORTHING	NORTHING	Northing (NAD83, UTM Z8N - nose of gradiometer loop)	F11.2	m	0.1
SURFACE	SURFACE	Drape surface altitude (to be used for magnetic data only)	F8.2	m	0.1
GPSALTRL	GPSALTRL	Raw helicopter GPS altitude, Real-time (MSL)	F8.2	m	0.1
GPSALT	GPSALT	Edited Helicopter GPS altitude above mean sea level (MSL)	F7.1	m	0.1
RALTRAW	RALTRAW	Raw Helicopter Radar altitude (Terrain Clearance)	F7.1	m	0.1
RALT	RALT	Edited Helicopter Radar altitude (Terrain Clearance),lagged	F8.2	m	0.1
BALTRAW	BALTRAW	Raw Helicopter Barometric Pressure altitude	F8.2	kPa	0.1
BALT	BALT	Helicopter Barometric altitude above sea level, corrected for drift (MSL)	F8.2	m	0.1
DEMLEV	DEMLEV	Levelled Digital Elevation Model / Topography (GPSALT - RALT + corrections) (Terrain Clearance)	F8.2	m	0.1
MGHEIGHT	MGHEIGHT	Magnetometer height (above terrain)	F9.2	m	0.1
MAGUNLAG_L	LMAGUCOM	Raw unlagged, uncompensated, magnetic total field, left sensor	F9.2	nT	0.1
MAGUNLAG_R	RMAGUCOM	Raw unlagged, uncompensated, magnetic total field, right sensor	F9.2	nT	0.1
MAGULED	MAGULED	Raw, edited, unlagged total magnetic field, mean of left and right sensors	F9.2	nT	0.1
MAGRAW	MAGRAW	Edited total magnetic field, mean of left and right sensors, lagged forward to nose of gradiometer loop	F8.4	nT	0.1
DIURNRAW	DIURNRAW	Raw Magnetic Diurnal ground base station 1	F8.4	nT	0.1
DIURNAL	DIURNAL	Edited, filtered Magnetic Diurnal ground	F8.4	nT	0.1

		Base station 1 (Livingstone Creek airstrip)			
DIURCOR	DIURNCOR	Magnetic Diurnal correction	F7.2	nT	0.1
MAGHFCOR	MAGHFCOR	HF magnetic noise correction	F9.2	nT	0.1
ALTCOR	ALTCOR	Taylor series correction factor for height variations	F9.2	nT	0.1
MAGTLCOR	MAGTLCOR	Manual levelling corrections to total magnetic field at tie line intersections	F8.2	nT	0.1
SRVMGLEV	SRVMGLEV	Final levelled total magnetic field	F10.2	nT	0.1
IGRF	IGRF	IGRF correction; Avg. alt (1375m), date: (2016/05/11)	F10.2	nT	0.1
SRVMGRES	SRVMGRES	Final levelled Residual total magnetic field	F10.2	nT	0.1
HG_INLINE	HG_LLEV	Calculated horizontal in-line magnetic gradient	F10.2	nT/m	0.1
HG_CXLINE	HG_OLEV	Measured horizontal cross-line magnetic gradient	F10.2	nT/m	0.1
EMTRANHT	EMTRANHT	Electromagnetic transmitter height (above terrain)	F10.2	m AGL	0.1
EMHEIGHT	EMHEIGHT	Electromagnetic receiver height (above terrain)	F10.2	m AGL	0.1
PRIMARY	PRIMARY	Primary field intensity (EM total field)	F10.2	Am ²	0.1
POWERLNE	POWERLNE	Power line monitor (EM noise monitor)	F10.2	μV	0.1
RXTEMOFF	RX_47_TEM	Raw X-coil TDEM Off channels array (20-46)	F10.2	pT/s	0.1
RYTEMOFF	RY_47_TEM	Raw Y-coil TDEM Off channels array (20-46)	F10.2	pT/s	0.1
RZTEMOFF	RZ_47_TEM	Raw Z-coil TDEM Off channels array (04-46)	F10.2	pT/s	0.1
RXBEMOFF	RX_47_BEM	Raw X-coil B-field Off channels array (20-46)	F10.2	fT	0.1
RYBEMOFF	RY_47_BEM	Raw Y-coil B-field Off channels array (20-46)	F10.2	fT	0.1
RZBEMOFF	RZ_47_BEM	Raw Z-coil B-field Off channels array (04-46)	F10.2	fT	0.1
PXTEMOFF	LX_47_TEM	Levelled X-coil TDEM Off channels array (20-46)	F10.2	pT/s	0.1
PYTEMOFF	LY_47_TEM	Levelled Y-coil TDEM Off channels array (20-46)	F10.2	pT/s	0.1
PZTEMOFF	LZ_47_TEM	Levelled Z-coil TDEM Off channels array (04-46)	F10.2	pT/s	0.1
PXBEMOFF	LX_47_BEM	Levelled X-coil B-field Off channels array (20-46)	F10.2	fT	0.1
LY_BEM	LY_47_BEM	Levelled Y-coil B-field Off channels array (20-46)	F10.2	fT	0.1
LZ_BEM	LZ_47_BEM	Levelled Z-coil B-field Off channels array (04-46)	F10.2	fT	0.1

COND	COND_47	Apparent Conductivity array (4-46)	F10.2	mS/m	0.1
TAUsf_EARLY	TAU_Z_EARLY	Decay constant (Tau) for dB/dt Z-component, calculated from channels 4-14	F10.2	millisec	0.1
TAUSF_MID	TAU_Z_MID	Decay constant (Tau) for dB/dt Z-component, calculated from channels 15-30	F10.2	millisec	0.1
TAUSF_LATE	TAU_Z_LATE	Decay constant (Tau) for dB/dt Z-component, calculated from channels 31-46	F10.2	millisec	0.1
TAU_BZ	TAU_BZ	Decay constant (Tau) for B-field Z-component	F10.2	millisec	0.1
APPCOND_EARLY	COND_EARLY	Apparent Conductivity calculated from early time channels 4-14	F10.2	mS/m	0.1
APPCOND_MID	COND_MID	Apparent Conductivity calculated from mid time channels 15-30	F10.2	mS/m	0.1
APPCOND_LATE	COND_LATE	Apparent Conductivity calculated from late time channels 31-46	F10.2	mS/m	0.1
FLIGHT	FLIGHT	Flight number	I9		0.1
DATE	DATE	Local date (YYMMDD)	I5		0.1
LINENAME	LINENAME	Line name An alpha-numeric string	A7		0.1
LINETYPE	LINETYPE	Line Type, L=Traverse, T=Tie, B=Background	A2		0.1

Electromagnetic B-field and dB/dt Z component data is found in array channel format between indexes 4 – 46, and X and Y component data from 20 – 46, as described above.

In this dataset all raw and processed EM data have been provided.

- Database of the Conductivity Depth Images in Geosoft GDB format, containing the following channels:

Table 8: Geosoft Conductivity Depth Image GDB Data Format

Channel name	GSC channel Name	Units	Description
	LINE		Line number
EASTING	EASTING	metres	UTM Easting NAD83 Zone 8 North
NORTHING	NORTHING	metres	UTM Northing NAD83 Zone 8 North
Depth	Depth_Terrain	metres	array channel, depth from the surface
Z	Depth_MSL	metres	array channel, depth from sea level
AppCond	COND_43	mS/m	Apparent conductivity array
EMHEIGHT	EMHEIGHT	metres	EM system height from sea level
DEMLEV	DEMLEV	metres	digital elevation model
DOI	DOI	metres	Depth of Investigation: a measure of VTEM depth effectiveness
PLM	POWERLNE	µV	60Hz Power Line Monitor

In this CDI database, the apparent conductivity (AppCond or COND_43) was calculated by Geotech software using a custom array of 44 channels from the measured dB/dt survey data having 43 channels (Note: the first 43 channels in the CDI database correspond to the 43 channels in the survey database).

- Database of the VTEM Waveform “GL160031_waveform.gdb” in Geosoft GDB format, containing the following channels:

Table 9: Geosoft database for the VTEM waveform

Channel name	Units	Description
Time:	milliseconds	Sampling rate interval, 5.2083 microseconds
Tx_Current:	amps	Output current of the transmitter

- Database containing the VTEM anomaly results in Geosoft GDB format and an Excel file, containing the following channels:

Table 10: Geosoft database describing the VTEM anomalies

Channel name	GSC Channel Name	Units	Description
	LINE		Line number
Anom_ID	ANOMALY_LETTER		Alpha identifier of the anomaly along the Line
Anom_type	ANOMALY_TYPE		Anomaly classification: “thick” (K) or “thin” (N) anomaly
EASTING	EASTING	metres	Easting (NAD83, UTM Z8N) – nose of gradiometer loop
NORTHING	NORTHING	metres	Northing (NAD83, UTM Z8N) – nose of gradiometer loop
GPSALT	GPSALT	metres	Edited helicopter GPS altitude (above mean sea level)
EMHeight	EMHEIGHT	metres	Electromagnetic receiver height above ground
AnConSF	COND_Z	mS/m	Apparent conductivity of dBz/dt data
AnTauSF	TAU_Z	milliseconds	Decay constant (Tau) for dBz/dt data
Anom_TgDepth	Anomaly_Depth	metres	Estimated Depth to conductor (below ground level)
cultural	Cultural		If “1”, the anomaly is cultural or is affected by cultural components
chan	Symbol_number		Number representing the EM anomaly symbol used on the maps (1-6)
AnChan	Anomaly_Extent		Last channel (element of array) of the array where the anomaly is identified

- Grids in Geosoft GRD and GeoTIFF format, as follows:

Livingstone_Creek_demlev	50m - Digital Elevation Model (m)
Livingstone_Creek_mag	50m - MAG (nT)
Livingstone_Creek_mag_res:	50m - MAG - Residual Total Field (nT)
Livingstone_Creek_mag_vd1	50m - MAG - 1st Vertical Derivative (nT/m)
Livingstone_Creek_mag_vd2	50m - MAG - 2nd Vertical Derivative (nT/m) ²

Livingstone_Creek_mag_vd1_rtp	50m - MAG - 1st Vertical Derivative of Magnetic Field reduced to the pole (nT/m)
Livingstone_Creek_em_tau_z_early	50m - EM - Z-coil decay constant (tau), early channels (ms)
Livingstone_Creek_em_tau_z_mid	50m - EM - Z-coil decay constant (tau), mid channels (ms)
Livingstone_Creek_em_tau_z_late	50m - EM - Z-coil decay constant (tau), late channels (ms)
Livingstone_Creek_em_cond_early	50m - EM - Apparent conductivity, early channels (mS/m)
Livingstone_Creek_em_cond_mid	50m - EM - Apparent conductivity, mid channels (mS/m)
Livingstone_Creek_em_cond_late	50m - EM - Apparent conductivity, late channels (mS/m)
Livingstone_Creek_tdr:	50m - Calculated Magnetic Tilt derivative (radians)
Livingstone_Creek_thdr:	50m - Calculated Magnetic Total Horizontal Gradient (nT/m)

A Geosoft .GRD file has a .GI metadata file associated with it, containing grid projection information. A grid cell size of 50 metres was used.

7. CONCLUSIONS AND RECOMMENDATIONS

A helicopter-borne versatile time domain electromagnetic (VTEMplus) and horizontal magnetic gradiometer geophysical survey has been completed over the Livingstone Creek area situated in the Yukon Territories.

The total area coverage is 711 km². Total survey line coverage 4227 line-kilometres. The principal sensors included a Time Domain EM system and a horizontal magnetic gradiometer using two caesium magnetometers. Results have been presented as stacked profiles, and contour colour images at a scale of 1:20,000.

Respectfully submitted⁶,

Neil Fiset
Geotech Ltd.

Marta Orta
Geotech Ltd.

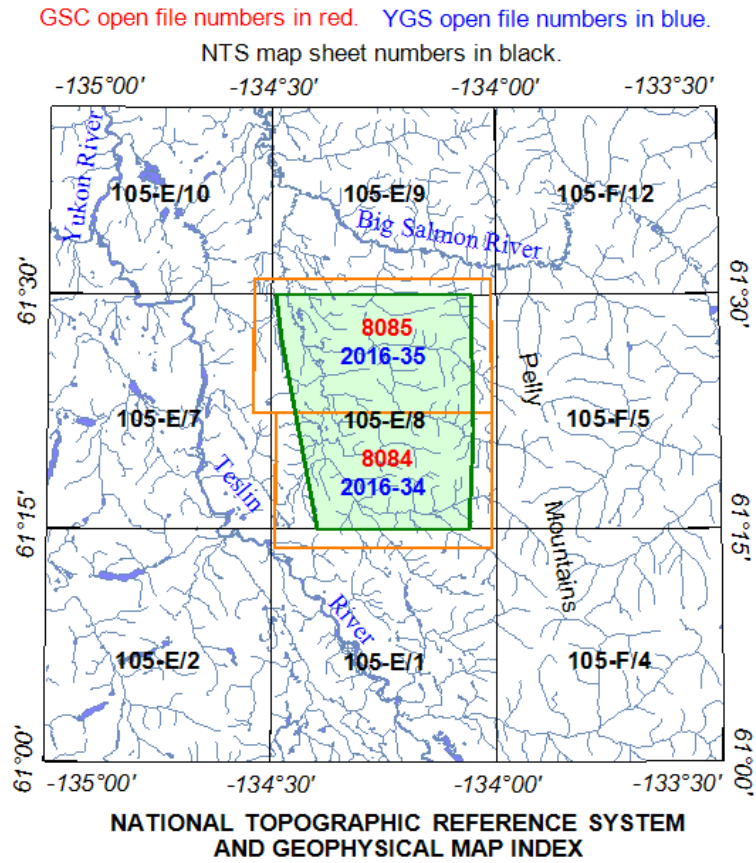
Geoffrey Plastow, P. Geo.
Data Processing Manager
Geotech Ltd.

August, 2016

⁶ Final data processing of the EM and magnetic data were carried out by Marta Orta, from the office of Geotech Ltd. in Aurora, Ontario, under the supervision of Geoffrey Plastow, P. Geo. Data Processing Manager.

APPENDIX A

SURVEY AREA LOCATION MAP



APPENDIX B

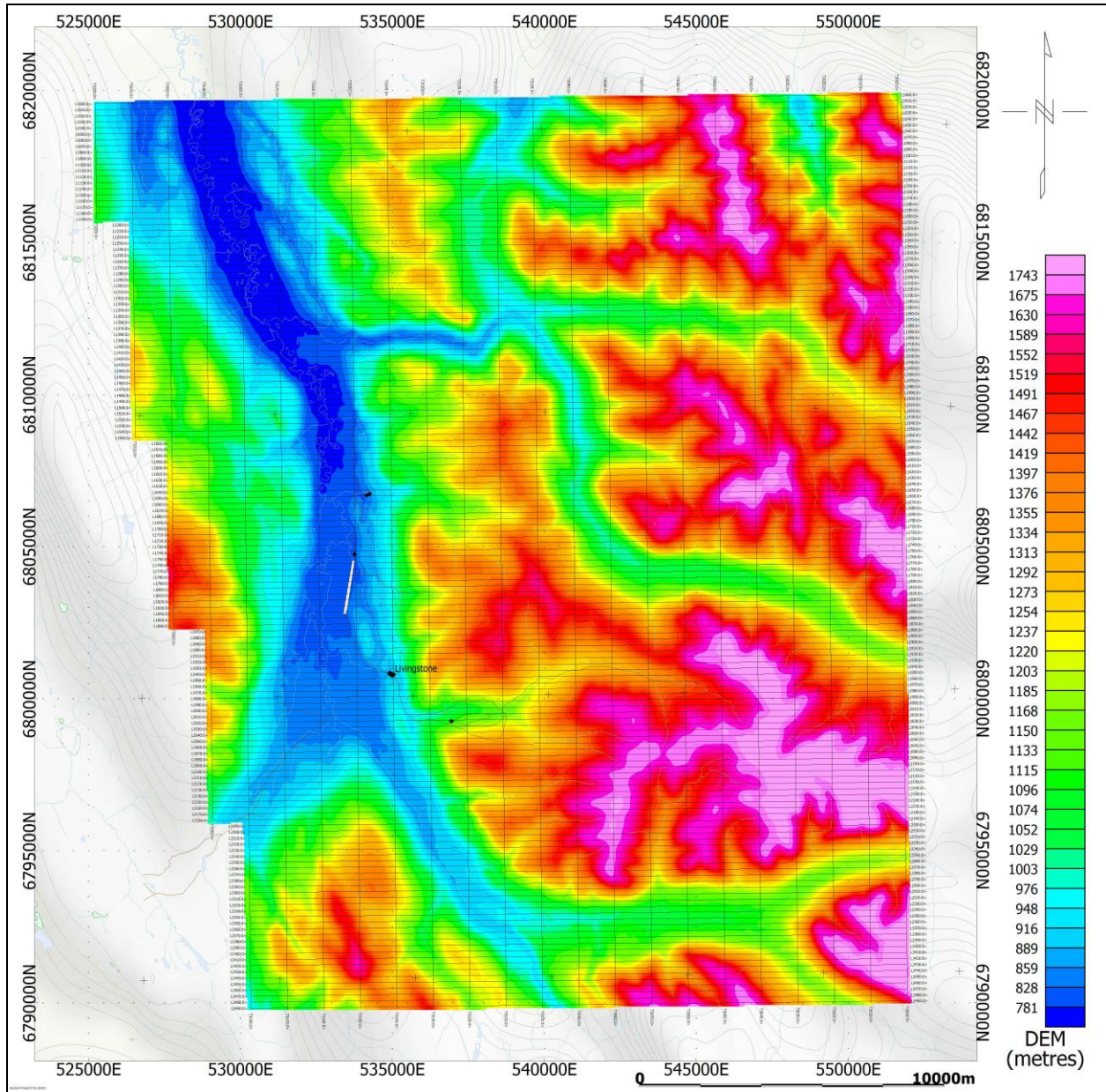
SURVEY AREA COORDINATES

The following coordinates define the main Block survey area:

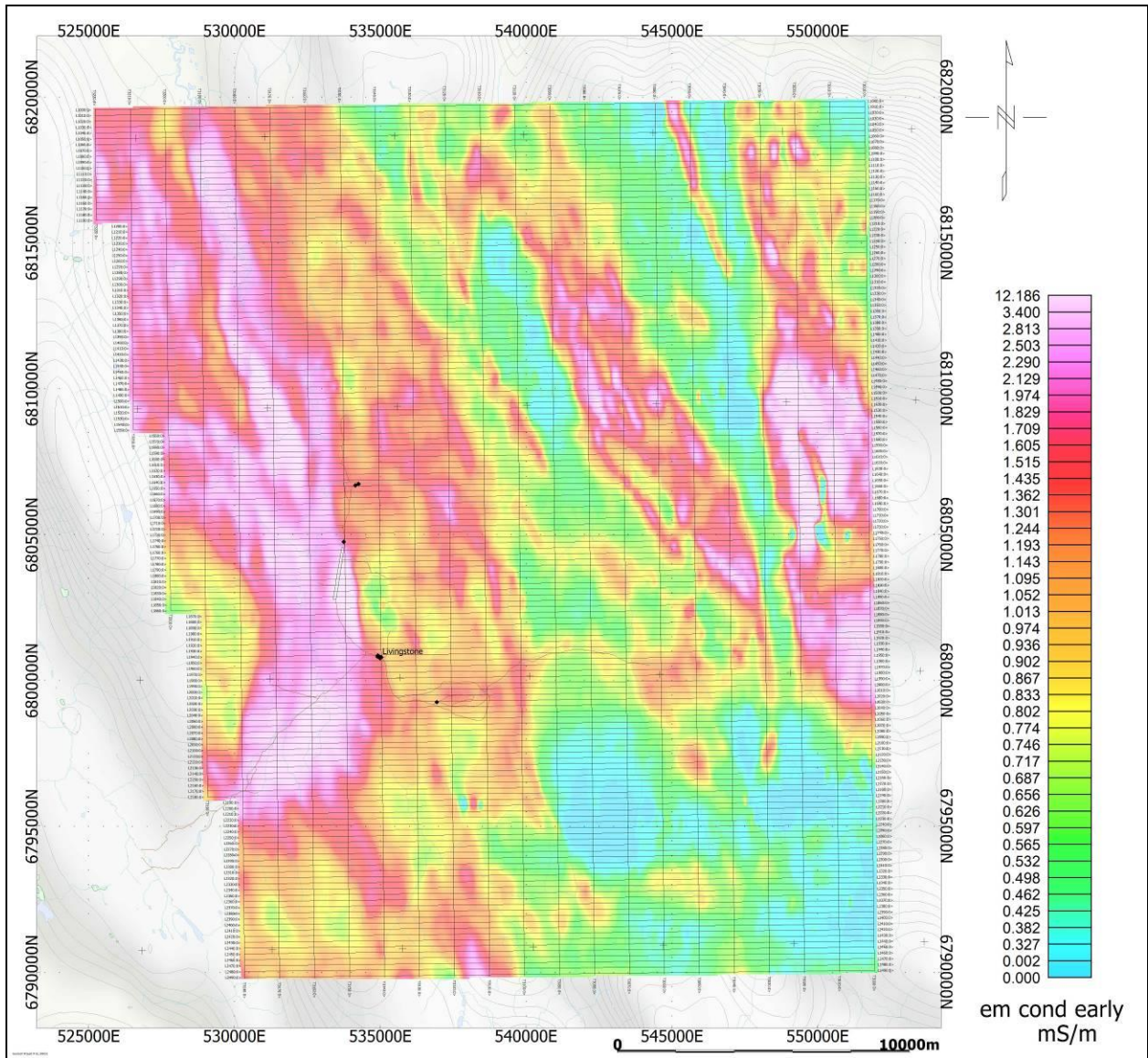
Main Block Boundaries WGS 84		
	LATITUDE	LONGITUDE
corner # 1	N 61°15'00"	W 134°23'52"
corner # 2	N 61°27'07"	W 134°28'41"
corner # 3	N 61°30'00"	W 134°29'32"
corner # 4	N 61°30'00"	W 134°03'23"
corner # 5	N 61°21'17"	W 134°03'03"
corner # 6	N 61°15'00"	W 134°03'36"
corner # 7	N 61°15'00"	W 134°23'52"

APPENDIX C

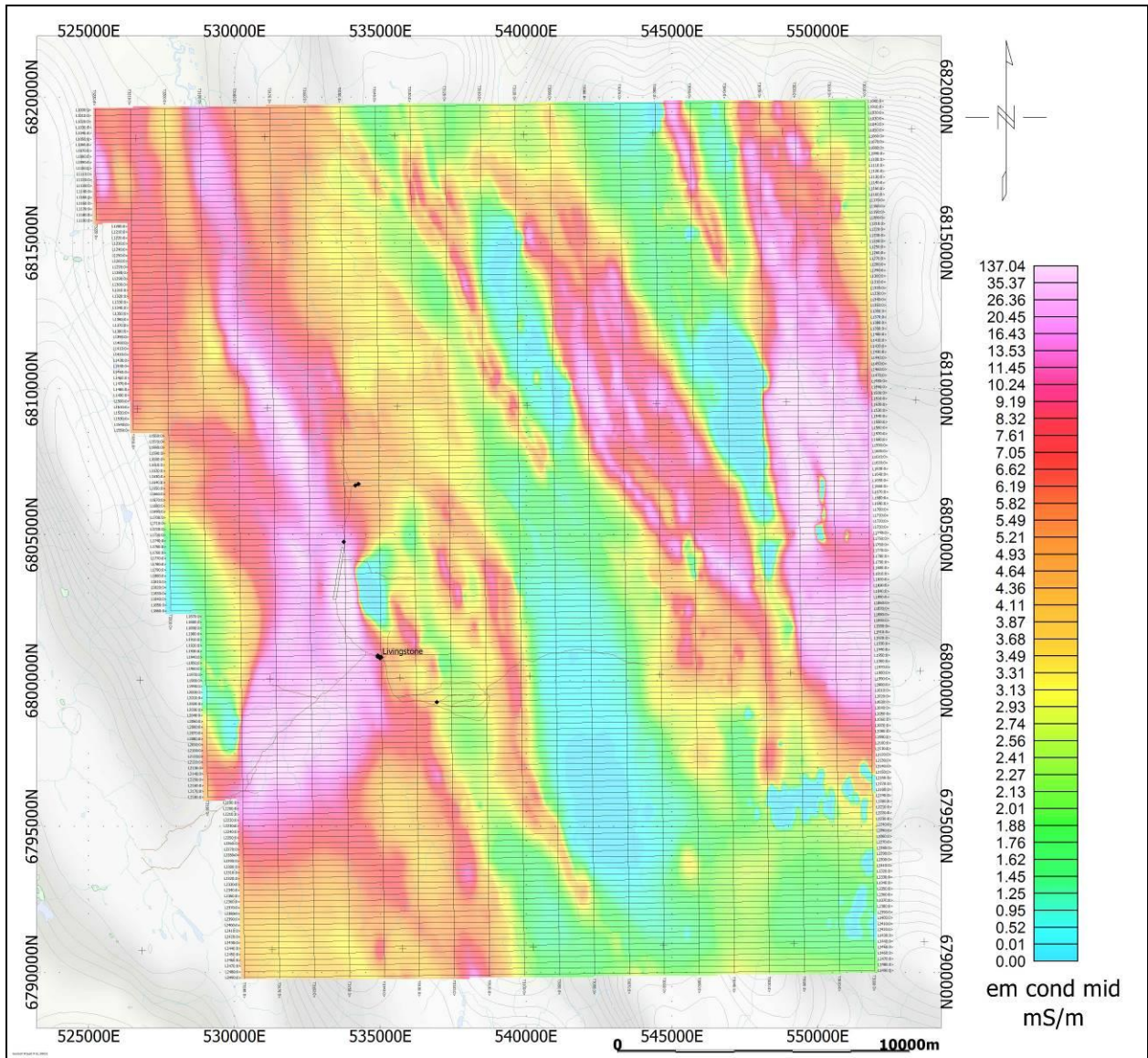
GEOPHYSICAL MAPS



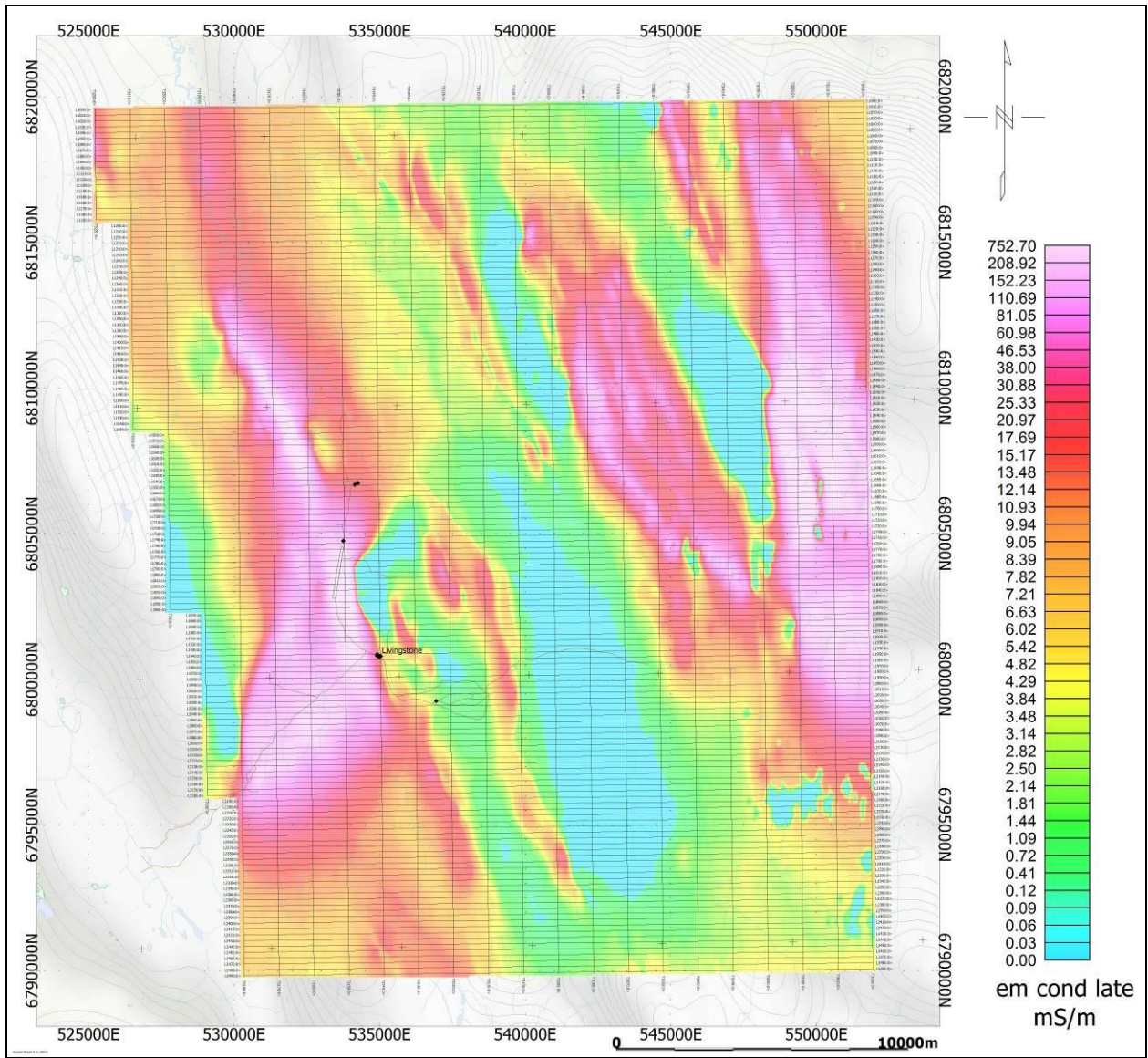
Livingstone Creek Digital Elevation



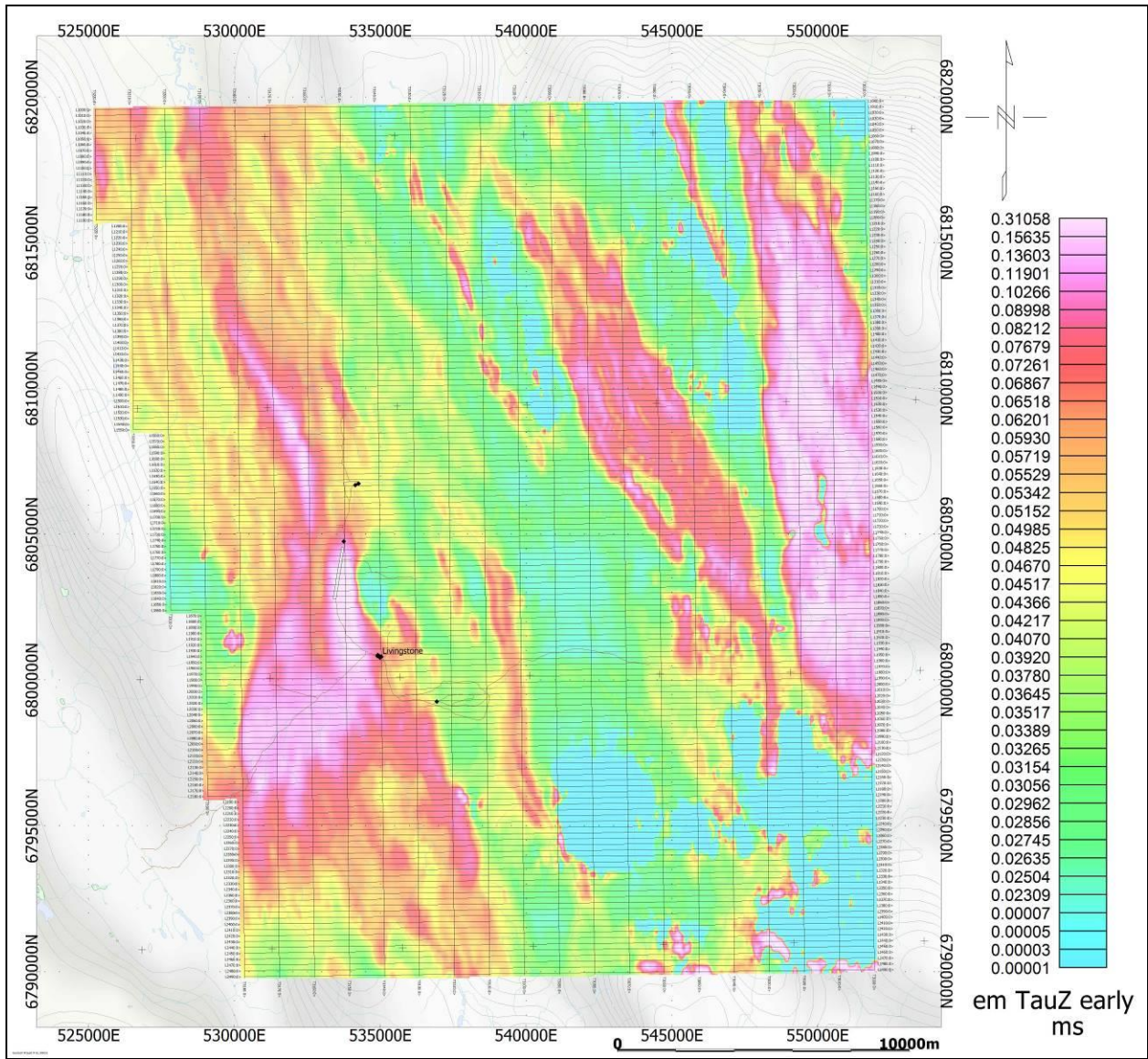
Livingstone Creek em conductivity early



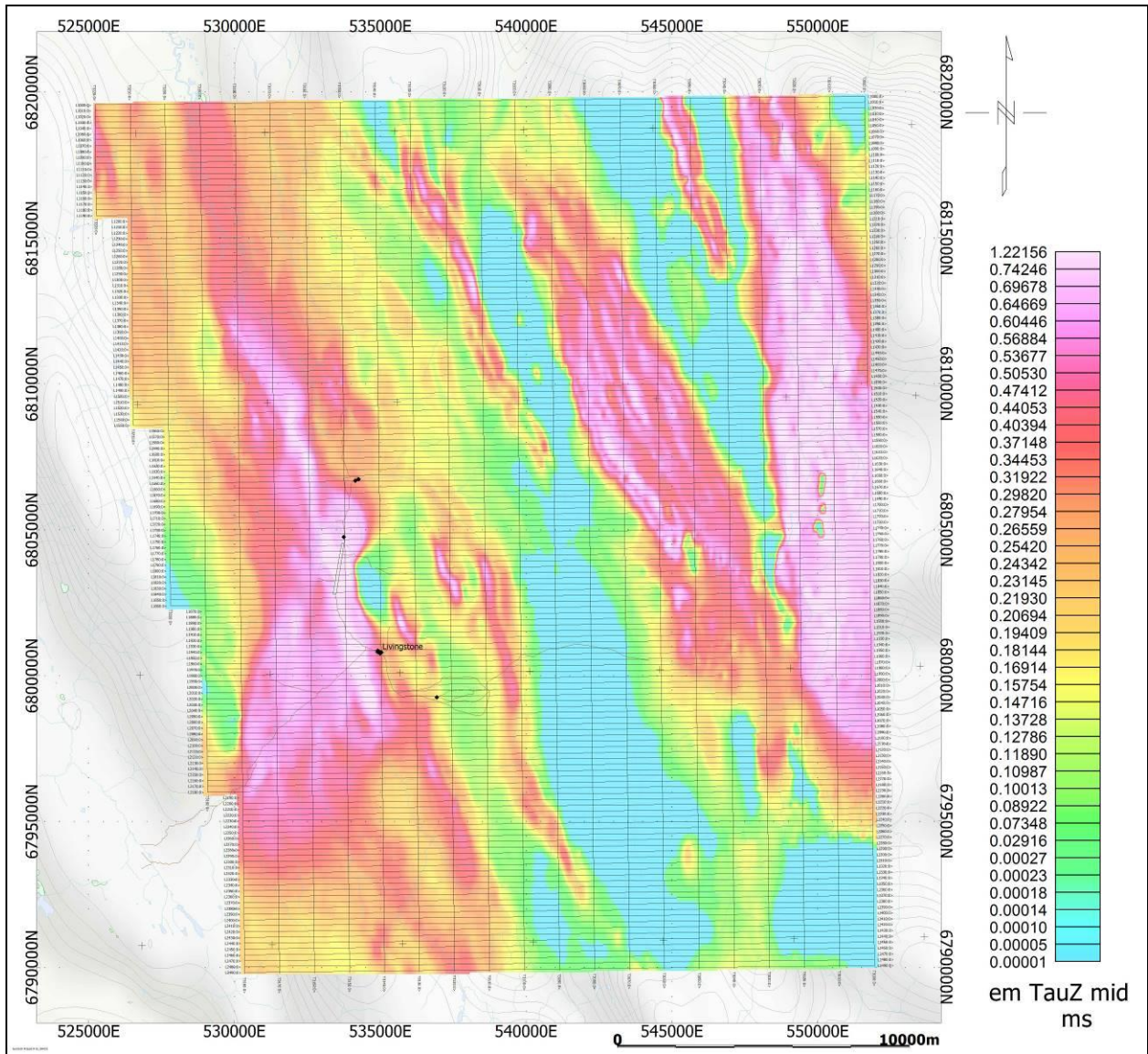
Livingstone_Creek em conductivity mid



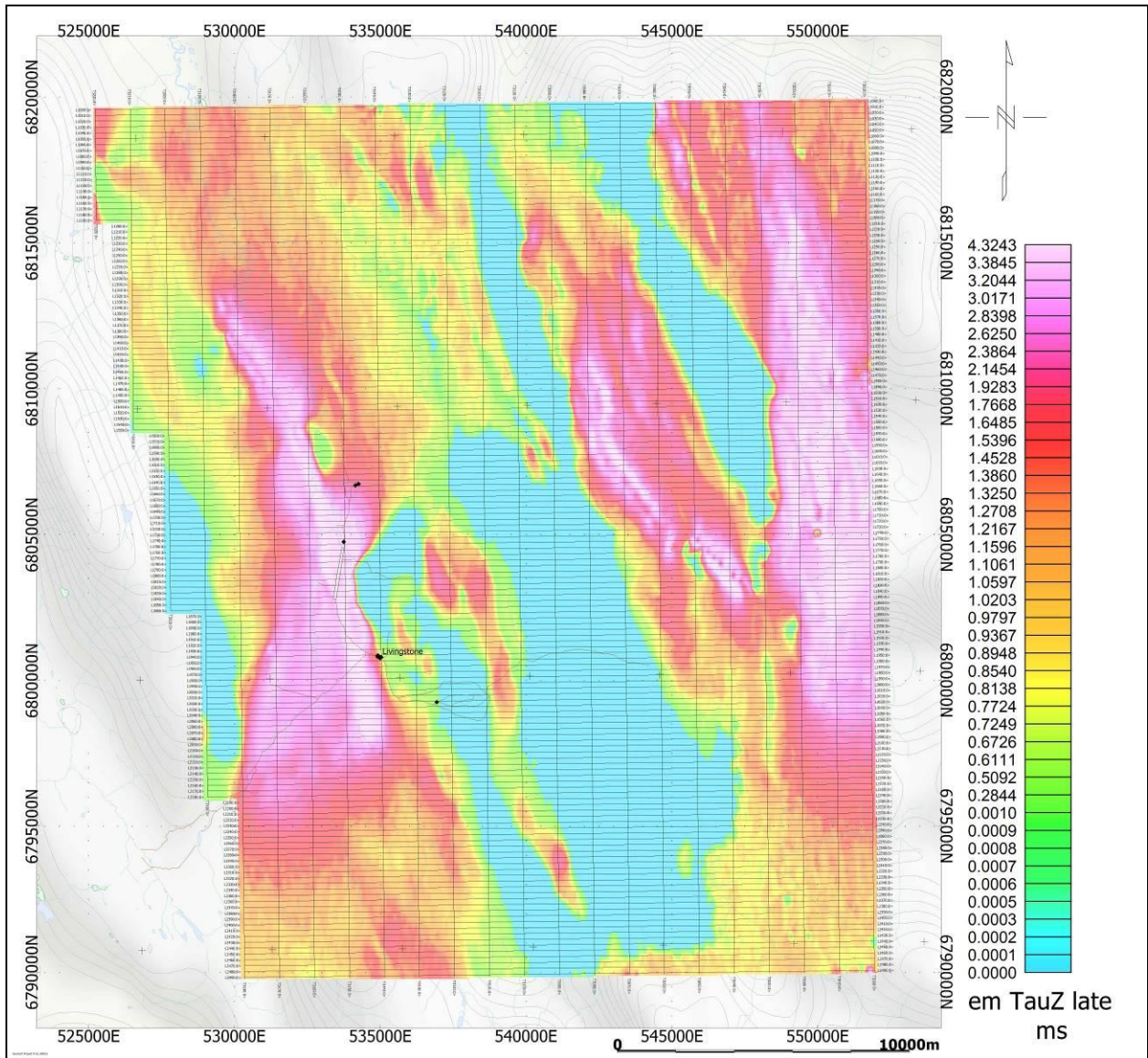
Livingstone Creek em conductivity late



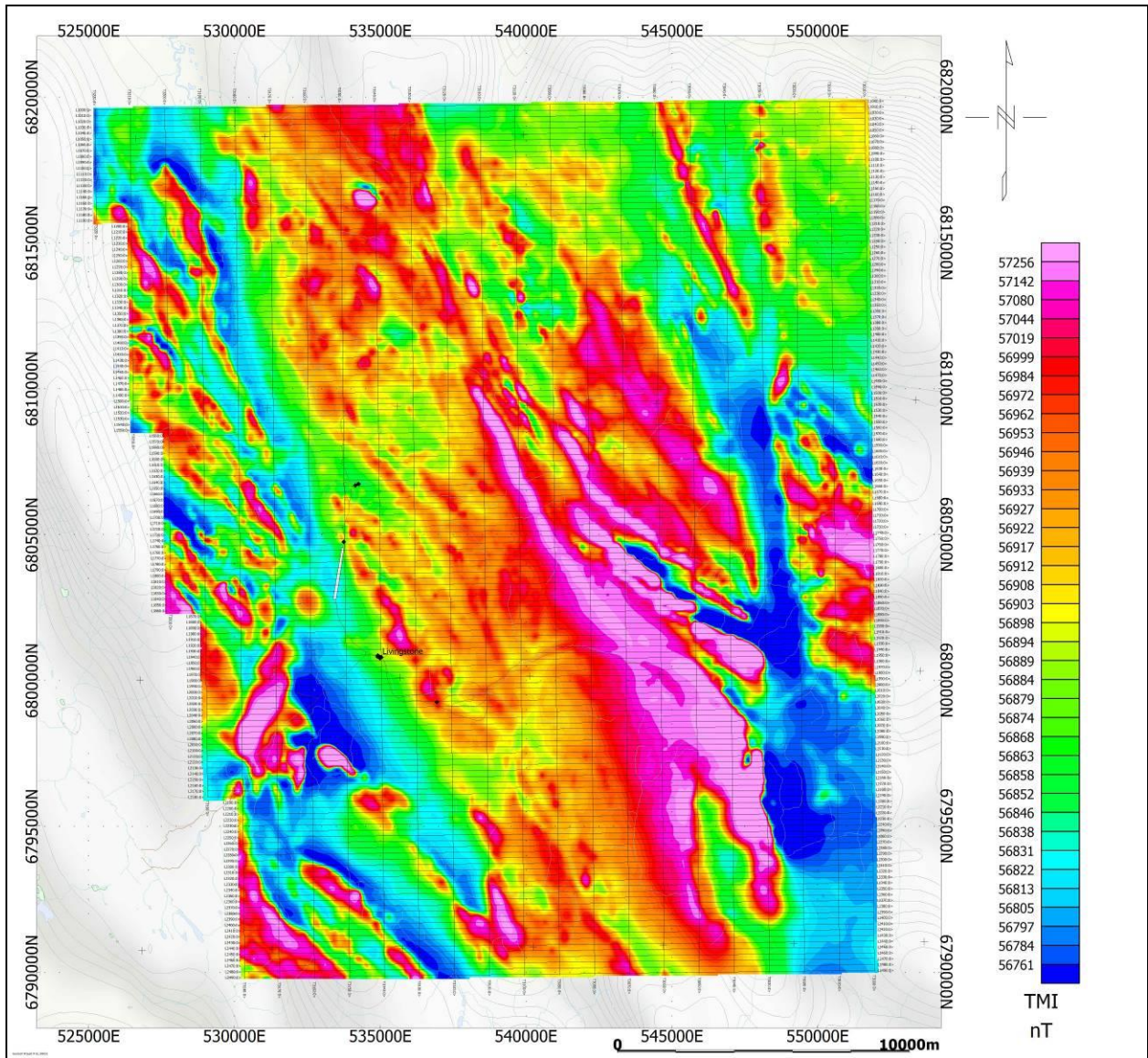
Livingstone_Creek em TauZ early



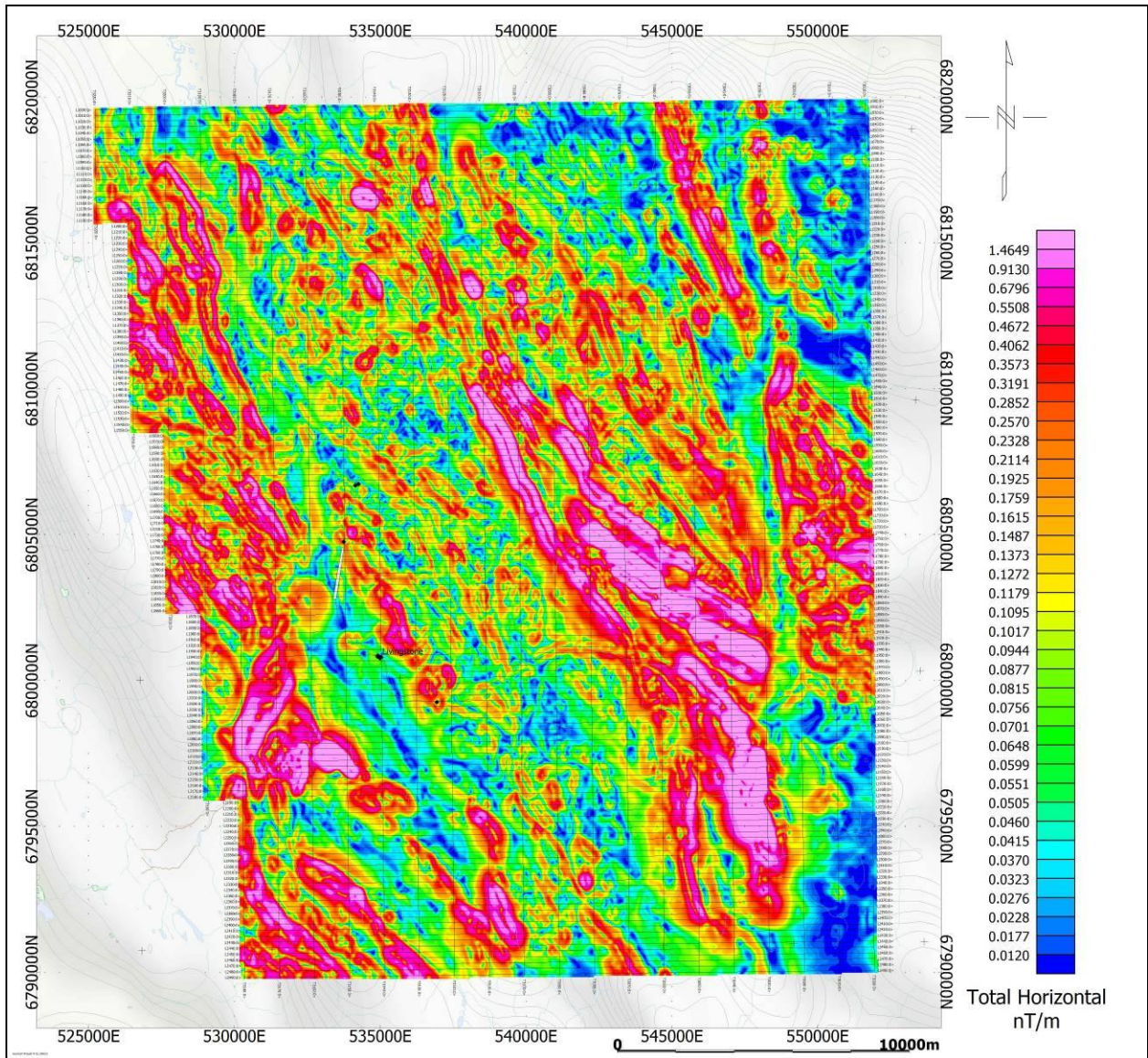
Livingstone Creek em TauZ mid



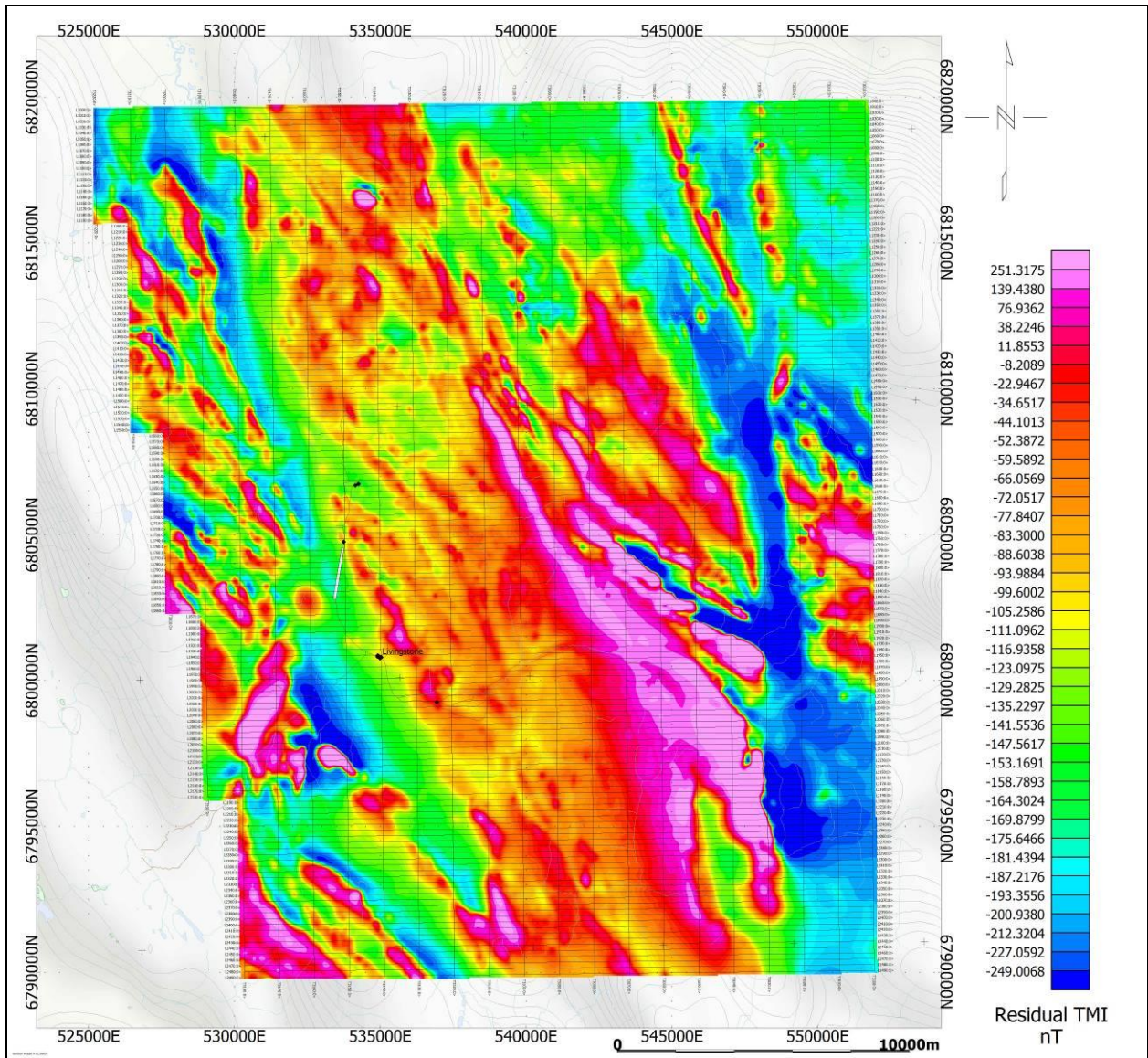
Livingstone Creek em TauZ late



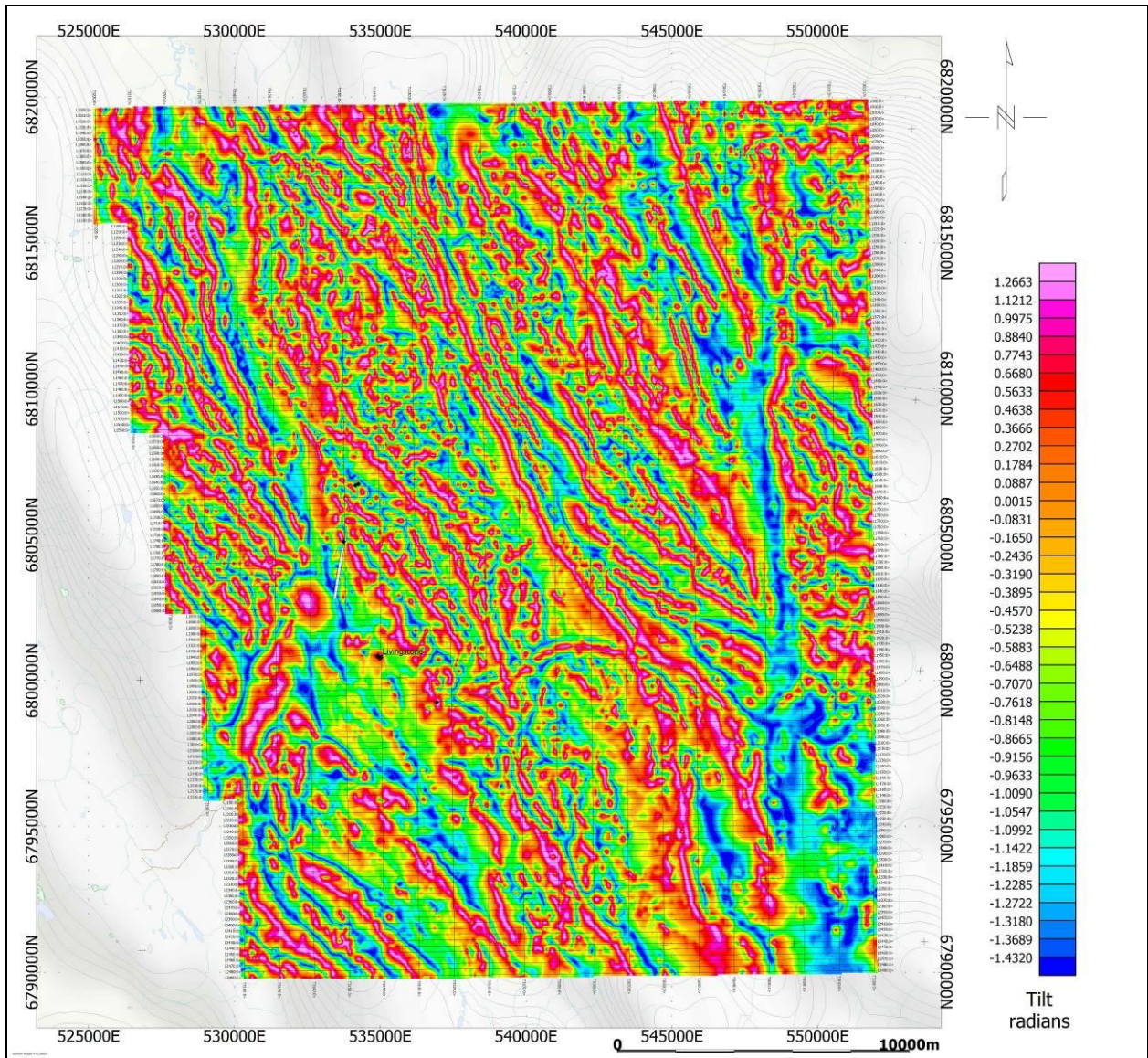
Livingstone Creek Total Magnetic Intensity



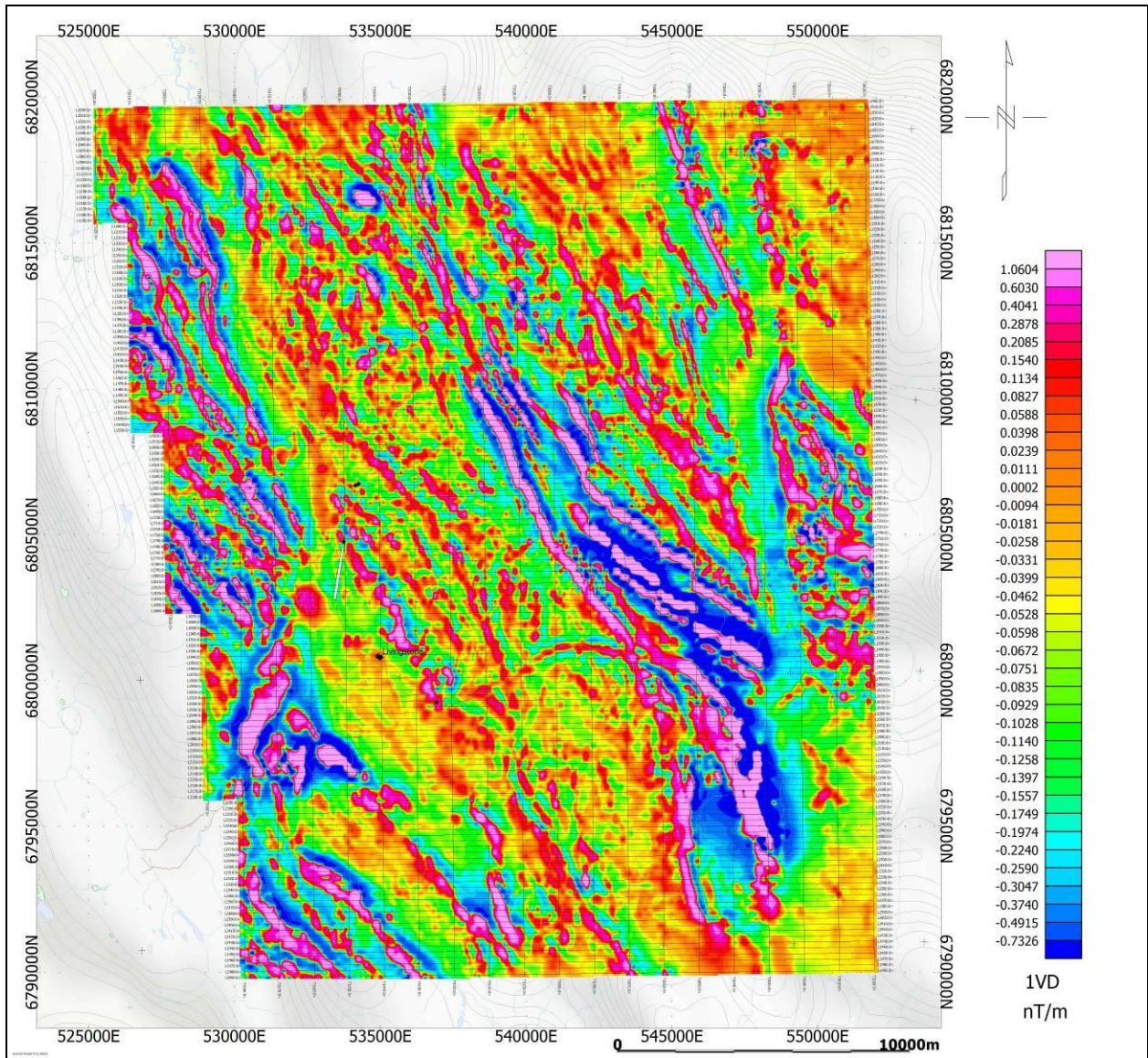
Livingstone Creek Magnetic Total Horizontal Gradient



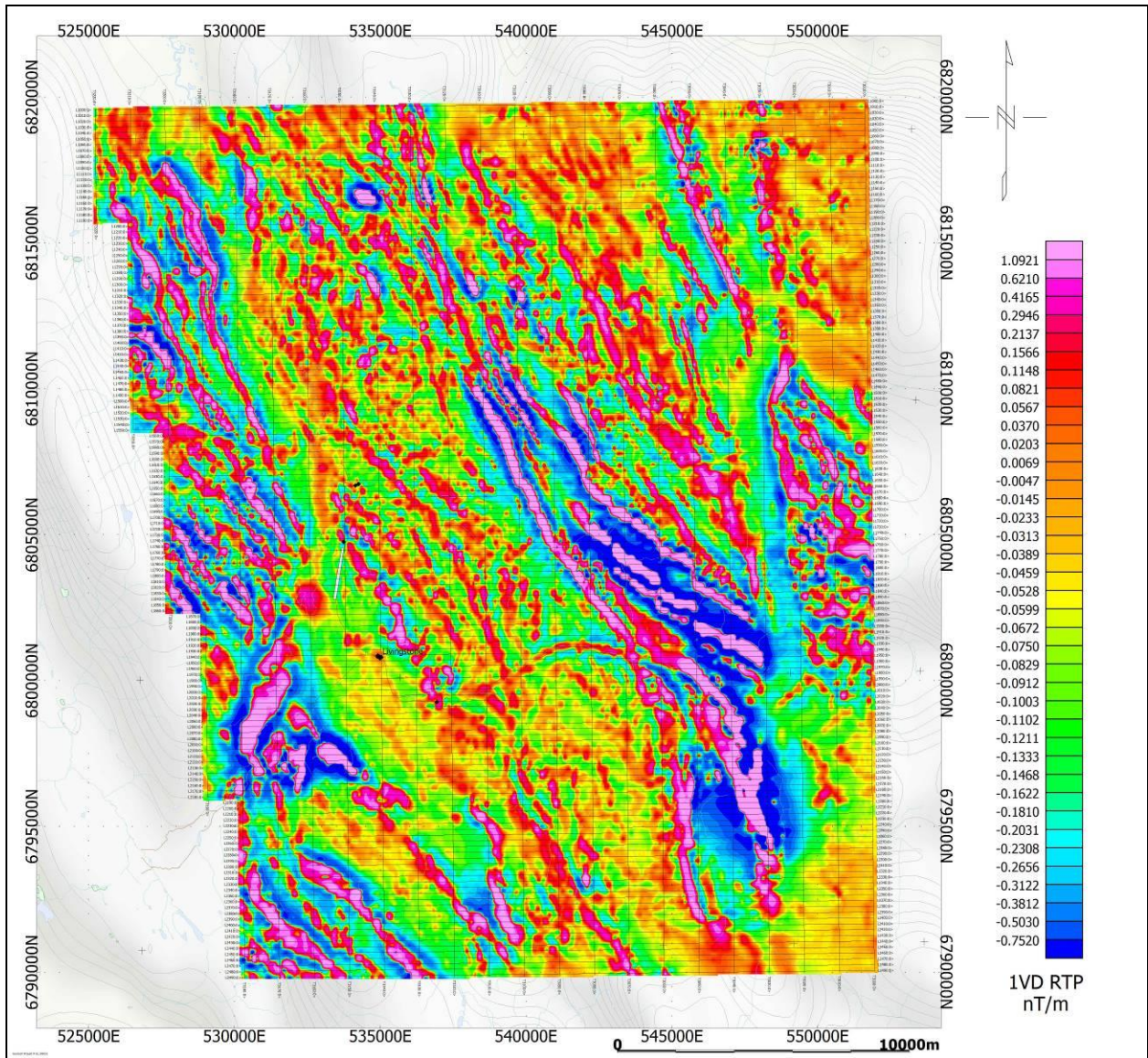
Livingstone Creek Residual Total Magnetic Intensity



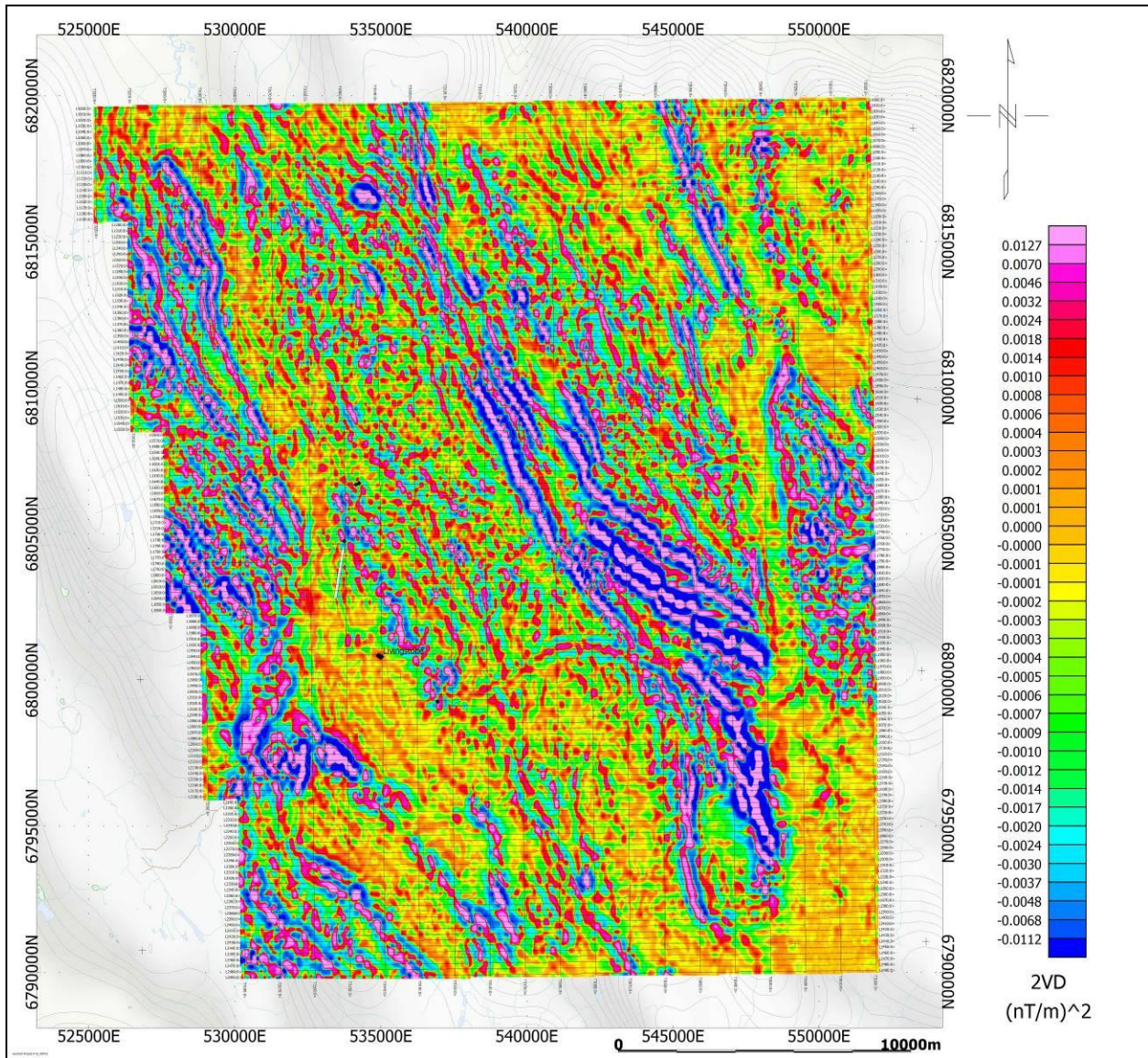
Livingstone Creek Magnetic Tilt Derivative



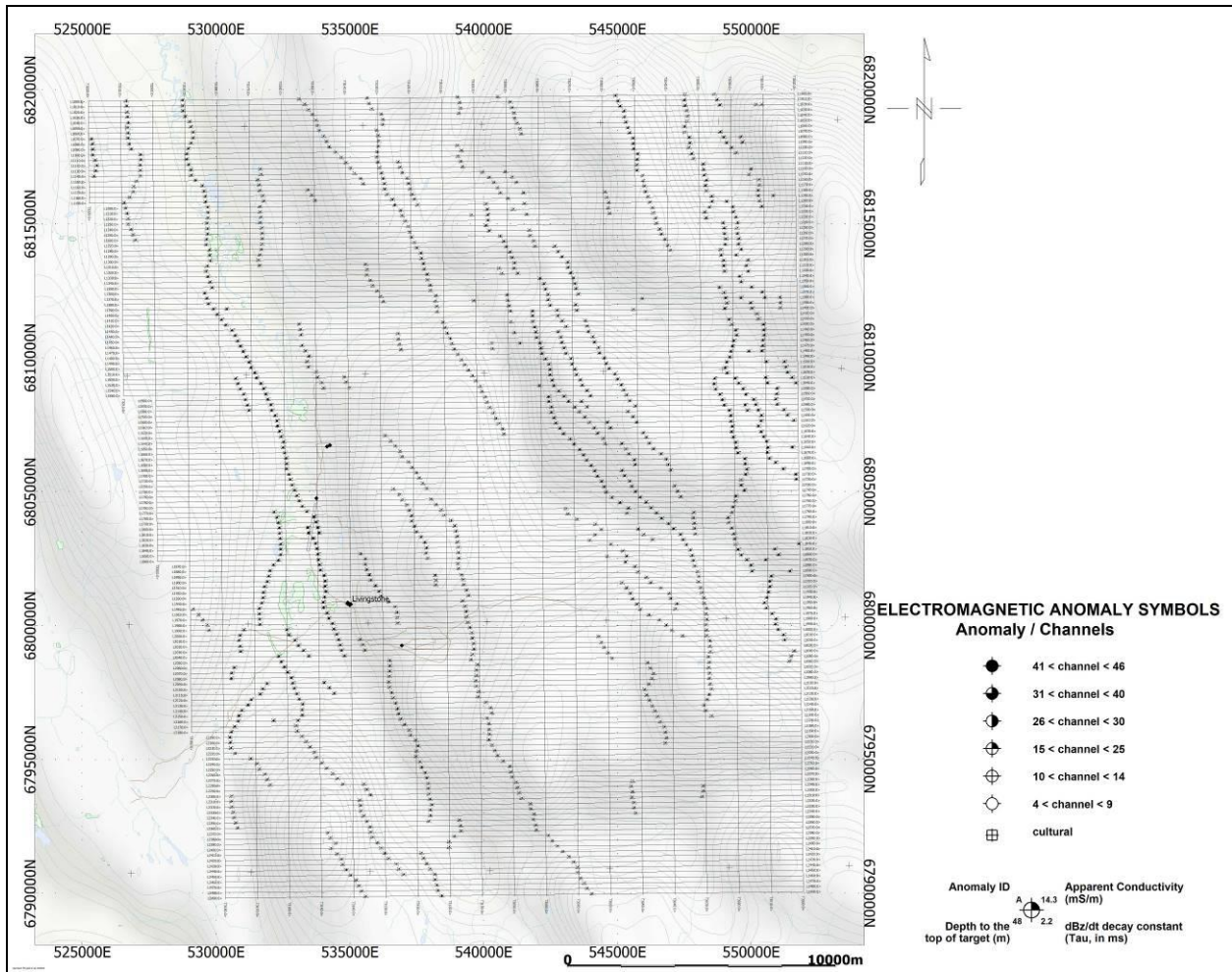
Livingstone Creek Magnetic First Vertical Derivative of TMI



Livingstone Creek Magnetic First Vertical Derivative of RTP

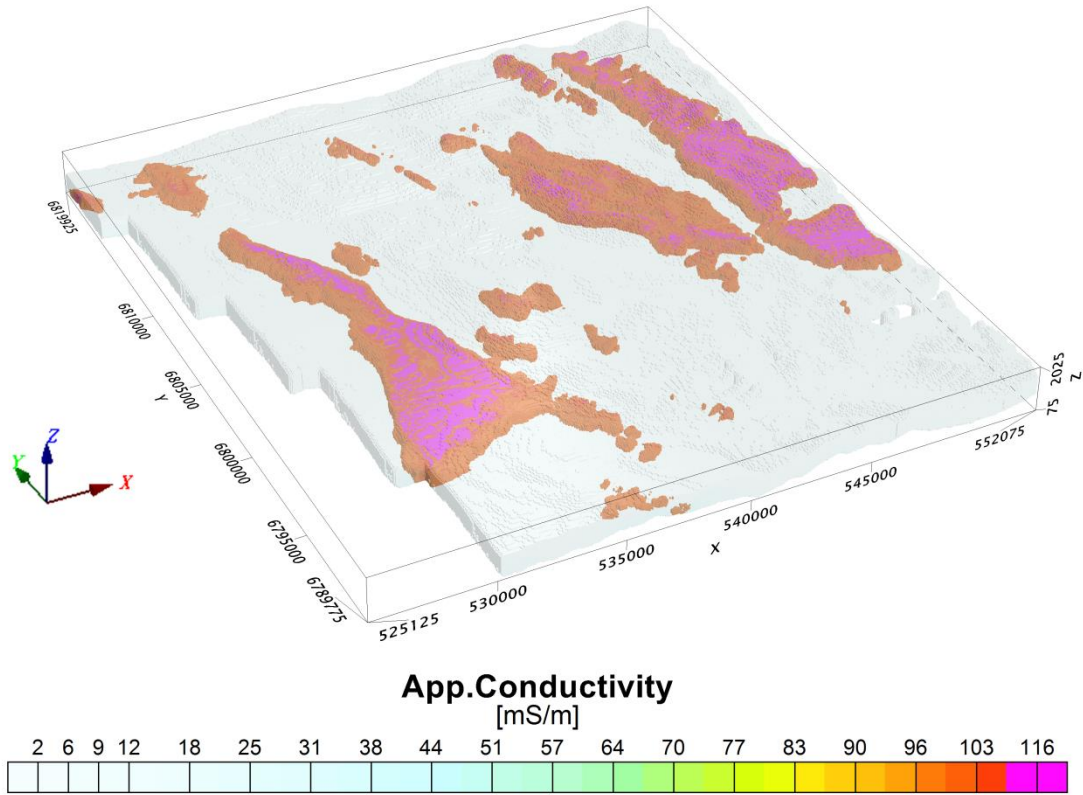


Livingstone Creek Magnetic Second Vertical Derivative of TMI



Livingstone Creek em Anomaly Interpretation

Apparent Conductivity Livingstone Creek



APPENDIX D

GENERALIZED MODELING RESULTS OF THE VTEM SYSTEM INTRODUCTION

The VTEM system is based on a concentric or central loop design, whereby, the receiver is positioned at the centre of a transmitter loop that produces a primary field. The wave form is a bi-polar, modified square wave with a turn-on and turn-off at each end.

During turn-on and turn-off, a time varying field is produced (dB/dt) and an electro-motive force (emf) is created as a finite impulse response. A current ring around the transmitter loop moves outward and downward as time progresses. When conductive rocks and mineralization are encountered, a secondary field is created by mutual induction and measured by the receiver at the centre of the transmitter loop.

Efficient modeling of the results can be carried out on regularly shaped geometries, thus yielding close approximations to the parameters of the measured targets. The following is a description of a series of common models made for the purpose of promoting a general understanding of the measured results.

A set of models has been produced for the Geotech VTEM® system dB/dT Z and X components (see models D1 to D15). The Maxwell™ modeling program (EMIT Technology Pty. Ltd. Midland, WA, AU) used to generate the following responses assumes a resistive half-space. The reader is encouraged to review these models, so as to get a general understanding of the responses as they apply to survey results. While these models do not begin to cover all possibilities, they give a general perspective on the simple and most commonly encountered anomalies.

As the plate dips and departs from the vertical position, the peaks become asymmetrical.

As the dip increases, the aspect ratio (Min/Max) decreases and this aspect ratio can be used as an empirical guide to dip angles from near 90° to about 30°. The method is not sensitive enough where dips are less than about 30°.

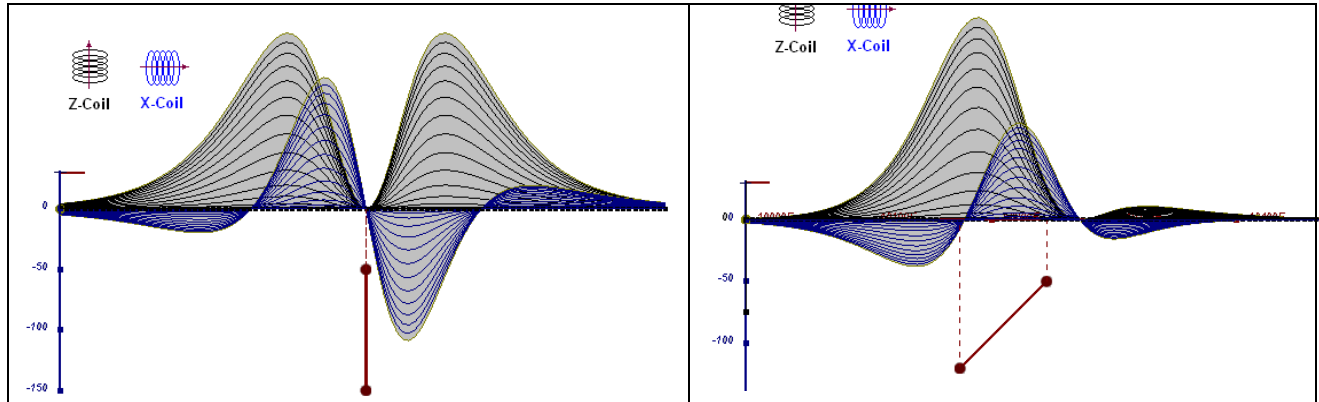


Figure D-1: vertical thin plate

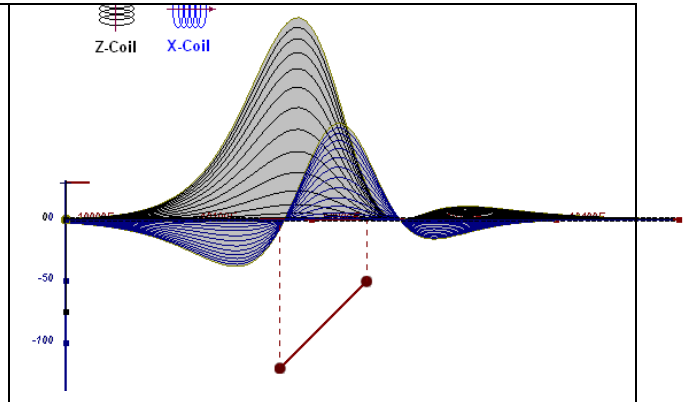


Figure D-2: inclined thin plate

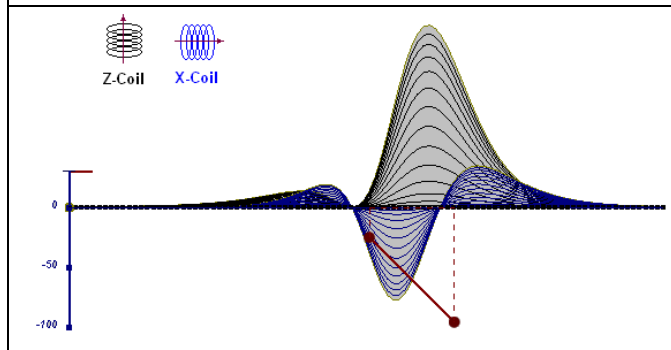


Figure D-3: inclined thin plate

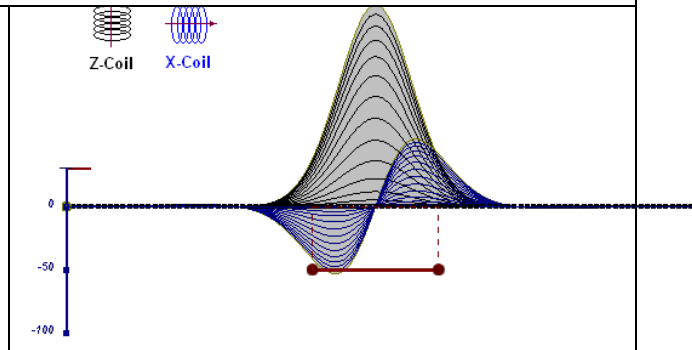


Figure D-4: horizontal thin plate

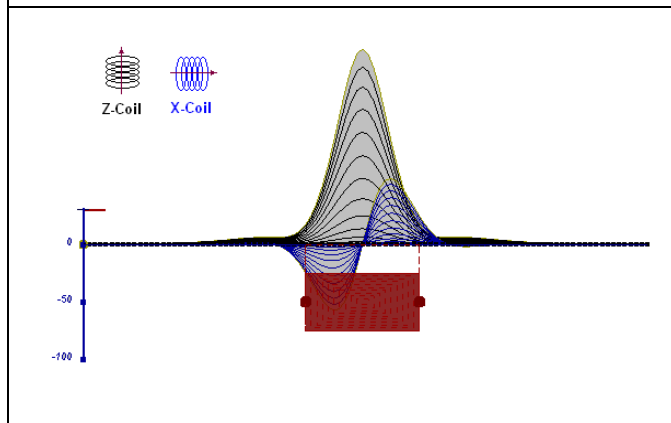


Figure D-5: horizontal thick plate (linear scale of the response)

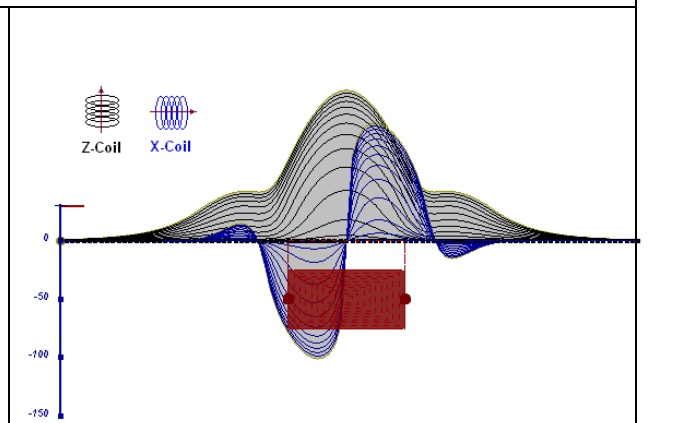


Figure D-6: horizontal thick plate (log scale of the response)

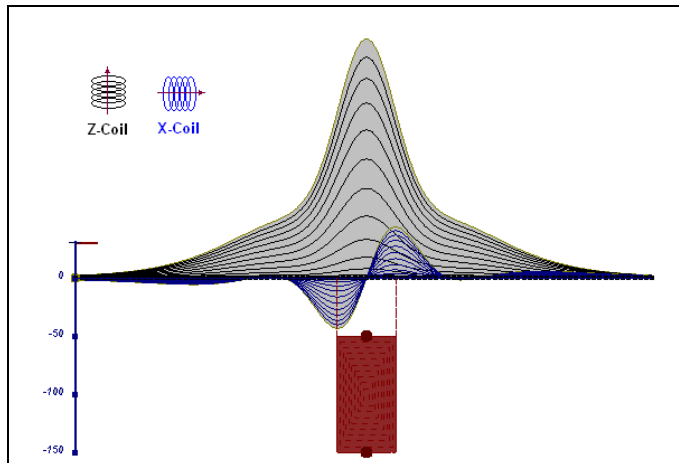


Figure D-7: vertical thick plate (linear scale of the response). 50 m depth

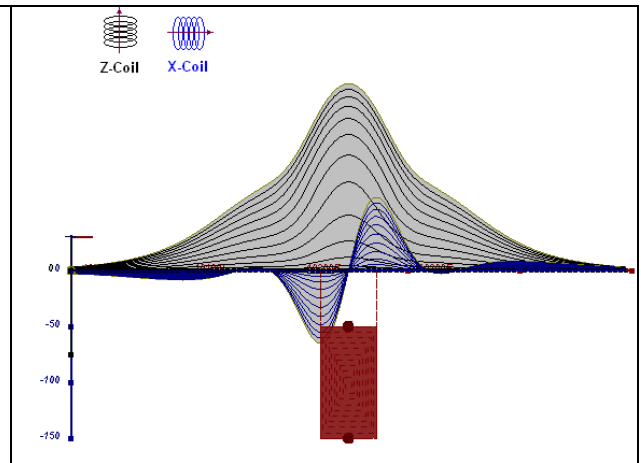


Figure D-8: vertical thick plate (log scale of the response). 50 m depth

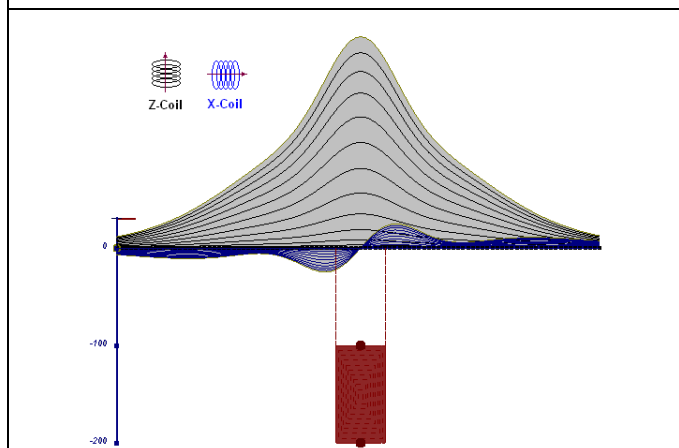


Figure D-9: vertical thick plate (linear scale of the response). 100 m depth

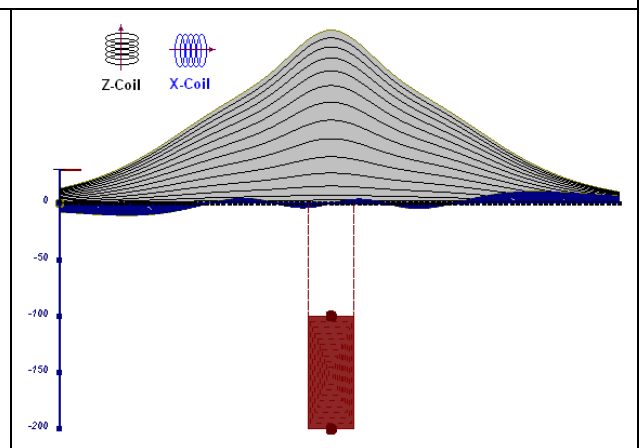


Figure D-10: vertical thick plate (linear scale of the response). Depth / horizontal thickness=2.5

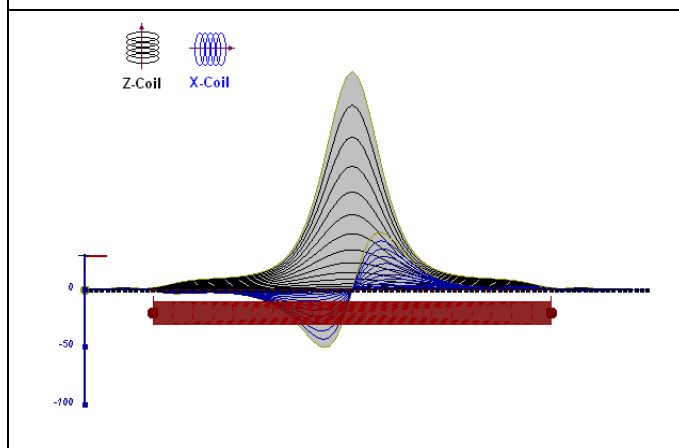


Figure D-11: horizontal thick plate (linear scale of the response)

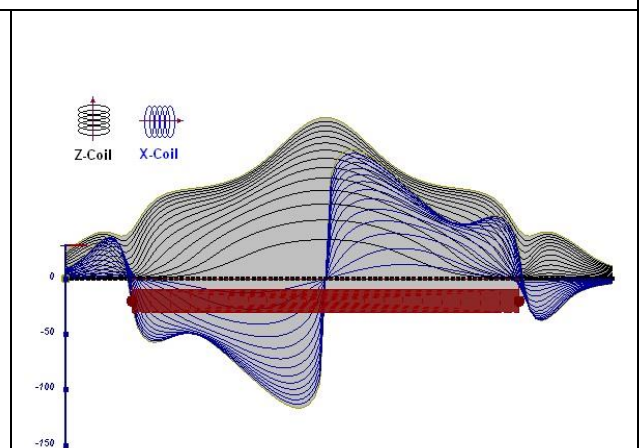


Figure D-12: horizontal thick plate (log scale of the response)

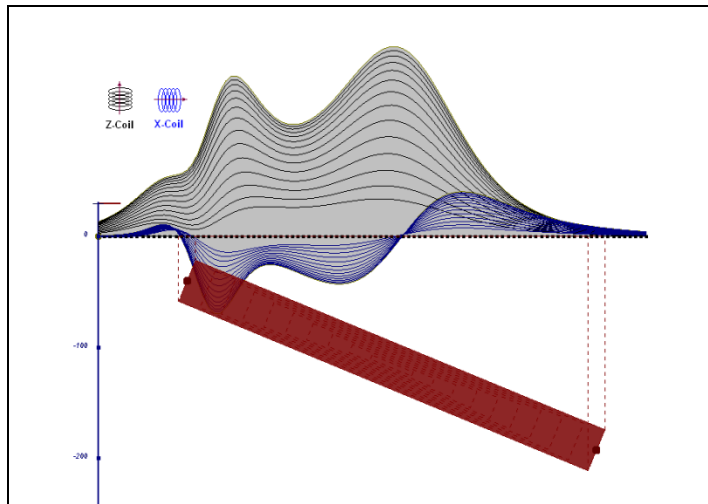


Figure D-13: inclined long thick plate

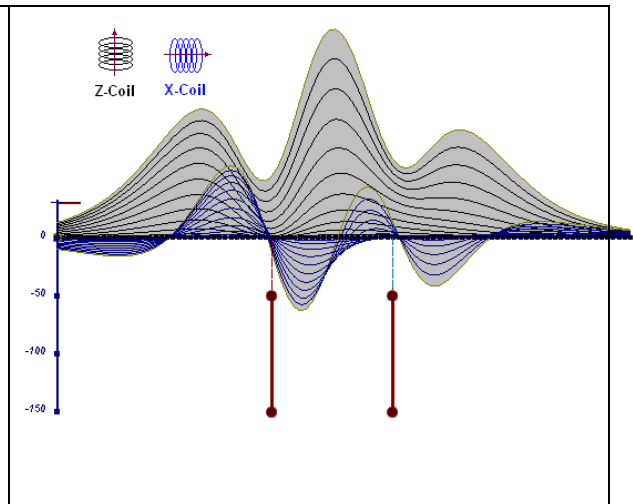


Figure D-14: two vertical thin plates

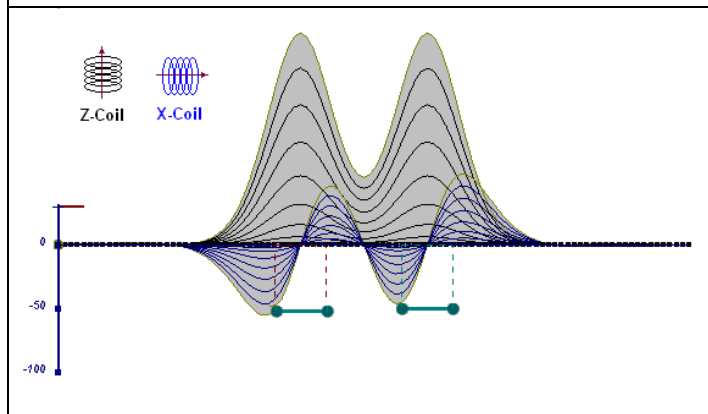


Figure D-15: two horizontal thin plates

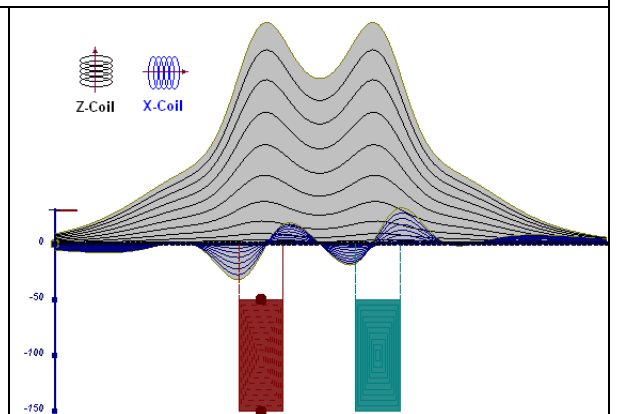


Figure D-16: two vertical thick plates

The same type of target but with different thickness, for example, creates different form of the response:

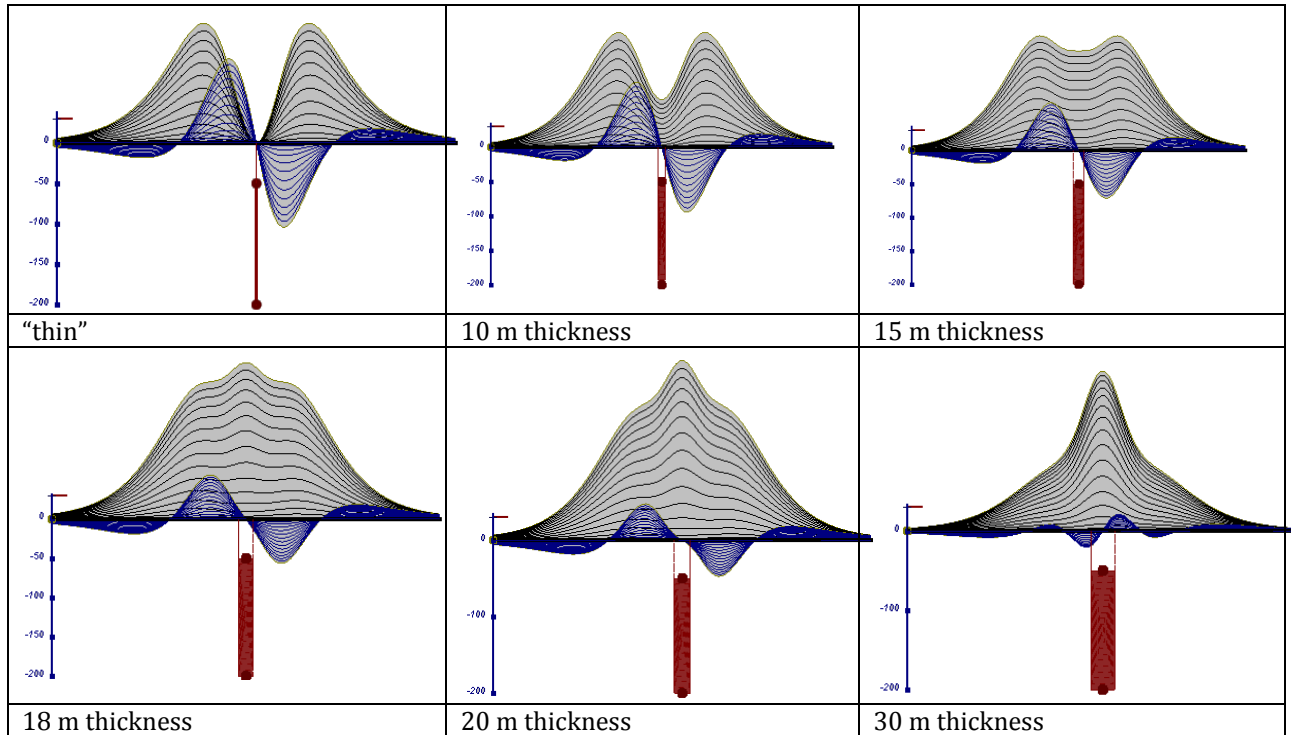


Figure D-17: Conductive vertical plate, depth 50 m, strike length 200 m, depth extends 150 m.

Alexander Prikhodko, PhD, P.Ge
Geotech Ltd.

September 2010

APPENDIX E

EM TIME CONSTANT (TAU) ANALYSIS

Estimation of time constant parameter⁷ in transient electromagnetic method is one of the steps toward the extraction of the information about conductances beneath the surface from TEM measurements.

The most reliable method to discriminate or rank conductors from overburden, background or one and other is by calculating the EM field decay time constant (TAU parameter), which directly depends on conductance despite their depth and accordingly amplitude of the response.

THEORY

As established in electromagnetic theory, the magnitude of the electro-motive force (emf) induced is proportional to the time rate of change of primary magnetic field at the conductor. This emf causes eddy currents to flow in the conductor with a characteristic transient decay, whose Time Constant (Tau) is a function of the conductance of the survey target or conductivity and geometry (including dimensions) of the target. The decaying currents generate a proportional secondary magnetic field, the time rate of change of which is measured by the receiver coil as induced voltage during the Off time.

The receiver coil output voltage (e_0) is proportional to the time rate of change of the secondary magnetic field and has the form,

$$e_0 \propto (1 / \tau) e^{-(t / \tau)}$$

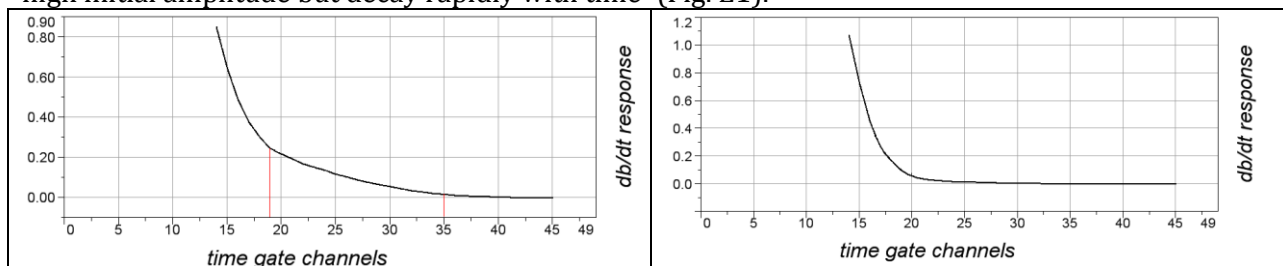
Where,

$\tau = L/R$ is the characteristic time constant of the target (TAU)

R = resistance

L = inductance

From the expression, conductive targets that have small value of resistance and hence large value of τ yield signals with small initial amplitude that decays relatively slowly with progress of time. Conversely, signals from poorly conducting targets that have large resistance value and small τ , have high initial amplitude but decay rapidly with time¹ (Fig. E1).



⁷ McNeill, JD, 1980, "Applications of Transient Electromagnetic Techniques", Technical Note TN-7 page 5, Geonics Limited, Mississauga, Ontario.

Figure E-1: Left – presence of good conductor, right – poor conductor.
EM Time Constant (Tau) Calculation

The EM Time-Constant (TAU) is a general measure of the speed of decay of the electromagnetic response and indicates the presence of eddy currents in conductive sources as well as reflecting the “conductance quality” of a source. Although TAU can be calculated using either the measured dB/dt decay or the calculated B-field decay, dB/dt is commonly preferred due to better stability (S/N) relating to signal noise. Generally, TAU calculated on base of early time response reflects both near surface overburden and poor conductors whereas, in the late ranges of time, deep and more conductive sources, respectively. For example early time TAU distribution in an area that indicates conductive overburden is shown in Figure 2.

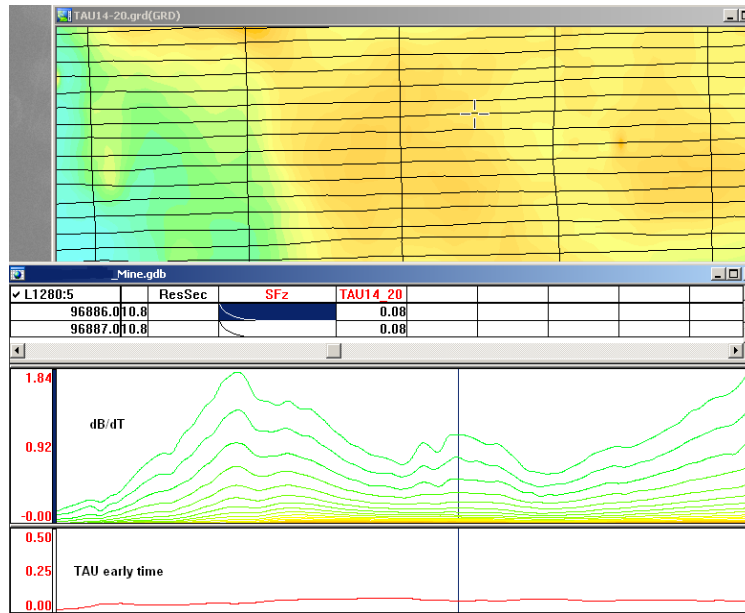


Figure E-2: Map of early time TAU. Area with overburden conductive layer and local sources.

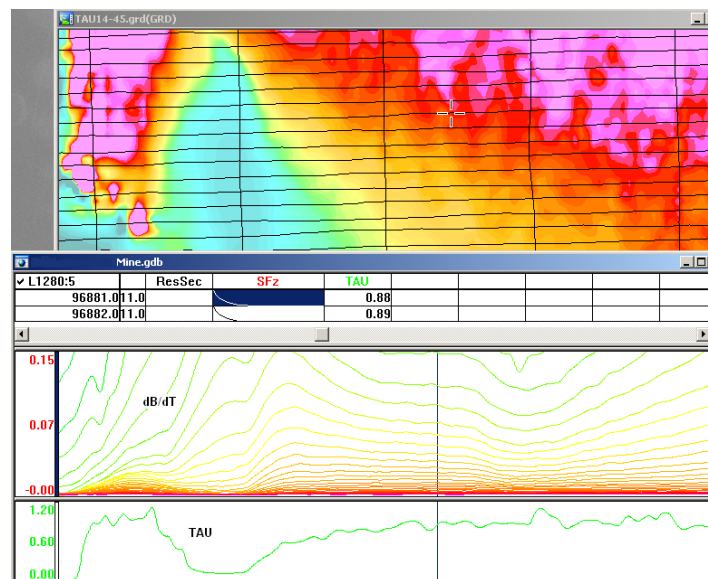


Figure E-3: Map of full time range TAU with EM anomaly due to deep highly conductive target.

There are many advantages of TAU maps:

- TAU depends only on one parameter (conductance) in contrast to response magnitude;
- TAU is integral parameter, which covers time range and all conductive zones and targets are displayed independently of their depth and conductivity on a single map.
- Very good differential resolution in complex conductive places with many sources with different conductivity.
- Signs of the presence of good conductive targets are amplified and emphasized independently of their depth and level of response accordingly.

In the example shown in Figure 4 and 5, three local targets are defined, each of them with a different depth of burial, as indicated on the resistivity depth image (RDI). All are very good conductors but the deeper target (number 2) has a relatively weak dB/dt signal yet also features the strongest total TAU (Figure 4). This example highlights the benefit of TAU analysis in terms of an additional target discrimination tool.

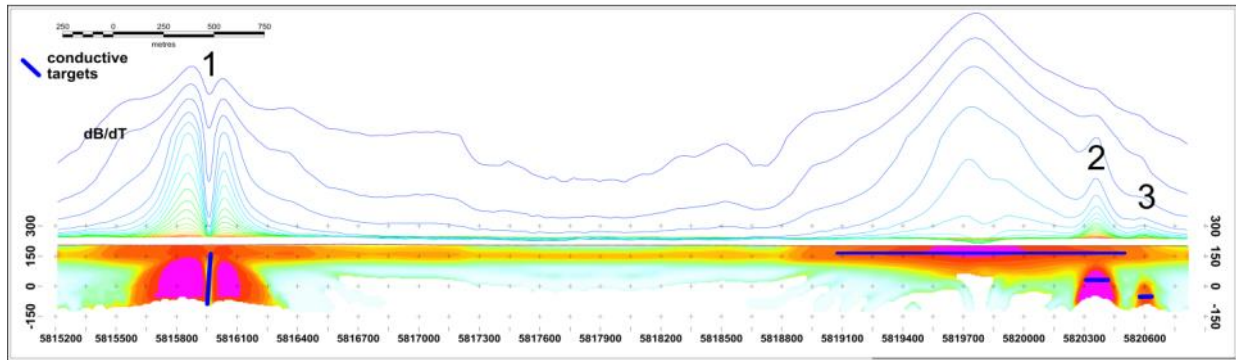


Figure E-4: dB/dt profile and RDI with different depths of targets.

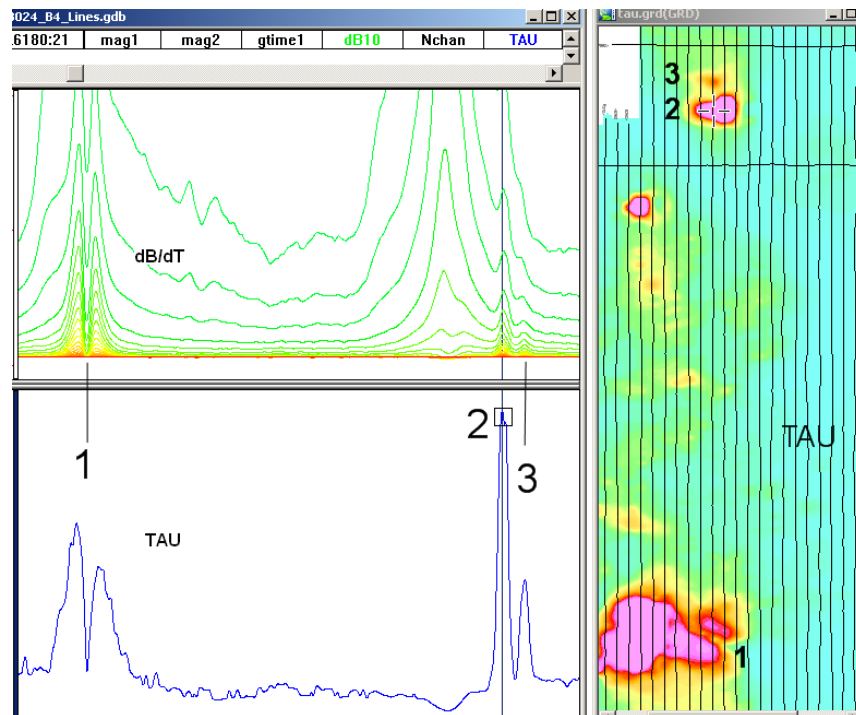


Figure E-5: Map of total TAU and dB/dt profile.

The EM Time Constants for dB/dt and B-field were calculated using the “sliding Tau” in-house program developed at Geotech⁸. The principle of the calculation is based on using of time window (4 time channels) which is sliding along the curve decay and looking for latest time channels which have a response above the level of noise and decay. The EM decays are obtained from all available decay channels, starting at the latest channel. Time constants are taken from a least square fit of a straight-line (log/linear space) over the last 4 gates above a pre-set signal threshold level (Figure F6). Threshold settings are pointed in the “label” property of TAU database channels. The sliding Tau method determines that, as the amplitudes increase, the time-constant is taken at progressively later times in the EM decay. Conversely, as the amplitudes decrease, Tau is taken at progressively earlier times in the decay. If the maximum signal amplitude falls below the threshold, or becomes negative for any of the 4 time gates, then Tau is not calculated and is assigned a value of “dummy” by default.

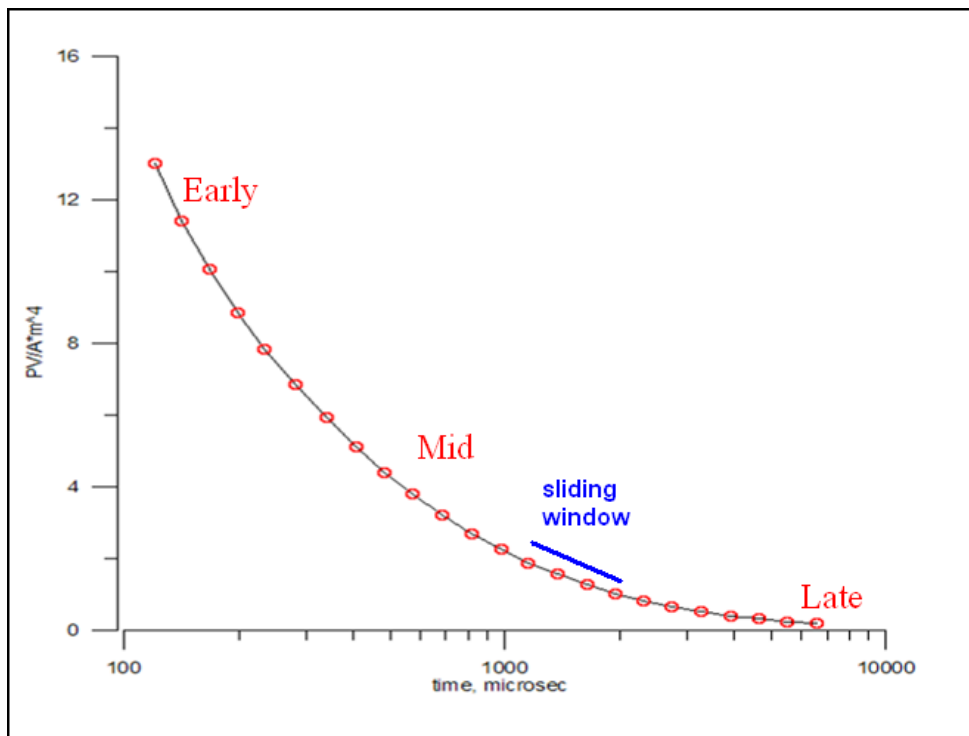


Figure E-6: Typical dB/dt decays of Vtem data

Alexander Prikhodko, PhD, P.Geo
Geotech Ltd.

September 2010

⁸ by A.Prikhodko

APPENDIX F

TEM RESISTIVITY DEPTH IMAGING (RDI)

Resistivity depth imaging (RDI) is technique used to rapidly convert EM profile decay data into an equivalent resistivity versus depth cross-section, by deconvolving the measured TEM data.

The used RDI algorithm of Resistivity-Depth transformation is based on scheme of the apparent resistivity transform of Maxwell A.Meju (1998)⁹ and TEM response from conductive half-space. The program is developed by Alexander Prikhodko and depth calibrated based on forward plate modeling for VTEM system configuration (Fig. 1-10).

RDI provide reasonable indications of conductor relative depth and vertical extent, as well as accurate 1D layered-earth apparent conductivity/resistivity structure across VTEM flight lines. Approximate depth of investigation of a TEM system, image of secondary field distribution in half space, effective resistivity, initial geometry and position of conductive targets is the information obtained on base of the RDI.

Maxwell forward modeling with RDI sections from the synthetic responses (VTEM system).

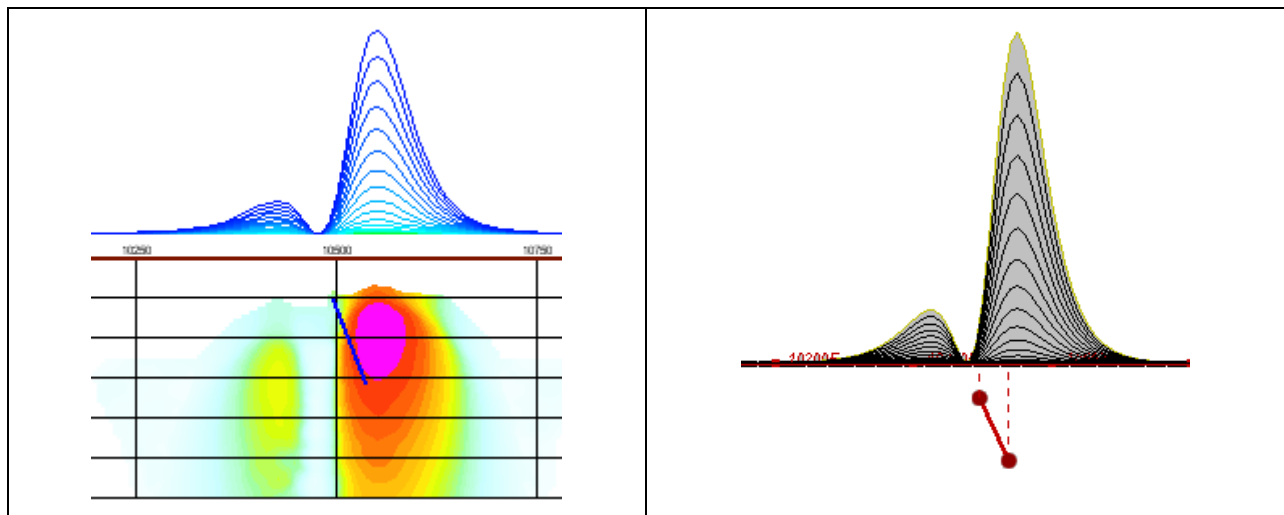


Figure F-1: Maxwell plate model and RDI from the calculated response for conductive “thin” plate (depth 50 m, dip 65 degree, depth extend 100 m).

⁹ Maxwell A.Meju, 1998, Short Note: A simple method of transient electromagnetic data analysis, *Geophysics*, **63**, 405–410.

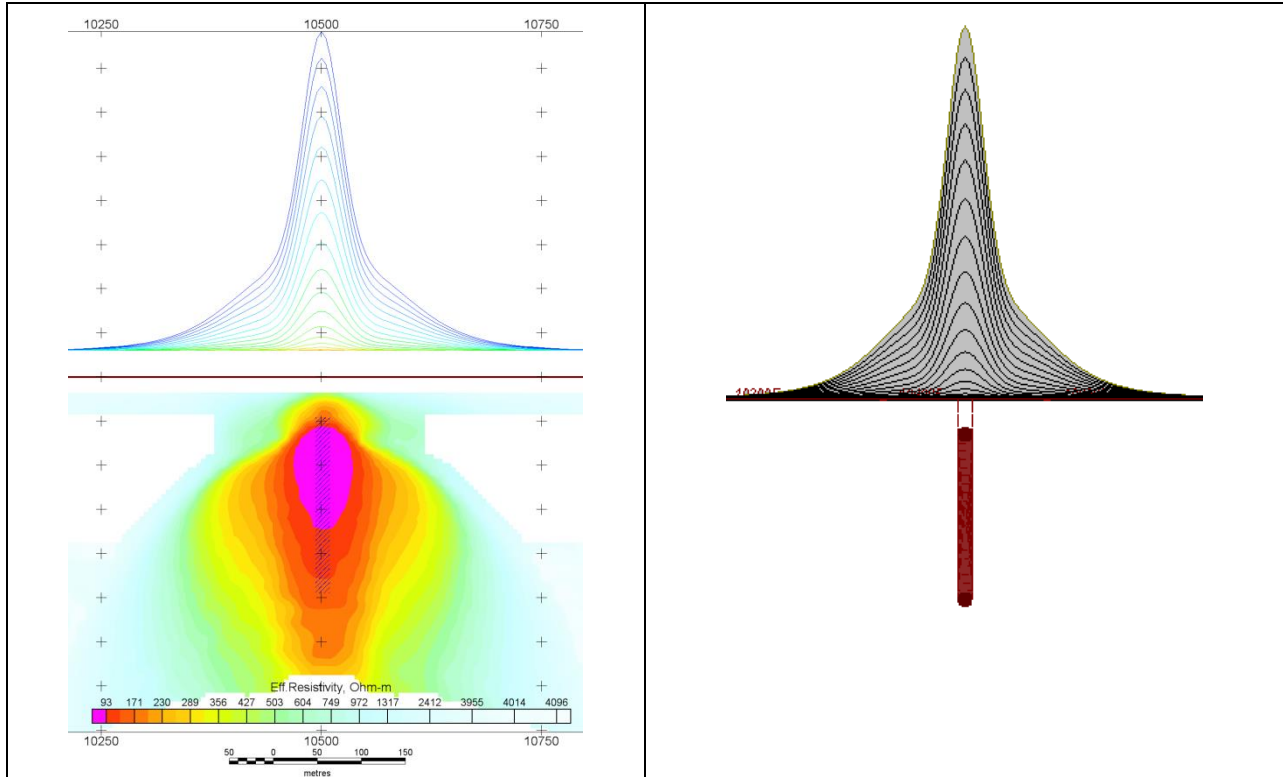


Figure F-2: Maxwell plate model and RDI from the calculated response for "thick" plate 18 m thickness, depth 50 m, depth extend 200 m).

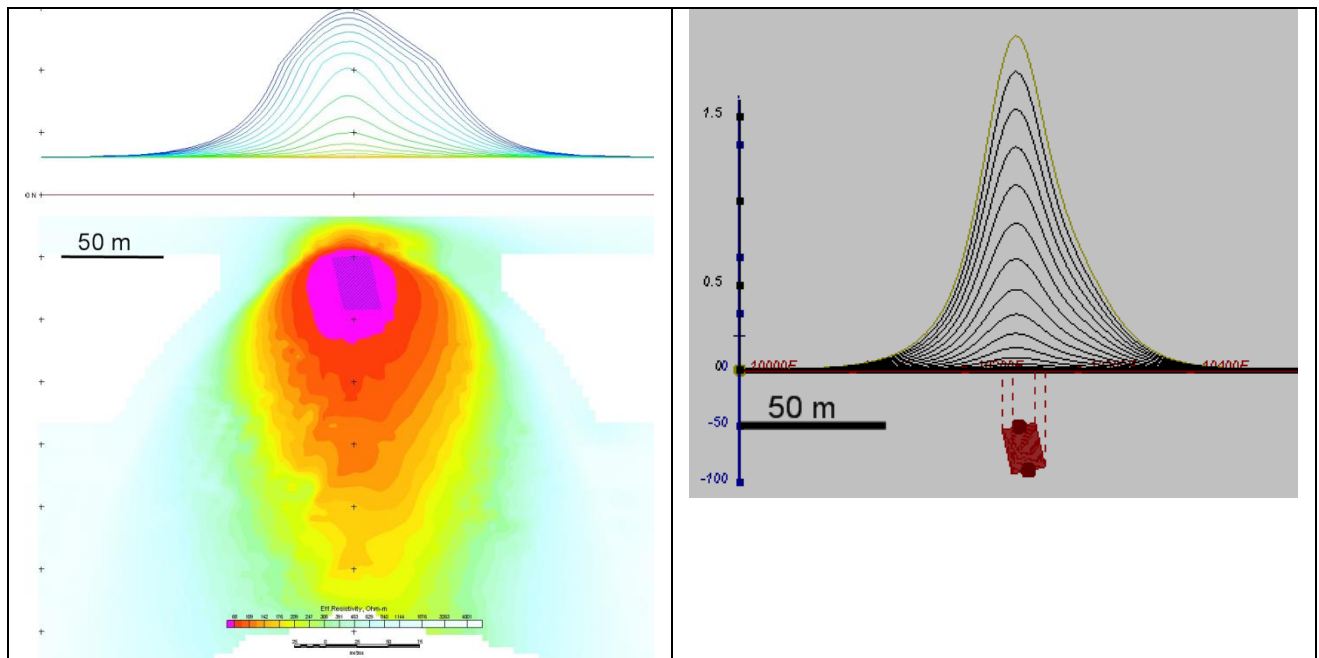


Figure F-3: Maxwell plate model and RDI from the calculated response for bulk ("thick") 100 m length, 40 m depth extend, 30 m thickness

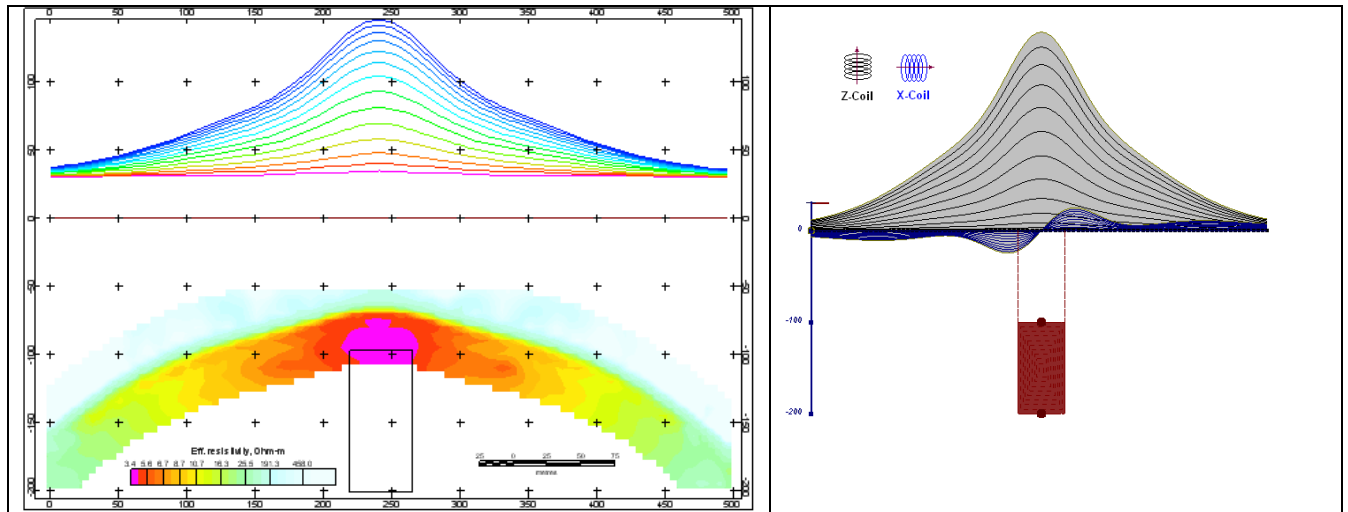


Figure F-4: Maxwell plate model and RDI from the calculated response for "thick" vertical target (depth 100 m, depth extend 100 m). 19-44 chan.

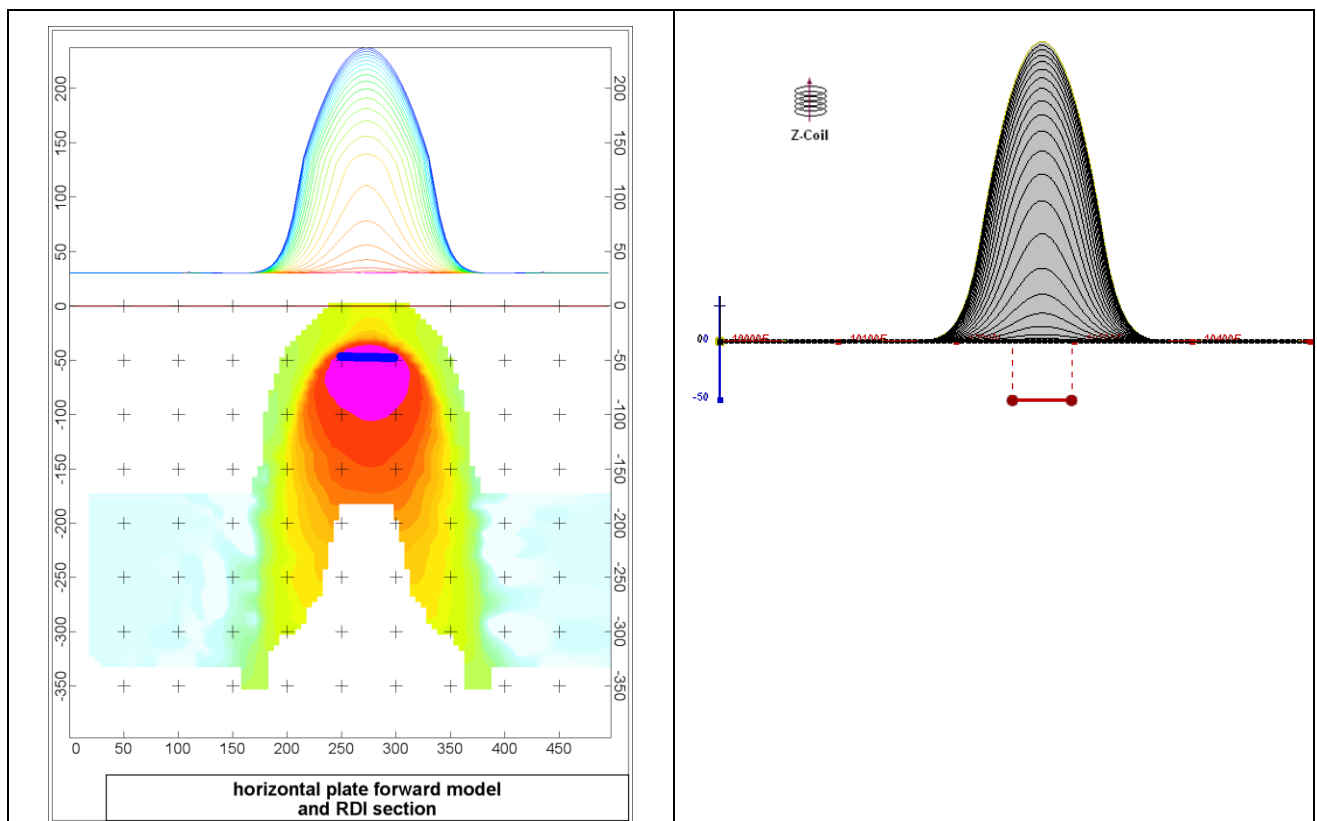


Figure F-5: Maxwell plate model and RDI from the calculated response for horizontal thin plate (depth 50 m, dim 50x100 m). 15-44 chan.

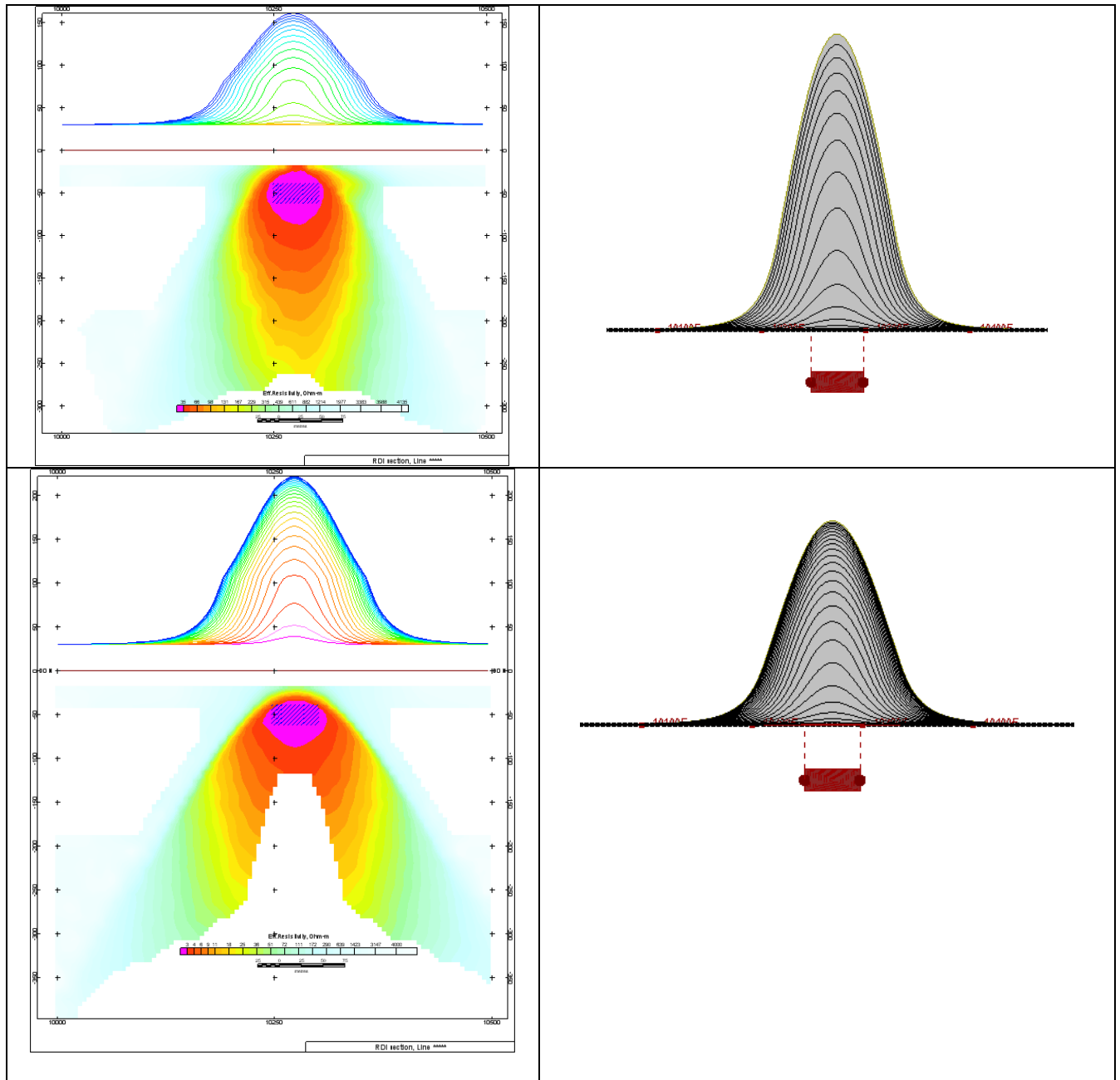


Figure F-6: Maxwell plate model and RDI from the calculated response for horizontal thick (20m) plate – less conductive (on the top), more conductive (below).

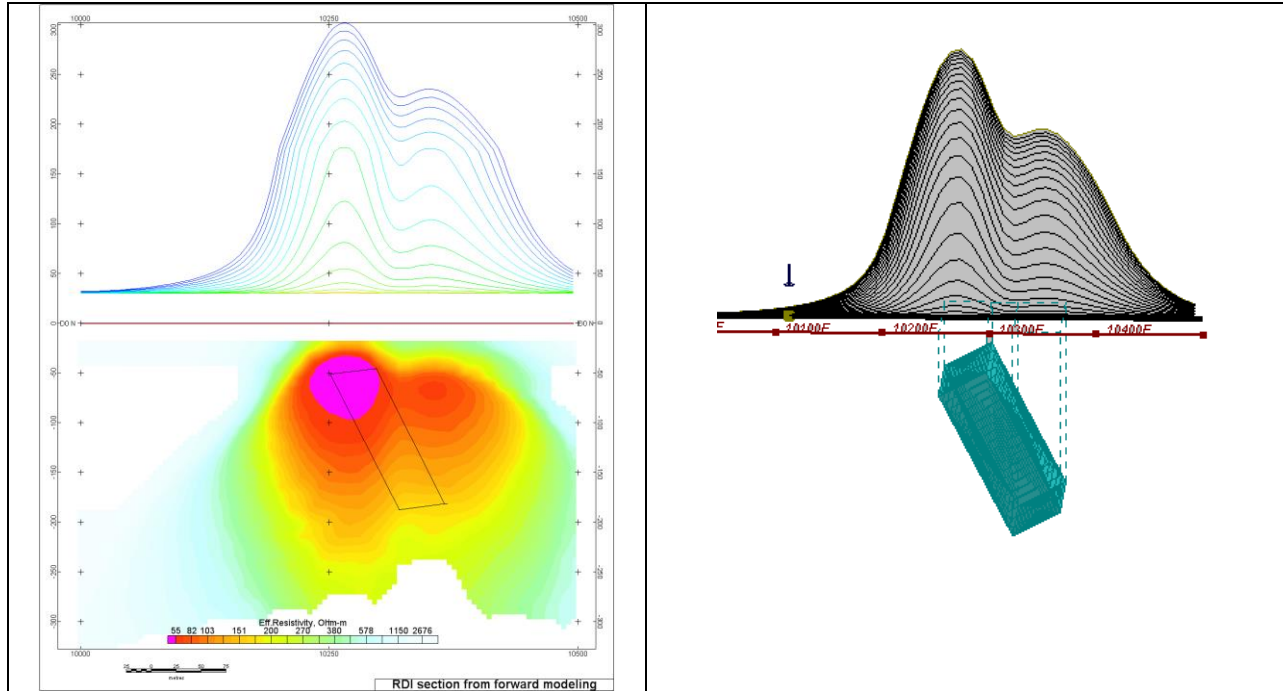


Figure F-7: Maxwell plate model and RDI from the calculated response for inclined thick (50m) plate. Depth extends 150 m, depth to the target 50 m.

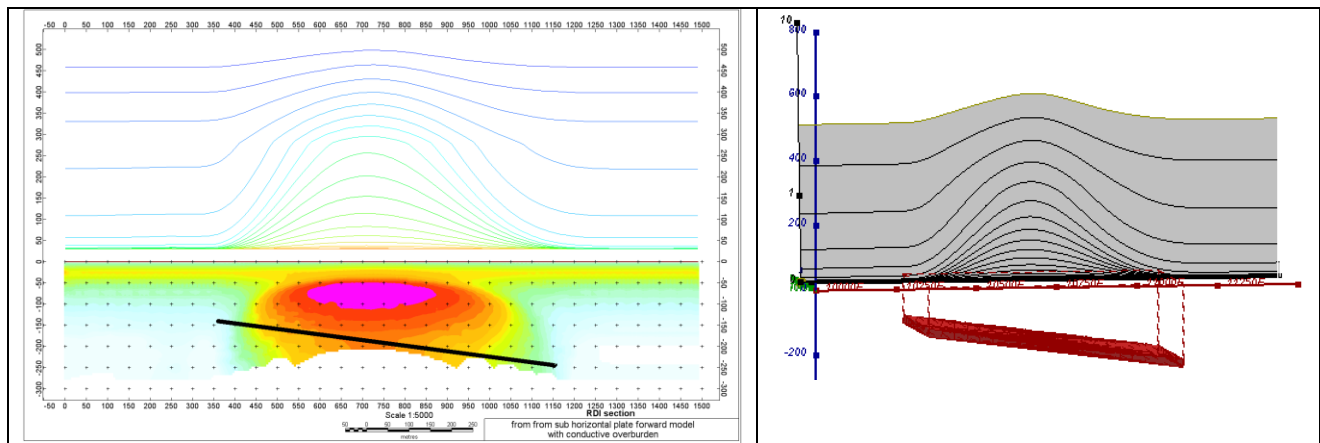


Figure F-8: Maxwell plate model and RDI from the calculated response for the long, wide and deep subhorizontal plate (depth 140 m, dim 25x500x800 m) with conductive overburden.

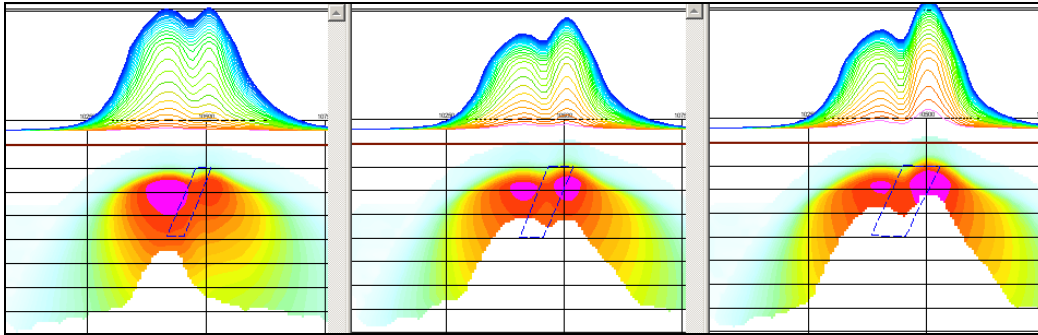


Figure F-9: Maxwell plate models and RDIs from the calculated response for "thick" dipping plates (35, 50, 75 m thickness), depth 50 m, conductivity 2.5 S/m.

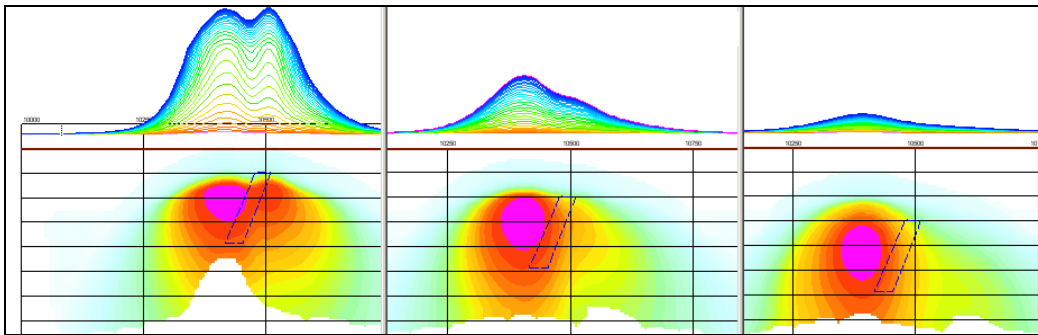


Figure F-10: Maxwell plate models and RDIs from the calculated response for "thick" (35 m thickness) dipping plate on different depth (50, 100, 150 m), conductivity 2.5 S/m.

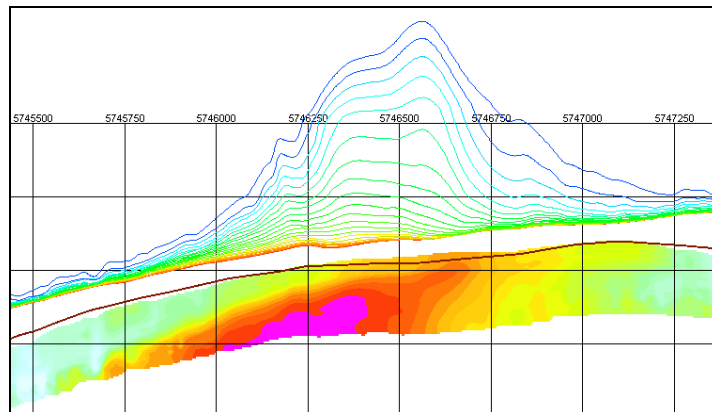
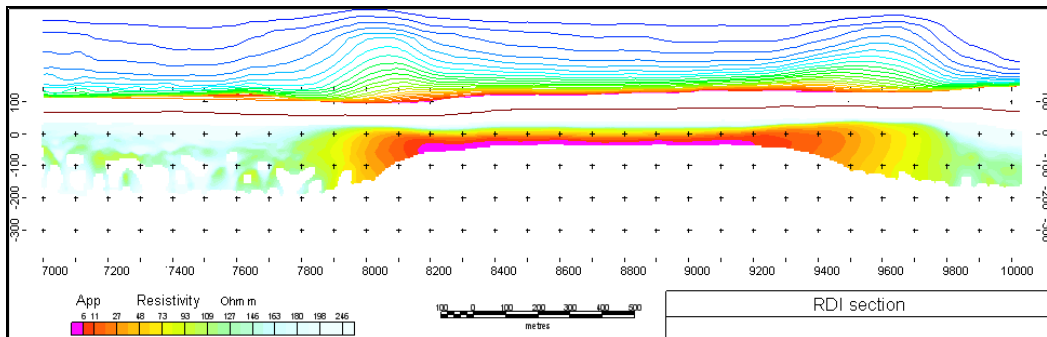
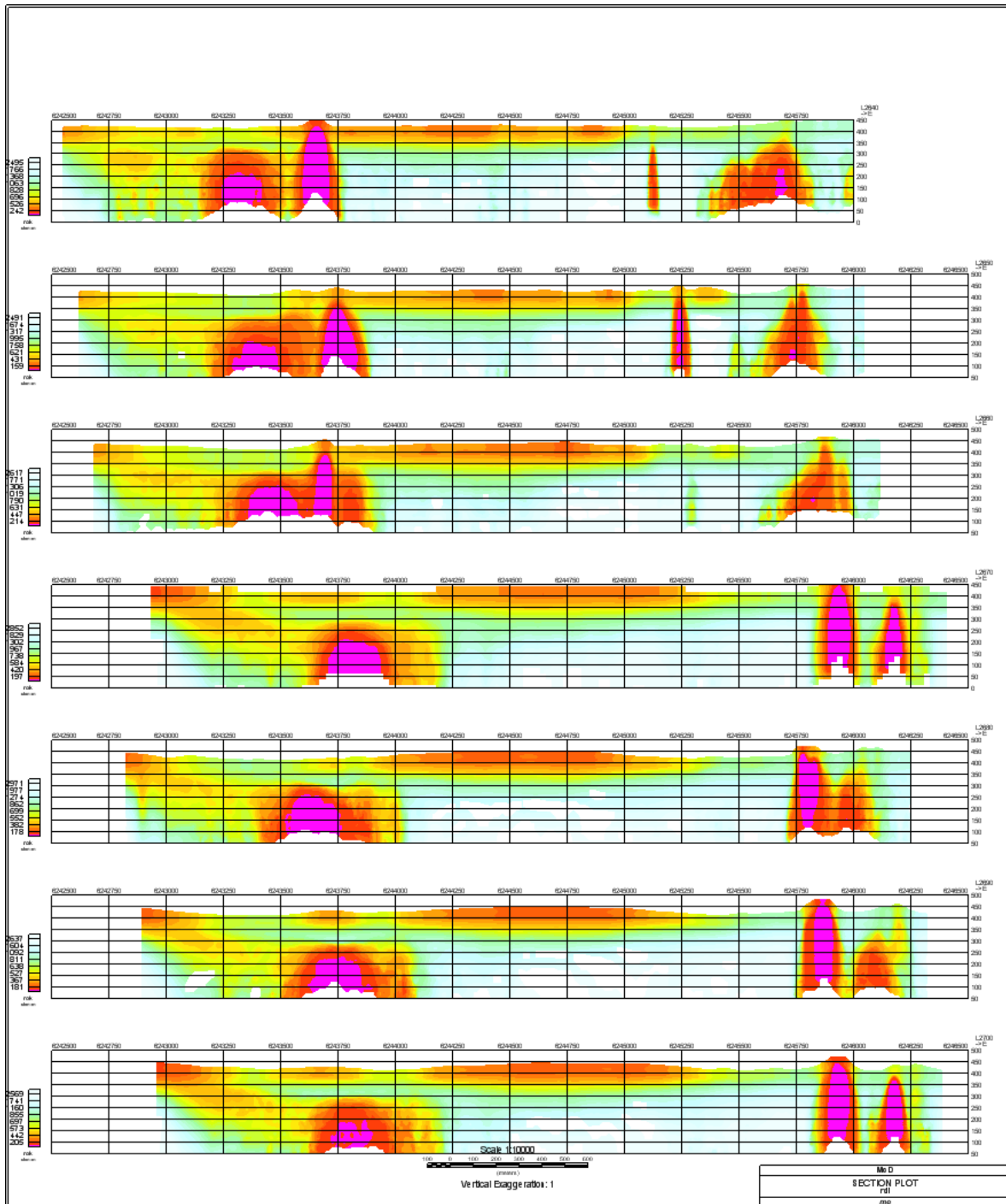


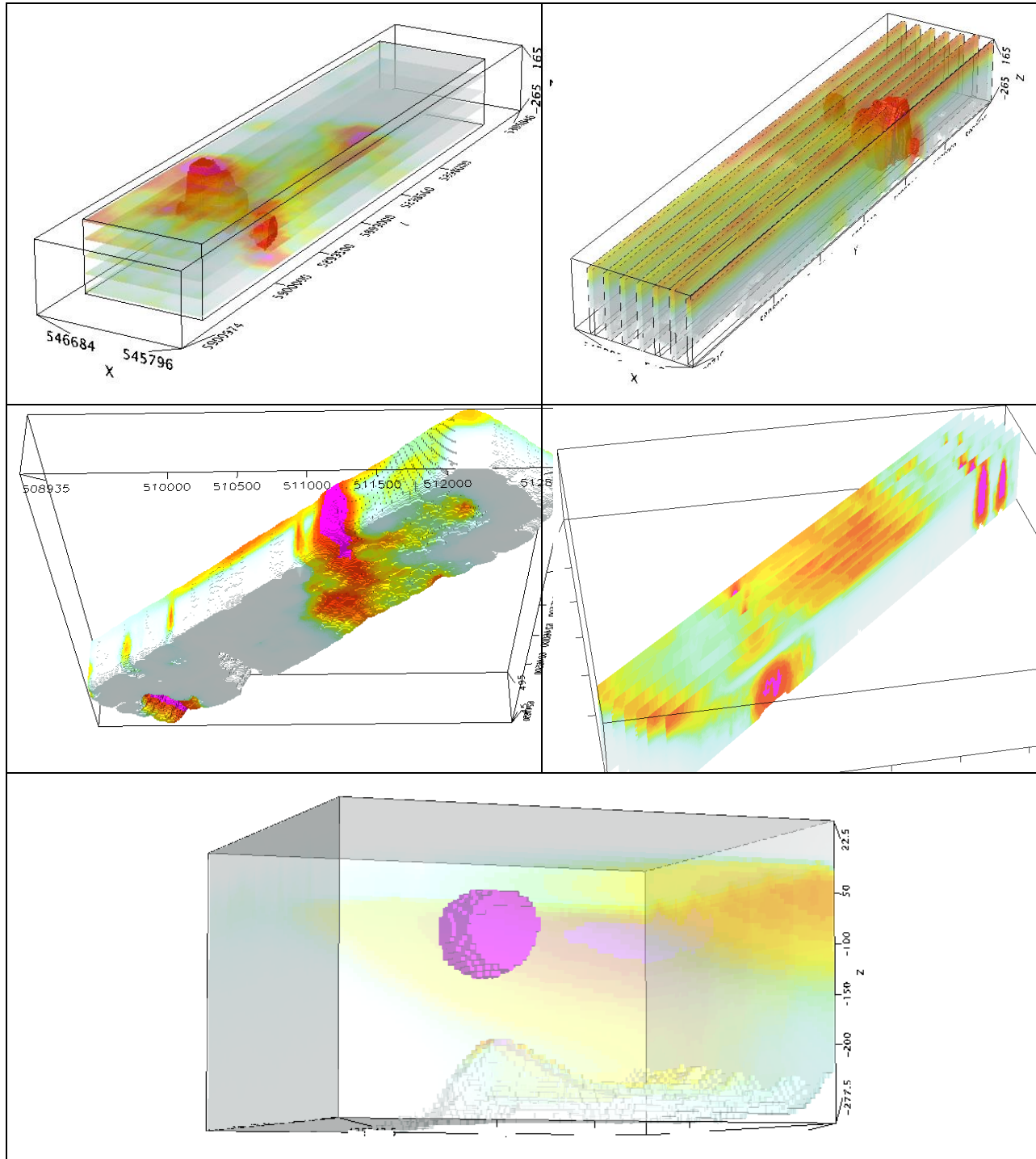
Figure F-11: RDI section for the real horizontal and slightly dipping conductive layers

FORMS OF RDI PRESENTATION

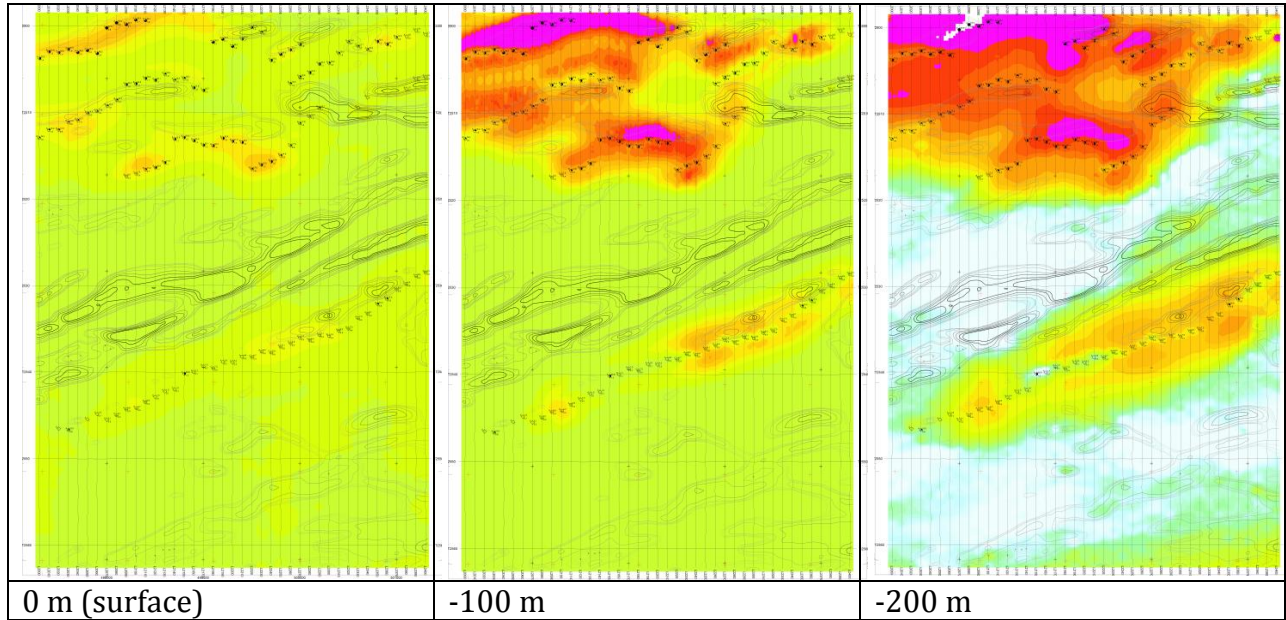
PRESENTATION OF SERIES OF LINES



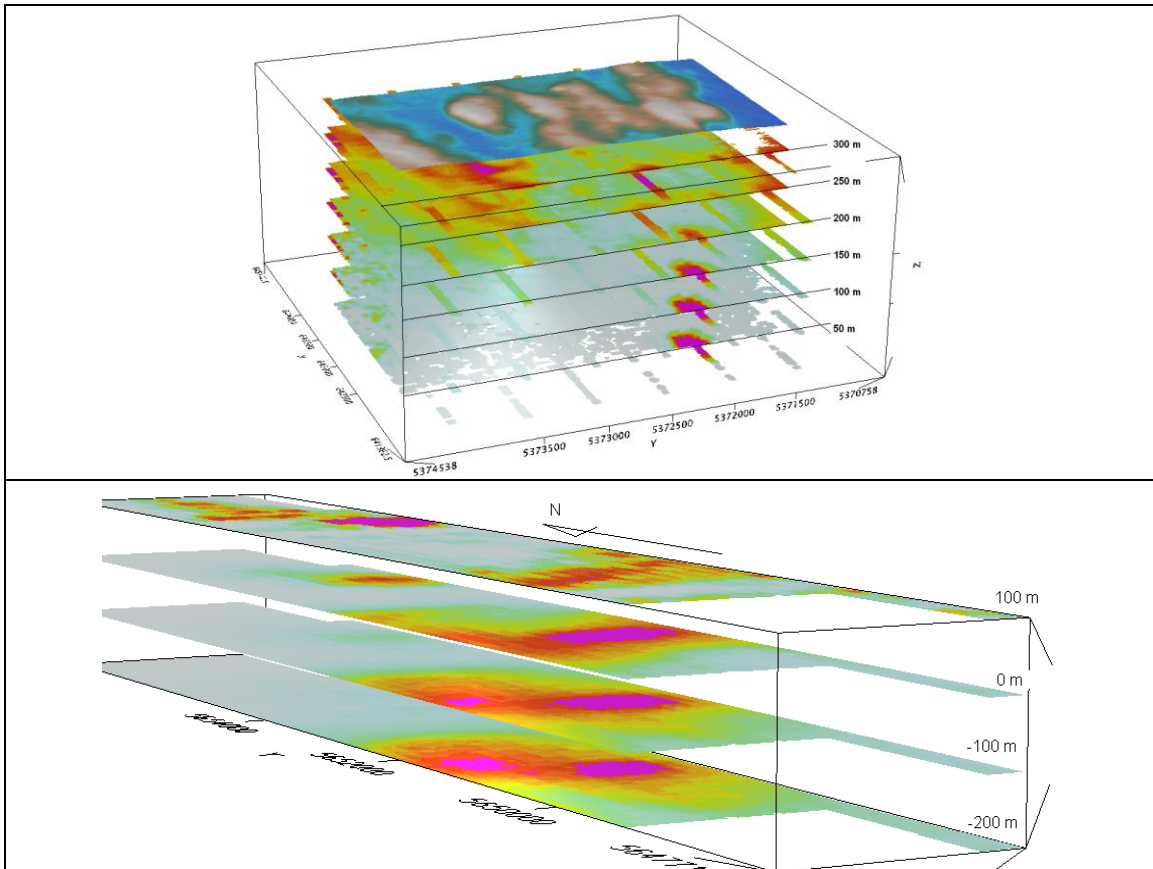
3D PRESENTATION OF RDIS



APPARENT RESISTIVITY DEPTH SLICES PLANS:

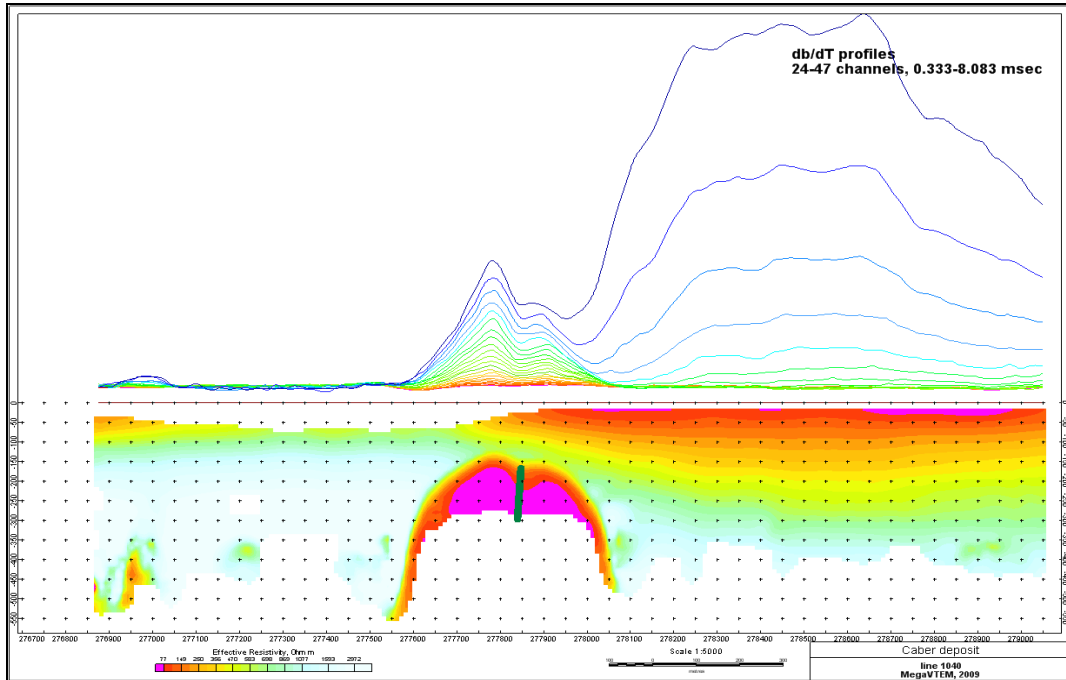


3D VIEWS OF APPARENT RESISTIVITY DEPTH SLICES:

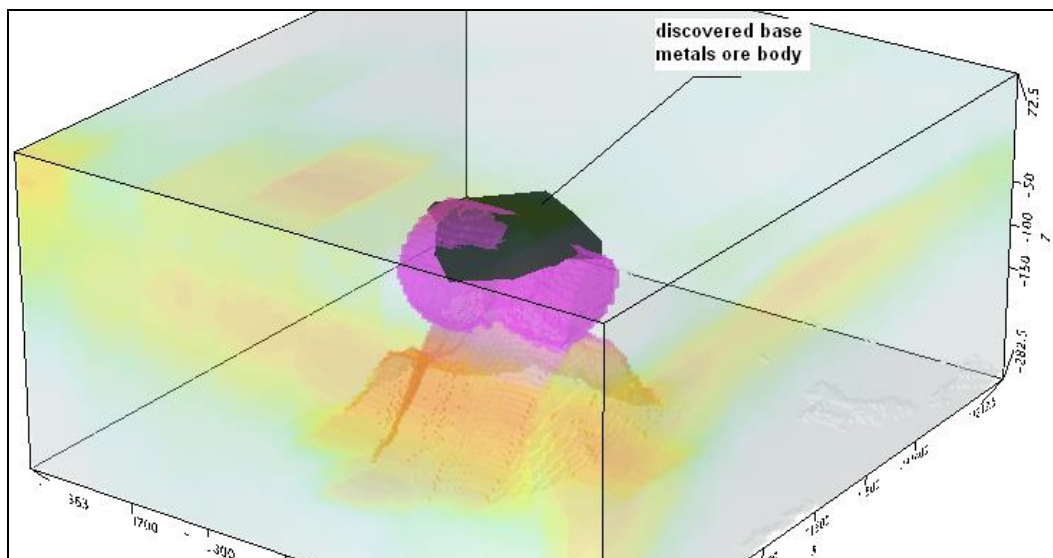


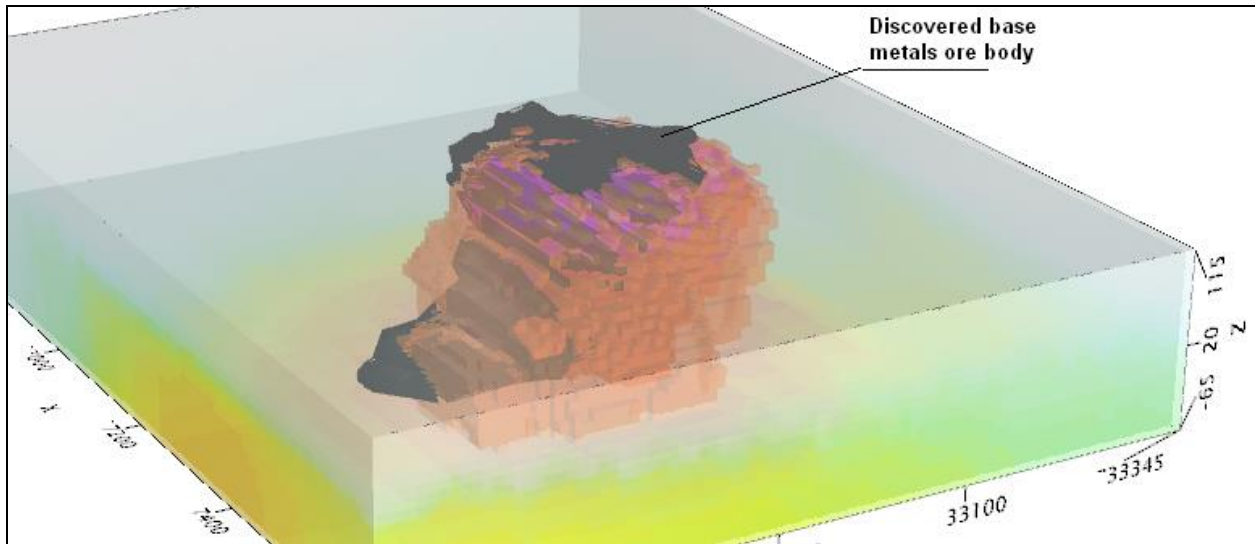
REAL BASE METAL TARGETS IN COMPARISON WITH RDIS:

RDI section of the line over Caber deposit ("thin" subvertical plate target and conductive overburden).



3D RDI VOXELS WITH BASE METALS ORE BODIES (MIDDLE EAST):





Alexander Prikhodko, PhD, P.Ge
Geotech Ltd.
April 2011

APPENDIX G

TEST AND CALIBRATIONS

G.1 Full Waveform VTEM Calibration

The calibration is performed with the completely assembled VTEM system connected to the helicopter at the survey site on the ground. Measurements of the half-cycles are collected and used to calculate a sensor calibration consisting of a single stacked half-cycle waveform. The purpose of the stacking is to attenuate natural and man-made magnetic signals, leaving only the response to the calibration signal. The stacked half-cycle allows the transfer functions between the receiver and data acquisition system, $H_D(\omega)$, and current sensor and data acquisition system, $H_R(\omega)$, to be determined. These transfer functions are used as a part of the system response correction during processing to correct the half-cycle waveforms and data acquired on a survey flight to a common transfer function:

$$D(\omega) = [H_C(\omega)/H_D(\omega)] D_R(\omega)$$
$$A(\omega) = [H_C(\omega)/H_R(\omega)] A_R(\omega)$$

where $H_C(\omega)$ is the common transfer function, and $D_R(\omega)$ and $A_R(\omega)$ are the FFT's of the raw receiver and current sensor responses recorded by the data acquisition system.

This process allows for the receiver response, $R(\omega)$, to become independent of the sensor characteristics determined by the transfer functions $H_D(\omega)$ and $H_R(\omega)$ and acts similar to a deconvolution of the data.

$$R(\omega) = \frac{D(\omega)I(\omega)}{A(\omega)}$$

where, $D(\omega)$ is the FFT of the actual receiver data sample $D(t)$, $I(\omega)$ is the FFT of a reference or "Ideal waveform" and $A(\omega)$ is the FFT of the actual waveform.

G.2 High Altitude Calibration

The high altitude calibration is conducted on each survey flight. At the beginning and at the end of each flight the helicopter climbs at 2000 feet above ground to check the EM "zero level". When at the required altitude, at least 60 seconds of data were acquired in normal operation mode.

Reference transmitter current and receiver voltage waveforms, each sampled at 192 kHz, were also recorded at high altitude for all survey flights. The recorded waveforms were transformed into an ideal form, having zero current at the beginning of the off-time, by the Full Waveform calibration (see Full Waveform VTEM Calibration section).

A waveform is provided for the fifty-nine (59) survey flights in Geosoft database format (see description in Table 9, section 6.3). A graphical representation of a VTEM waveform is shown in Figure 5.

G.3 Aluminium Plate Test

This test is performed on ground to verify the sensitivity of the system. An aluminium plate of known conductive response is positioned in alternated positions (vertical and horizontal) for about 10 seconds for 3 time measurements. Response of corresponding dB/dt and Bfield data is then verified.

The test results performed on March 22, 2016 are presented in figure below. When the aluminum plate is horizontal with respect to the loop, measured signal will show positive response, indicating a proper polarity (see H1, H2, H3, H4 in figure below).

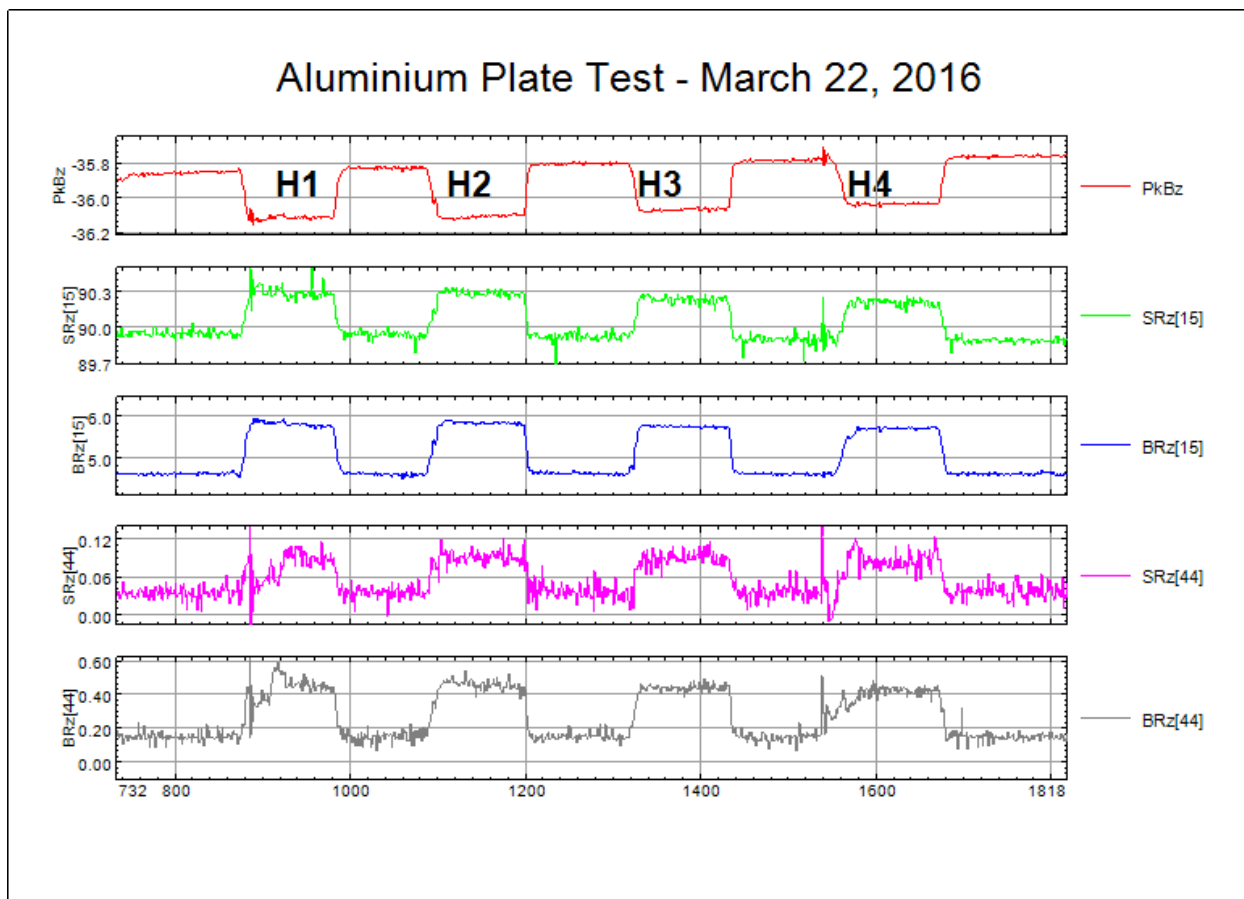


Figure G3: Plate Test results performed on March 22, 2016

G.4 Test Lines

Test lines were acquired to ensure that the airborne system is operating repeatably and as expected. The lines are flown in opposite direction and the same anomalies should be of roughly the same amplitude allowing for the variation in altitude.

Two Test lines were flown on March 22, 2016 about 10 Km north-east of Whitehorse, YT. Location of the test lines is presented in figure below.

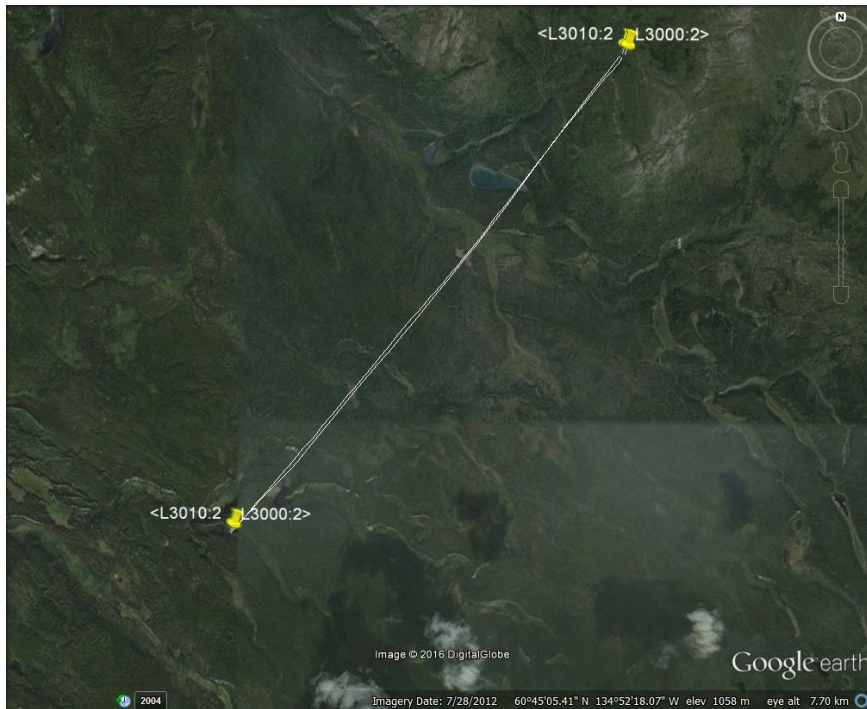


Figure G4.1: Location of Test Lines flown in opposite direction before survey production

Figure below shows a summary of the results of test line T3000 flown in SW-NE direction. The first panel from top represents the altitude channels: EM bird altitude (EMHEIGHT in blue profile), magnetic sensor altitude (MGHEIGHT in magenta) and radar altimeter mounted in helicopter (RALT in red). The second panel from top shows a view of the late times of the off-time dBz/dt array (PZTEMOFF). The third panel from top shows the off-time B-field array of the Z component (PZBEMOFF). The fourth panel from top shows the off-time dBx/dt array (PXTEMOFF). The bottom panel shows the power line monitor (POWERLINE).

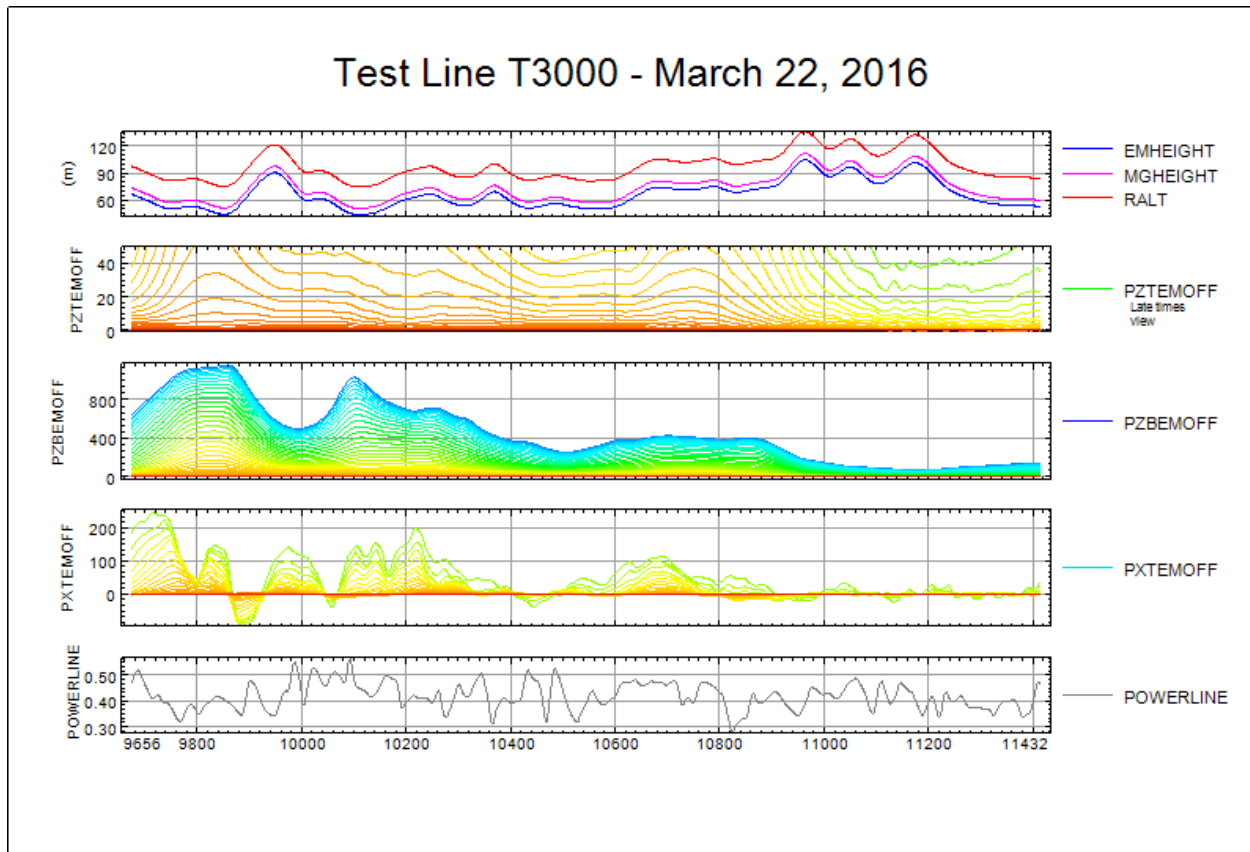


Figure G4.2: Test line T3000 flown in SW-NE direction

Figure below shows a summary of the results of test line T3010 flown in NE-SW direction. A database in Geosoft format containing the results is part of the client's deliverables.

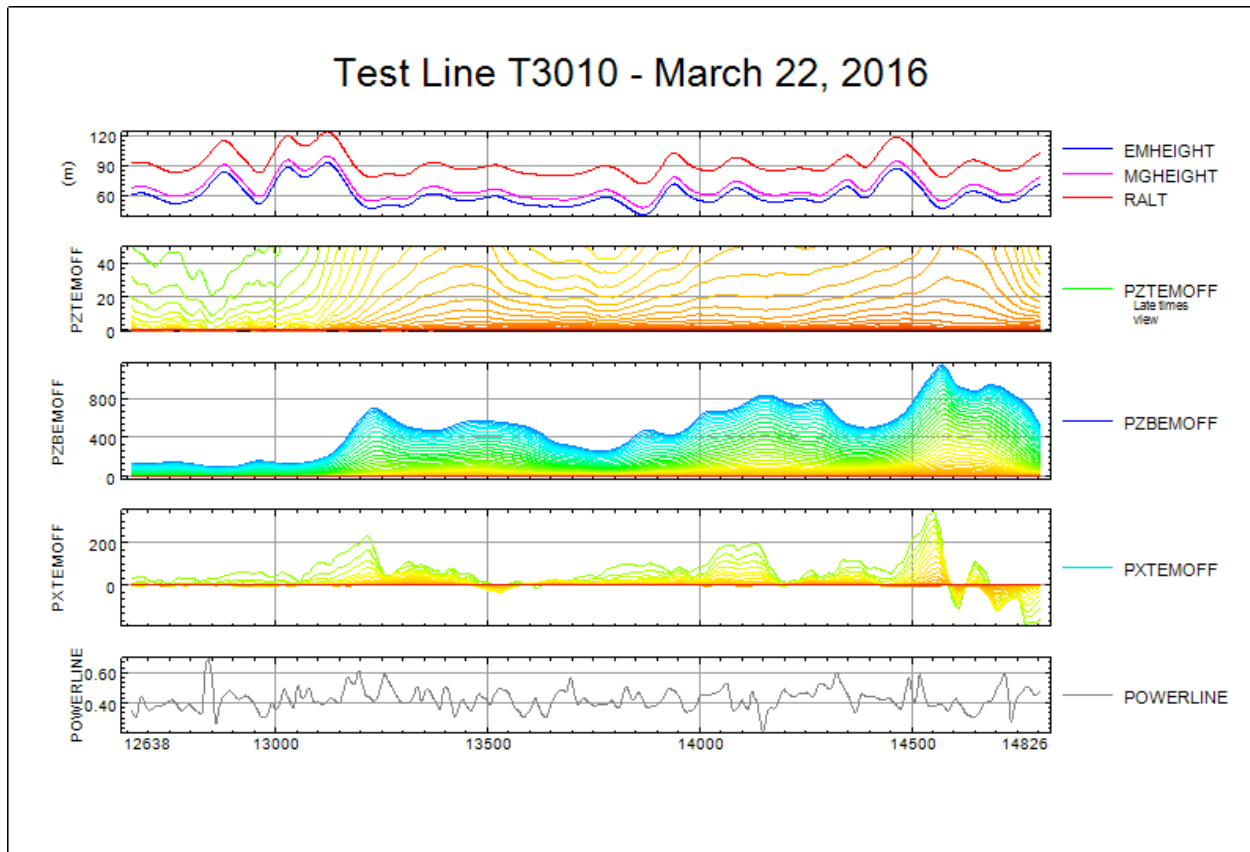


Figure G4.3: Test line T3010 flown in NE-SW direction

G.5 Radar Altimeter Calibration Test

The purpose of the radar altimeter calibration is to verify the performance of radar altimeter readings using the GPS elevation data as the reference.

The calibration is performed flying over the same spot at various altitudes, ranging from 76 m (250 feet) to 130 m (430 feet). The selected spot has known elevation and flat terrain. This test was performed at the beginning of the survey on March 22, 2016 in the Whitehorse International Airport. Another line was flown at 76 m (250 feet) over water at Schwatka Lake to verify altitude consistency with land measurement.

As observed in the graphical results presented below, where the GPS elevations versus radar readings are plotted, the relationship between radar and GPS readings are linear, and the radar readings are very accurate ($R^2 \sim 1.0$), for the range of flying heights to be expected for the survey. The line flown over water correlates well with the linear-regression trend established from the lines flown over land.

Radar checks were performed once per day. These checks consisted of the ground crew communicating with the operator/pilot via radio when the tail of the system would leave the ground.

Nominal Altitude above ground (m)	Radar Altitude Raw Data (m)	DGPS Altitude Ellipsoidal Height (m)	DTM = DGPS - Radar Alt Ellipsoidal Height WGS84 (m)	DGPS Altitude (ALT) ALT=DGPS - AVERAGE(DTM) (m)
76.22	74.6	778.1	703.50	73.84
85.37	87.1	790.9	703.80	86.64
94.51	90.7	794.6	703.90	90.34
103.66	105.1	809.4	704.30	105.14
112.80	112.4	817	704.60	112.74
121.95	123	827.6	704.60	123.34
131.10	130.5	835.6	705.10	131.34
76.22 (over water)	83.3	761.6		

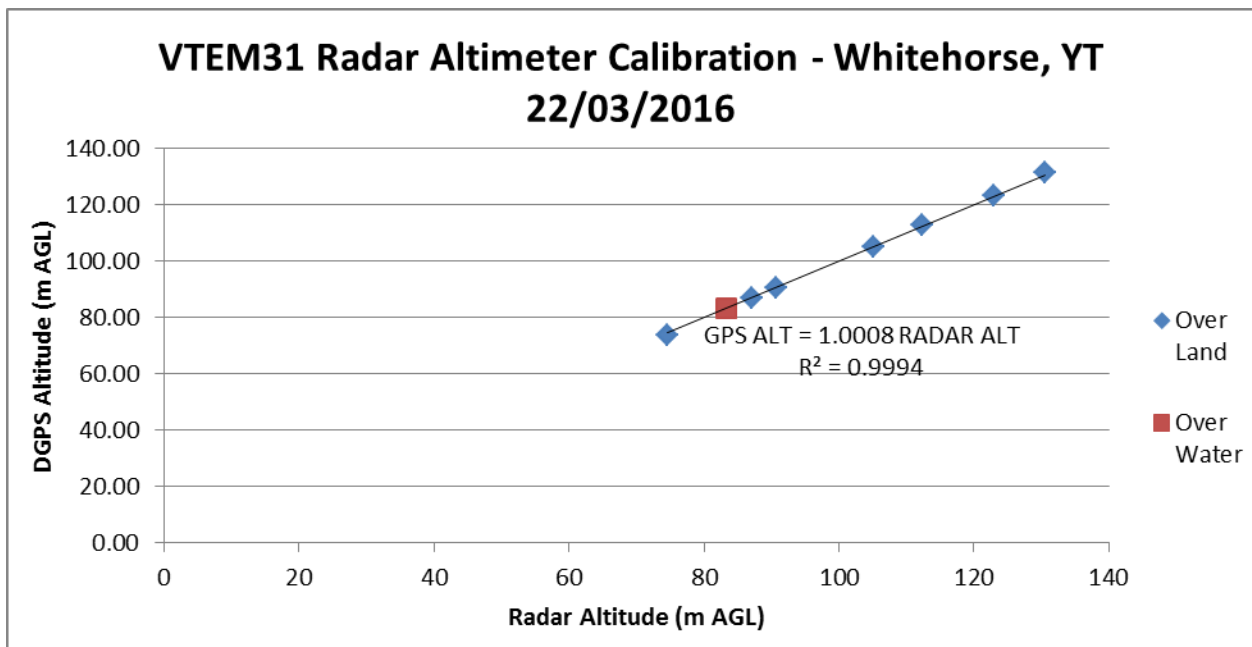


Figure G5: Radar altimeter Test

APPENDIX H

EM ANOMALIES

Line	Anom ID	Anom Type	X (m)	Y (m)	Z (m)	EMheight (m)	CondSFz (mS/m)	Tau_dB/dt (ms)	Estimated depth (m)	Cultural Affected	last Channel
L1000	A	K	548602	6819831	1590	566	28.98	1.50	74		7
L1000	B	K	547510	6819817	1687	597	42.44	2.50	75		7
L1000	C	N	544919	6819785	1738	75	48.80	2.87	96		28
L1000	D	K	540528	6819739	1222	200	2.61	0.57	73		14
L1000	E	K	539021	6819722	1169	265	2.53	0.77	70		15
L1000	F	N	535646	6819693	1454	145	1.94	0.13	80		16
L1000	G	N	533103	6819651	1238	121	7.99	0.86	66		24
L1000	H	K	528740	6819608	875	118	24.71	1.25	57		29
L1000	I	K	526633	6819582	984	147	8.53	0.64	62		26
L1010	A	K	526655	6819393	948	125	8.63	0.61	60		27
L1010	B	K	528745	6819402	855	97	24.67	1.23	55		30
L1010	C	N	533311	6819454	1286	154	6.35	0.89	69		22
L1011	A	K	547498	6819617	1233	97	56.20	2.41	69		33
L1012	A	N	548725	6819630	1060	74	44.32	1.58	75		34
L1013	A	N	545018	6819584	1696	51	68.76	2.89	75		34
L1013	B	N	540991	6819544	1148	57	2.17	0.16	69		21
L1013	C	K	539105	6819526	971	70	2.21	0.68	58		21
L1013	D	N	535719	6819485	1337	70	2.50	0.13	77		18
L1020	A	N	533444	6819247	1281	140	6.03	0.91	71		22
L1020	B	K	528755	6819211	872	112	22.55	1.23	54		29
L1020	C	K	526671	6819166	1037	178	8.18	0.60	56		24
L1021	A	N	535812	6819281	1268	60	2.59	0.62	76		18
L1021	B	K	539140	6819314	976	67	2.73	0.71	53		19
L1021	C	N	541062	6819327	1125	80	2.31	0.54	67		22
L1021	D	N	545098	6819389	1682	50	72.55	2.77	80		33
L1021	E	K	547525	6819410	1298	87	51.65	2.23	66		31
L1022	A	K	550395	6819451	1484	48	7.78	1.20	87		14
L1022	B	K	550179	6819441	1402	66	8.22	1.22	84		18
L1022	C	N	548824	6819432	1076	67	48.14	1.85	69		34
L1030	A	K	526689	6818988	954	95	7.87	0.59	54		26
L1030	B	K	528844	6819003	880	120	24.58	1.24	53		28
L1030	C	N	533605	6819075	1338	170	6.15	0.90	72		21
L1030	D	K	536177	6819082	1273	119	2.93	0.70	76		17
L1031	A	N	539072	6819124	1019	108	3.17	0.76	66		19

Line	Anom ID	Anom Type	X (m)	Y (m)	Z (m)	EMheight (m)	CondSFz (mS/m)	Tau_dB/dt (ms)	Estimated depth (m)	Cultural Affected	last Channel
L1031	B	N	541130	6819133	1106	55	2.35	0.50	70		22
L1032	A	N	545241	6819204	1765	87	52.52	1.68	59		27
L1033	A	K	547580	6819219	1608	388	43.19	2.22	72		12
L1041	A	K	526714	6818773	943	93	7.27	0.61	52		26
L1041	B	K	529012	6818810	871	103	25.23	1.24	50		29
L1041	C	N	533729	6818860	1309	133	7.10	1.04	71		21
L1041	D	K	536237	6818888	1298	115	3.15	0.71	77		16
L1041	E	N	541157	6818931	1298	181	2.36	0.55	74		19
L1041	F	N	545255	6818983	1779	46	52.56	1.85	61		29
L1041	G	K	547611	6819010	1457	262	36.03	2.05	78		24
L1051	A	K	547586	6818821	1665	460	35.38	2.01	79		9
L1051	B	N	545312	6818794	1795	78	53.69	2.15	66		29
L1051	C	N	541246	6818754	1285	104	2.63	0.54	74		21
L1051	D	K	536227	6818699	1319	88	3.89	0.68	77		17
L1051	E	N	533789	6818663	1276	126	7.65	1.02	70		23
L1051	F	K	529055	6818616	859	79	25.92	1.25	47		30
L1051	G	K	526688	6818587	1004	155	7.80	0.61	54		24
L1061	A	K	526704	6818385	947	99	7.98	0.64	52		26
L1061	B	K	529138	6818415	882	101	27.05	1.23	45		29
L1061	C	N	533857	6818473	1285	130	8.09	1.13	71		22
L1061	D	N	535999	6818487	1355	71	4.24	0.84	74		17
L1061	E	N	541357	6818542	1402	105	2.27	0.53	76		19
L1061	F	N	545388	6818586	1767	58	66.63	2.35	67		32
L1061	G	K	547502	6818630	1437	196	35.20	1.90	77		28
L1070	A	K	525347	6818166	1122	96	40.55	1.62	52		31
L1070	B	K	526706	6818195	948	95	7.89	0.64	52		26
L1070	C	K	529137	6818201	866	79	28.42	1.25	43		30
L1070	D	N	534010	6818259	1312	161	8.84	1.19	71		20
L1070	E	N	536060	6818286	1388	81	6.26	0.84	72		15
L1071	A	K	548840	6818428	1060	65	62.76	2.48	96		34
L1072	A	K	547512	6818415	1658	434	41.46	1.77	68		7
L1073	A	N	545451	6818396	1759	62	69.65	2.74	68		33
L1073	B	N	541404	6818355	1437	55	2.21	0.16	73		20
L1080	A	K	525381	6817979	1118	90	35.16	1.52	49		31
L1080	B	K	526752	6817974	937	83	8.29	0.66	49		26
L1080	C	K	529065	6818010	834	48	30.72	1.30	40		30
L1080	D	N	534127	6818068	1315	156	9.59	1.30	72		20
L1080	E	N	536079	6818085	1339	58	6.67	0.83	73		18

Line	Anom ID	Anom Type	X (m)	Y (m)	Z (m)	EMheight (m)	CondSFz (mS/m)	Tau_dB/dt (ms)	Estimated depth (m)	Cultural Affected	last Channel
L1082	A	N	545582	6818195	1786	73	72.71	2.63	68		29
L1082	B	K	547678	6818228	1246	95	75.42	2.64	49		34
L1082	C	K	548968	6818231	1103	88	85.46	2.20	71		36
L1083	A	K	549607	6818241	1350	108	23.74	1.31	65		24
L1090	A	N	536065	6817891	1315	72	13.08	1.05	72		22
L1090	B	N	534225	6817864	1241	83	6.01	0.61	71		26
L1090	C	K	528963	6817807	809	48	33.43	1.27	39		31
L1090	D	K	526828	6817787	943	78	9.61	0.83	44		26
L1090	E	K	525391	6817776	1109	66	25.37	0.59	45		32
L1091	A	K	549673	6818046	1366	58	49.77	1.56	55		35
L1092	A	K	547701	6818019	1243	58	76.45	2.54	45		35
L1092	B	K	549080	6818023	1145	88	82.80	2.15	64		35
L1093	A	N	545589	6817994	1727	57	94.41	2.53	60		36
L1093	B	N	539016	6817918	1068	64	2.10	0.15	63		22
L1100	A	N	525391	6817569	1106	49	16.85	0.94	48		30
L1100	B	K	527177	6817581	949	57	10.93	0.85	53		28
L1100	C	K	528903	6817607	818	56	34.67	1.22	39		32
L1100	D	N	534463	6817667	1323	95	7.18	1.16	70		20
L1100	E	N	536019	6817680	1253	57	14.16	1.11	71		26
L1101	A	K	549262	6817839	1349	195	57.37	1.76	58		27
L1101	B	K	547660	6817837	1596	355	60.06	2.16	55		16
L1102	A	N	545608	6817799	1721	85	77.48	2.89	67		31
L1102	B	N	539166	6817729	1093	63	2.45	0.51	63		23
L1110	A	N	535995	6817485	1327	160	19.37	1.27	73		18
L1110	B	N	534678	6817470	1331	71	7.51	0.83	73		21
L1110	C	K	528896	6817408	816	52	35.39	1.19	38		32
L1110	D	K	527187	6817390	948	67	11.40	0.89	53		27
L1110	E	N	525481	6817371	1136	69	17.64	0.82	48		29
L1111	A	K	539040	6817517	1150	164	2.72	0.52	60		21
L1111	B	N	545750	6817603	1793	60	54.74	2.21	61		28
L1111	C	K	547776	6817613	1376	116	60.25	1.94	60		33
L1111	D	K	549430	6817641	1398	252	36.03	1.91	62		20
L1120	A	N	525541	6817173	1129	56	14.98	0.81	49		28
L1120	B	K	527167	6817188	955	73	11.32	0.98	48		26
L1120	C	K	528975	6817208	812	49	36.93	1.30	37		31
L1120	D	N	534851	6817273	1386	94	5.67	0.68	69		20
L1120	E	N	536042	6817294	1227	56	26.68	1.60	72		29
L1120	F	N	536798	6817302	1159	77	2.36	0.57	75		20

Line	Anom ID	Anom Type	X (m)	Y (m)	Z (m)	EMheight (m)	CondSFz (mS/m)	Tau_dB/dt (ms)	Estimated depth (m)	Cultural Affected	last Channel
L1121	A	K	547835	6817425	1670	410	60.11	2.26	61		14
L1121	B	N	545733	6817400	1712	70	54.80	2.43	69		31
L1122	A	K	539149	6817325	1061	81	3.69	0.54	62		24
L1130	A	N	536865	6817103	1224	108	3.53	0.55	76		20
L1130	B	N	536099	6817087	1306	95	27.64	1.69	72		25
L1130	C	N	535022	6817073	1369	54	7.85	0.76	71		25
L1130	D	K	531652	6817036	1016	103	7.87	0.98	64		24
L1130	E	K	529059	6817006	820	57	34.82	1.35	37		31
L1130	F	K	527162	6816989	939	52	11.97	0.97	44		26
L1130	G	N	525505	6816978	1153	52	10.84	0.51	49		28
L1131	A	K	539212	6817128	1134	97	3.81	0.51	62		23
L1131	B	K	545726	6817198	1795	243	24.94	1.07	54		20
L1131	C	K	548204	6817228	1395	101	59.18	2.05	60		34
L1140	A	N	525434	6816769	1180	54	7.80	0.47	49		26
L1140	B	K	527169	6816783	951	54	11.20	0.96	43		25
L1140	C	K	529065	6816806	818	51	31.86	1.40	38		30
L1140	D	K	531681	6816838	1053	126	7.91	0.90	63		22
L1140	E	N	535176	6816877	1382	64	6.64	0.62	73		24
L1140	F	N	536176	6816889	1299	52	29.38	1.62	69		28
L1140	G	N	536961	6816901	1213	71	5.88	0.74	72		23
L1141	A	N	549989	6817044	1443	112	35.75	2.06	76		27
L1141	B	K	548221	6817021	1581	198	70.55	2.13	57		28
L1142	A	N	545725	6816996	1634	64	57.45	2.46	72		36
L1142	B	N	540812	6816941	1273	69	6.56	0.79	69		23
L1142	C	N	539962	6816922	1096	80	4.26	0.53	69		24
L1151	A	K	527019	6816583	941	45	9.49	0.97	40		25
L1151	B	K	529229	6816617	818	52	27.46	1.28	36		30
L1151	C	K	531562	6816638	1050	145	8.06	0.91	60		23
L1151	D	N	535403	6816678	1397	74	3.28	0.58	77		21
L1151	E	N	536242	6816687	1314	51	27.18	1.77	72		26
L1151	F	N	537134	6816699	1212	92	9.75	0.77	71		24
L1151	G	N	540213	6816731	1226	206	8.23	1.02	69		20
L1151	H	N	541063	6816738	1296	115	8.23	1.02	70		20
L1151	I	N	545933	6816791	1850	130	23.72	1.14	73		16
L1151	J	K	548241	6816815	1512	92	87.74	1.90	50		36
L1151	K	K	549913	6816834	1592	229	34.38	1.93	77		22
L1160	A	K	526920	6816387	959	55	8.53	0.83	43		25
L1160	B	K	529483	6816415	828	58	24.26	1.26	42		29

Line	Anom ID	Anom Type	X (m)	Y (m)	Z (m)	EMheight (m)	CondSFz (mS/m)	Tau_dB/dt (ms)	Estimated depth (m)	Cultural Affected	last Channel
L1160	C	K	531609	6816444	1023	118	8.32	1.02	60		23
L1160	D	N	535499	6816491	1399	70	1.72	0.16	76		18
L1160	E	N	536289	6816495	1296	47	23.73	1.42	70		28
L1160	F	N	537190	6816503	1189	82	12.82	0.89	68		27
L1160	G	N	540384	6816540	1127	104	8.71	0.98	72		22
L1160	H	N	541226	6816543	1225	86	9.27	0.96	68		24
L1160	I	N	545958	6816600	1878	183	19.53	1.38	77		13
L1160	J	N	548328	6816627	1434	122	76.69	2.31	65		34
L1160	K	K	550286	6816641	1679	201	18.62	1.58	76		15
L1170	A	N	537250	6816296	1148	70	10.44	0.83	66		25
L1170	B	N	536301	6816291	1291	73	20.29	1.31	67		26
L1170	C	K	533434	6816263	1207	63	3.93	0.67	58		19
L1170	D	K	531639	6816239	1008	109	8.57	0.98	59		23
L1170	E	K	529541	6816211	820	52	21.57	1.25	40		29
L1170	F	K	526900	6816185	995	72	8.57	0.78	45		25
L1171	A	N	540520	6816335	1268	197	8.98	1.00	70		21
L1171	B	K	546002	6816399	1854	198	6.39	0.93	70		16
L1171	C	N	548290	6816426	1434	171	67.94	2.70	67		31
L1171	D	N	550304	6816442	1591	133	41.32	1.97	76		24
L1181	A	N	536391	6816090	1303	130	16.13	1.23	68		21
L1181	B	K	533572	6816064	1220	63	3.43	0.69	57		20
L1181	C	K	531747	6816041	972	75	8.92	1.02	59		24
L1181	D	K	529590	6816014	825	56	20.24	1.11	40		28
L1181	E	K	526764	6815982	994	67	7.85	0.70	48		25
L1182	A	N	550254	6816247	1544	172	19.44	1.18	73		27
L1182	B	K	548325	6816224	1708	432	69.50	2.76	64		14
L1182	C	N	546044	6816197	1789	82	24.73	1.38	80		28
L1182	D	N	544534	6816185	1499	107	2.47	0.79	83		15
L1182	E	N	541491	6816154	1146	64	10.84	0.87	65		26
L1182	F	N	540618	6816152	1198	80	14.14	1.19	69		20
L1182	G	N	537329	6816096	1127	78	10.34	0.97	65		26
L1190	A	K	526561	6815777	1000	60	8.55	0.71	46		26
L1190	B	K	529603	6815817	845	59	19.50	1.11	40		27
L1190	C	K	531781	6815845	1002	94	9.06	1.01	58		23
L1190	D	K	533700	6815864	1256	83	4.09	0.74	59		19
L1190	E	N	536584	6815902	1209	76	24.85	1.20	69		28
L1191	A	N	537408	6815912	1174	122	8.70	1.01	67		21
L1191	B	N	540910	6815944	1236	117	10.56	0.81	68		25

Line	Anom ID	Anom Type	X (m)	Y (m)	Z (m)	EMheight (m)	CondSFz (mS/m)	Tau_dB/dt (ms)	Estimated depth (m)	Cultural Affected	last Channel
L1191	C	K	544604	6815977	1574	144	1.79	0.11	86		15
L1192	A	N	546132	6816003	1870	69	18.55	1.55	78		22
L1192	B	K	548522	6816026	1415	112	103.77	2.37	66		38
L1192	C	N	550257	6816042	1404	104	51.78	2.01	75		30
L1192	D	N	550826	6816052	1502	83	15.37	1.09	65		28
L1200	A	N	550301	6815852	1443	84	48.75	2.02	71		25
L1200	B	N	549079	6815832	1495	144	51.09	3.06	70		27
L1200	C	K	548528	6815831	1566	281	89.79	2.59	70		26
L1200	D	N	546211	6815801	1884	57	18.86	1.42	96		25
L1200	E	K	544673	6815786	1593	91	1.63	0.14	87		17
L1200	F	K	541517	6815753	1258	57	10.27	0.83	61		24
L1200	G	K	540081	6815728	1362	127	24.28	1.37	67		23
L1200	H	N	537526	6815701	1138	100	10.31	1.12	68		24
L1200	I	N	536674	6815699	1254	98	21.11	1.19	69		30
L1200	J	K	531640	6815638	944	65	9.94	1.00	55		24
L1200	K	K	529678	6815617	838	52	18.65	1.16	41		27
L1200	L	K	526615	6815583	1001	47	9.64	0.74	43		26
L1210	A	K	526673	6815381	1024	55	10.02	0.75	44		26
L1210	B	K	529699	6815419	834	52	17.90	1.15	41		27
L1210	C	K	531646	6815435	973	98	9.88	1.05	55		23
L1210	D	N	536895	6815494	1228	72	14.96	1.04	73		26
L1210	E	K	540134	6815538	1388	100	44.78	1.69	63		28
L1210	F	N	541098	6815539	1317	99	11.32	0.88	66		25
L1210	G	K	544660	6815584	1692	91	2.00	0.12	89		11
L1210	H	N	546304	6815593	1884	53	19.29	1.47	81		25
L1210	I	K	548432	6815617	1502	169	78.60	3.08	74		29
L1210	J	N	549300	6815631	1467	73	69.20	3.37	74		30
L1210	K	N	550390	6815646	1453	55	37.60	1.96	69		27
L1220	A	N	549322	6815442	1495	84	65.85	2.44	74		29
L1220	B	K	548261	6815431	1612	214	80.28	2.76	68		27
L1220	C	N	546337	6815399	1858	60	22.98	1.53	102		24
L1220	D	K	544720	6815388	1730	68	1.88	0.10	95		13
L1220	E	K	541611	6815352	1346	65	11.17	0.86	64		24
L1220	F	K	540156	6815333	1457	76	69.44	2.11	60		33
L1220	G	K	539548	6815325	1466	57	1.19	0.03	78		19
L1220	H	N	536946	6815299	1235	87	10.34	0.87	75		24
L1220	I	K	531670	6815240	935	62	9.90	1.01	55		23
L1220	J	K	529689	6815216	829	57	17.72	1.16	41		26

Line	Anom ID	Anom Type	X (m)	Y (m)	Z (m)	EMheight (m)	CondSFz (mS/m)	Tau_dB/dt (ms)	Estimated depth (m)	Cultural Affected	last Channel
L1220	K	K	526712	6815183	1015	48	10.05	0.77	45		25
L1230	A	K	526713	6814977	1024	55	9.93	0.80	47		25
L1230	B	K	529657	6815017	824	55	17.91	1.23	42		26
L1230	C	K	531648	6815038	967	123	9.87	1.04	58		23
L1230	D	N	537071	6815093	1223	98	8.78	0.84	78		21
L1230	E	K	540167	6815133	1503	51	77.25	2.29	57		35
L1230	F	N	546423	6815204	1803	58	25.28	1.73	88		26
L1230	G	K	548316	6815217	1559	161	88.72	2.90	62		33
L1230	H	N	549427	6815250	1522	158	70.92	2.66	78		29
L1240	A	N	549486	6815039	1542	159	69.94	2.78	80		29
L1240	B	K	548944	6815032	1603	130	98.91	3.13	72		32
L1240	C	N	546445	6815010	1794	92	25.53	1.71	95		24
L1240	D	N	540086	6814935	1529	57	29.26	1.65	62		29
L1240	E	N	537183	6814894	1230	129	9.83	0.72	77		23
L1240	F	K	531708	6814837	953	91	10.10	1.06	59		23
L1240	G	K	529672	6814814	824	53	19.46	1.21	43		26
L1240	H	K	526820	6814787	1044	51	9.64	0.83	48		25
L1250	A	K	526892	6814586	1070	64	9.51	0.88	45		24
L1250	B	K	529678	6814614	848	81	20.35	1.22	44		26
L1250	C	K	531724	6814640	994	91	10.29	1.15	58		22
L1250	D	N	537236	6814690	1219	112	10.54	0.66	75		24
L1250	E	N	540203	6814734	1509	68	26.37	1.52	66		29
L1250	F	K	541706	6814754	1550	133	9.40	0.96	68		22
L1250	G	N	546576	6814795	1774	74	32.53	1.47	82		30
L1250	H	K	548988	6814839	1568	143	109.21	3.25	76		34
L1250	I	K	549461	6814836	1592	145	70.86	3.16	80		24
L1260	A	K	549480	6814637	1570	89	83.64	2.98	75		31
L1260	B	K	548997	6814632	1533	136	117.14	3.26	77		35
L1260	C	N	546642	6814613	1738	71	33.71	1.55	87		31
L1260	D	K	541735	6814555	1555	96	10.32	1.01	63		23
L1260	E	N	540613	6814539	1496	76	11.59	0.85	60		26
L1260	F	N	537296	6814497	1197	96	14.84	0.75	77		29
L1260	G	K	531725	6814441	987	64	10.42	1.12	57		22
L1260	H	K	529642	6814416	839	54	21.10	1.42	45		27
L1260	I	K	526982	6814388	1069	52	9.31	0.94	45		24
L1270	A	K	529627	6814214	844	60	24.43	1.43	44		28
L1270	B	K	531719	6814235	987	51	10.83	1.21	56		22
L1270	C	N	537403	6814299	1215	121	13.14	0.75	74		23

Line	Anom ID	Anom Type	X (m)	Y (m)	Z (m)	EMheight (m)	CondSFz (mS/m)	Tau_dB/dt (ms)	Estimated depth (m)	Cultural Affected	last Channel
L1270	D	N	540754	6814344	1481	63	12.75	1.05	59		26
L1270	E	K	541871	6814352	1562	81	8.79	0.90	63		24
L1270	F	N	546770	6814416	1726	85	18.02	1.35	78		27
L1270	G	K	549044	6814435	1548	158	108.30	3.56	79		29
L1270	H	K	549537	6814445	1601	91	89.59	2.92	68		31
L1280	A	K	549524	6814244	1638	98	95.87	2.87	66		34
L1280	B	K	549027	6814231	1529	118	110.95	3.49	77		31
L1280	C	N	546887	6814193	1732	59	10.99	1.33	76		23
L1280	D	N	542653	6814157	1589	49	26.30	1.26	66		27
L1280	E	K	541920	6814157	1533	91	10.26	1.01	61		24
L1280	F	N	540842	6814138	1445	55	14.34	0.97	60		26
L1280	G	N	537498	6814099	1202	117	17.79	0.81	72		27
L1280	H	K	531694	6814037	955	41	11.40	1.31	55		22
L1280	I	K	529748	6814018	844	63	22.53	1.38	45		27
L1290	A	K	529756	6813818	853	73	26.04	1.35	43		28
L1290	B	K	531638	6813835	940	69	13.16	1.22	56		23
L1290	C	N	537650	6813903	1142	71	19.52	0.76	67		28
L1290	D	N	540980	6813943	1403	60	19.64	1.19	58		26
L1290	E	N	542778	6813956	1539	63	45.24	1.67	63		30
L1290	F	N	546984	6814011	1669	43	6.70	1.05	72		22
L1290	G	K	548856	6814030	1609	223	127.39	3.26	65		25
L1290	H	K	549619	6814041	1694	66	97.44	2.80	57		33
L1300	A	K	549433	6813834	1605	66	107.73	3.31	77		36
L1300	B	K	548875	6813829	1451	64	159.96	3.11	60		40
L1300	C	N	542929	6813767	1472	60	51.13	1.75	61		33
L1300	D	N	541062	6813738	1357	85	16.65	0.90	53		28
L1300	E	N	537681	6813703	1130	58	16.99	0.68	63		30
L1300	F	K	531577	6813640	907	60	14.04	1.26	58		24
L1300	G	K	529777	6813613	844	48	29.84	1.60	41		29
L1310	A	N	529666	6813415	883	60	38.00	1.97	48		29
L1310	B	K	531624	6813437	899	69	14.85	1.46	60		23
L1310	C	N	535587	6813481	1307	58	3.15	0.57	57		21
L1310	D	N	537749	6813511	1136	69	19.95	0.69	67		31
L1310	E	N	541150	6813539	1327	79	18.91	0.96	53		29
L1310	F	N	543133	6813560	1403	74	45.95	2.15	63		29
L1310	G	K	548969	6813632	1622	227	170.71	3.30	65		27
L1310	H	K	549876	6813642	1724	96	83.25	2.94	65		28
L1320	A	K	549818	6813441	1730	91	106.71	3.06	66		32

Line	Anom ID	Anom Type	X (m)	Y (m)	Z (m)	EMheight (m)	CondSFz (mS/m)	Tau_dB/dt (ms)	Estimated depth (m)	Cultural Affected	last Channel
L1320	B	K	548979	6813433	1467	83	214.47	3.31	66		43
L1320	C	N	543154	6813369	1331	59	52.57	1.82	59		32
L1320	D	N	541133	6813337	1249	50	14.91	0.77	50		30
L1320	E	N	540578	6813337	1239	50	3.41	1.04	65		19
L1320	F	N	537777	6813305	1162	69	15.43	0.67	69		29
L1320	G	N	535646	6813283	1276	51	3.30	0.61	54		22
L1320	H	N	529621	6813216	902	61	52.42	2.35	50		30
L1330	A	N	529694	6813021	903	63	63.21	2.69	44		32
L1330	B	K	535631	6813084	1247	47	3.24	0.50	54		23
L1330	C	N	537884	6813108	1163	76	19.75	0.84	75		30
L1330	D	N	540679	6813136	1183	48	3.28	0.86	61		22
L1330	E	N	541271	6813143	1195	52	20.98	1.03	52		29
L1330	F	N	543251	6813165	1258	75	51.60	1.79	63		32
L1330	G	K	549003	6813228	1617	200	153.14	3.27	68		29
L1330	H	K	549887	6813228	1736	86	121.00	3.14	70		34
L1341	A	N	549560	6813036	1712	136	114.92	3.42	70		33
L1341	B	N	543351	6812968	1242	123	46.89	1.74	59		28
L1341	C	N	542107	6812956	1160	78	31.06	1.55	50		27
L1341	D	N	537903	6812904	1226	133	14.06	0.85	80		25
L1341	E	K	535764	6812886	1286	84	2.66	0.53	57		21
L1341	F	N	529772	6812820	977	111	59.59	3.40	46		28
L1350	A	N	529851	6812618	947	80	72.54	2.23	46		34
L1350	B	K	535850	6812681	1258	54	3.19	0.54	59		21
L1350	C	N	538001	6812706	1185	137	14.28	0.94	83		26
L1350	D	N	542252	6812755	1114	58	38.97	1.69	50		31
L1350	E	N	543403	6812763	1137	54	41.88	1.76	57		30
L1350	F	N	549624	6812837	1679	116	117.97	3.27	69		34
L1360	A	K	550008	6812639	1660	115	136.66	3.29	70		37
L1360	B	K	548814	6812629	1436	110	130.17	2.82	58		37
L1360	C	N	543445	6812578	1136	58	41.97	1.80	53		30
L1360	D	N	542310	6812558	1153	55	34.47	1.40	49		31
L1360	E	N	538015	6812506	1249	215	9.25	0.84	90		15
L1360	F	K	536020	6812487	1180	56	2.75	0.56	58		21
L1360	G	N	529575	6812408	1001	70	72.54	2.55	50		31
L1370	A	N	529656	6812217	1002	57	92.68	2.98	48		31
L1370	B	K	536155	6812283	1098	73	3.15	0.64	57		22
L1370	C	N	538225	6812316	1102	176	9.32	0.96	89		18
L1370	D	N	540880	6812344	1187	58	13.21	0.74	59		28

Line	Anom ID	Anom Type	X (m)	Y (m)	Z (m)	EMheight (m)	CondSFz (mS/m)	Tau_dB/dt (ms)	Estimated depth (m)	Cultural Affected	last Channel
L1370	E	N	542405	6812356	1187	63	41.08	1.62	52		30
L1370	F	N	543535	6812370	1153	50	41.66	1.80	56		29
L1370	G	K	548978	6812429	1575	228	183.20	3.08	58		28
L1370	H	N	550415	6812454	1715	62	146.63	3.13	66		36
L1380	A	N	551064	6812253	1680	70	40.15	2.36	71		28
L1380	B	N	550509	6812246	1675	70	140.64	2.98	67		38
L1380	C	K	549612	6812237	1504	95	124.83	3.66	70		38
L1380	D	K	549044	6812234	1369	64	251.07	3.26	53		43
L1380	E	N	545930	6812198	1177	55	1.52	0.07	67		19
L1380	F	N	542408	6812162	1256	65	39.09	1.62	60		32
L1380	G	N	540900	6812137	1256	61	10.54	0.64	60		29
L1380	H	N	539628	6812121	1039	100	1.58	0.16	83		24
L1380	I	N	538194	6812111	1055	144	6.98	0.80	82		18
L1380	J	K	536251	6812089	981	60	3.22	0.63	56		23
L1380	K	N	529716	6812015	1042	77	122.72	2.86	48		34
L1390	A	N	529904	6811819	1016	56	163.80	3.08	42		40
L1390	B	K	530400	6811819	923	81	86.31	2.74	50		33
L1390	C	N	538247	6811911	1059	122	7.78	0.88	85		20
L1390	D	N	540951	6811938	1300	55	10.41	0.70	62		28
L1390	E	N	542485	6811956	1299	54	46.17	1.77	60		31
L1390	F	N	543431	6811973	1242	74	44.86	1.86	54		30
L1390	G	K	549087	6812035	1552	268	215.31	3.09	53		25
L1390	H	K	549975	6812049	1683	89	154.26	3.32	64		38
L1390	I	K	551081	6812050	1740	135	48.96	2.42	77		27
L1400	A	K	551083	6811856	1744	132	50.95	2.70	81		24
L1400	B	K	550025	6811846	1718	70	138.92	3.31	64		30
L1400	C	K	549014	6811836	1308	79	296.90	2.68	46		44
L1400	D	K	545589	6811795	1339	81	1.78	0.11	81		17
L1400	E	N	543477	6811766	1295	84	39.21	1.89	58		28
L1400	F	K	542742	6811766	1357	100	42.97	1.82	61		29
L1400	G	K	541821	6811742	1405	67	44.06	1.87	56		29
L1400	H	N	540998	6811743	1298	51	10.93	0.82	64		26
L1400	I	N	538258	6811713	1059	85	7.64	0.82	78		23
L1400	J	N	530042	6811618	1036	65	164.32	2.95	42		39
L1410	A	N	530205	6811419	1017	51	164.99	3.05	43		39
L1410	B	K	541821	6811564	1487	83	45.47	1.98	53		28
L1410	C	K	542771	6811562	1385	86	38.81	1.83	62		30
L1410	D	K	550210	6811638	1766	79	118.66	3.28	65		18

Line	Anom ID	Anom Type	X (m)	Y (m)	Z (m)	EMheight (m)	CondSFz (mS/m)	Tau_dB/dt (ms)	Estimated depth (m)	Cultural Affected	last Channel
L1420	A	K	550261	6811447	1751	133	118.91	3.33	64		21
L1420	B	K	549169	6811432	1439	210	168.07	3.18	57		32
L1420	C	K	543793	6811374	1425	124	40.83	2.79	71		24
L1420	D	K	542929	6811366	1469	152	39.66	1.84	62		26
L1420	E	K	541832	6811347	1490	54	55.67	1.93	52		30
L1420	F	N	541019	6811336	1250	74	4.00	0.90	72		20
L1420	G	N	538485	6811313	1282	88	4.47	0.66	79		20
L1420	H	K	533099	6811251	891	58	14.66	1.11	53		25
L1420	I	N	530362	6811219	1020	89	140.47	2.64	43		38
L1430	A	N	530594	6811021	980	69	194.70	3.20	43		39
L1430	B	K	533152	6811048	938	103	17.08	1.21	54		26
L1430	C	N	538557	6811118	1337	58	5.94	0.57	77		23
L1430	D	K	541908	6811141	1473	50	74.97	2.23	51		33
L1430	E	K	543078	6811159	1464	123	43.63	1.75	61		27
L1430	F	K	543862	6811174	1524	201	41.13	2.52	72		20
L1430	G	K	549267	6811237	1547	303	183.24	3.24	56		20
L1430	H	K	550456	6811242	1627	126	146.34	3.67	62		35
L1440	A	K	550471	6811038	1562	119	159.34	3.43	60		36
L1440	B	K	549421	6811027	1410	163	207.82	3.46	54		32
L1440	C	K	543913	6810975	1476	119	45.89	2.30	75		30
L1440	D	N	542784	6810961	1522	65	33.63	1.52	61		31
L1440	E	K	541946	6810950	1456	65	87.51	2.60	51		34
L1440	F	N	541146	6810940	1218	83	10.99	0.77	80		30
L1440	G	N	538638	6810911	1357	51	7.11	0.68	77		26
L1440	H	N	536803	6810893	1209	93	2.42	0.48	60		22
L1440	I	K	533166	6810851	889	62	19.80	1.20	54		27
L1440	J	N	530712	6810827	1010	67	190.55	2.88	40		39
L1450	A	N	530802	6810622	1013	56	246.08	3.03	37		39
L1450	B	N	536818	6810692	1216	62	2.58	0.45	60		22
L1450	C	N	538746	6810714	1382	60	7.44	0.65	73		26
L1450	D	K	541980	6810750	1474	131	107.19	2.60	53		34
L1450	E	N	542885	6810759	1557	59	52.52	1.68	62		30
L1450	F	K	544070	6810774	1614	157	45.11	2.37	74		26
L1450	G	K	549454	6810841	1366	136	240.97	3.53	50		36
L1450	H	K	550487	6810847	1510	104	170.92	3.29	59		35
L1460	A	K	550433	6810654	1485	142	195.52	3.08	54		35
L1460	B	K	549347	6810635	1318	87	344.17	3.38	43		42
L1460	C	K	544142	6810581	1614	60	49.73	2.25	70		31

Line	Anom ID	Anom Type	X (m)	Y (m)	Z (m)	EMheight (m)	CondSFz (mS/m)	Tau_dB/dt (ms)	Estimated depth (m)	Cultural Affected	last Channel
L1460	D	N	542922	6810567	1572	40	59.98	1.56	62		34
L1460	E	K	542106	6810548	1447	73	129.75	2.67	52		37
L1460	F	N	541356	6810538	1217	101	16.66	1.10	84		30
L1460	G	K	540314	6810536	1257	189	0.28	0.14	100		13
L1460	H	N	538807	6810521	1395	55	7.67	0.50	70		25
L1460	I	N	536851	6810496	1267	60	2.26	0.17	58		23
L1460	J	N	533201	6810453	863	61	21.83	1.22	55		27
L1460	K	N	530912	6810429	1024	55	306.99	2.87	33		41
L1470	A	N	531016	6810230	1038	49	358.00	2.70	32		44
L1470	B	K	533338	6810251	967	142	20.93	1.01	54		26
L1470	C	N	536910	6810303	1312	67	2.44	0.49	56		20
L1470	D	N	538900	6810318	1365	58	8.78	0.60	69		29
L1470	E	K	540329	6810335	1237	98	1.41	0.21	95		25
L1470	F	K	542139	6810354	1475	81	134.80	2.67	49		36
L1470	G	N	543004	6810362	1571	39	62.40	1.48	54		35
L1470	H	K	544283	6810374	1682	46	49.47	2.07	60		30
L1470	I	K	549299	6810432	1359	103	443.15	3.22	37		41
L1470	J	K	550425	6810448	1466	160	284.50	2.65	46		36
L1480	A	K	550404	6810253	1323	53	388.87	2.60	42		45
L1480	B	N	549913	6810243	1285	44	213.78	3.16	53		40
L1480	C	K	549240	6810232	1333	48	578.60	3.04	31		45
L1480	D	K	544332	6810175	1670	52	50.89	2.17	55		31
L1480	E	N	543077	6810161	1542	47	53.69	1.60	50		34
L1480	F	K	542177	6810157	1434	51	143.35	2.82	48		38
L1480	G	N	539037	6810119	1371	85	5.77	0.65	68		24
L1480	H	N	533470	6810056	881	65	30.23	1.53	60		31
L1480	I	N	531118	6810028	1055	62	322.27	2.91	34		43
L1490	A	K	531233	6809826	1077	74	299.01	2.88	37		42
L1490	B	K	533399	6809851	988	167	27.77	1.60	54		25
L1490	C	N	539169	6809917	1401	84	4.75	0.75	68		19
L1490	D	K	542309	6809954	1402	92	149.39	2.99	46		36
L1490	E	N	543262	6809968	1523	91	53.48	1.91	51		31
L1490	F	K	544507	6809986	1680	49	59.50	1.79	52		33
L1490	G	K	549201	6810024	1373	53	617.77	3.02	31		46
L1500	A	N	551240	6809856	1349	49	155.77	2.74	46		36
L1500	B	K	550566	6809853	1308	51	178.08	3.09	46		37
L1500	C	K	549086	6809836	1417	49	547.09	3.10	30		44
L1500	D	K	544587	6809782	1682	45	65.37	1.69	53		35

Line	Anom ID	Anom Type	X (m)	Y (m)	Z (m)	EMheight (m)	CondSFz (mS/m)	Tau_dB/dt (ms)	Estimated depth (m)	Cultural Affected	last Channel
L1500	E	N	543304	6809762	1427	47	59.89	2.13	55		34
L1500	F	N	542441	6809759	1304	56	151.28	3.16	45		39
L1500	G	N	539296	6809726	1441	74	3.58	0.59	68		24
L1500	H	K	533447	6809648	896	89	29.15	1.65	61		28
L1500	I	K	531307	6809629	1076	70	306.88	3.02	36		43
L1510	A	K	531449	6809433	1064	66	409.89	2.78	34		44
L1510	B	N	533737	6809457	1011	156	26.14	1.69	67		25
L1510	C	N	539436	6809532	1465	57	4.57	0.47	65		27
L1510	D	N	542481	6809558	1346	70	147.40	2.95	46		37
L1510	E	N	543408	6809566	1496	64	92.21	2.19	55		32
L1510	F	K	544688	6809593	1675	55	64.01	1.75	61		34
L1510	G	K	549028	6809627	1479	52	648.27	3.28	30		46
L1510	H	N	551294	6809655	1334	49	139.03	2.69	44		36
L1520	A	N	551355	6809455	1321	45	149.39	2.44	43		37
L1520	B	K	549100	6809427	1525	46	598.62	3.21	30		46
L1520	C	K	544900	6809386	1614	103	57.96	1.78	71		34
L1520	D	N	543468	6809366	1528	54	87.27	1.79	53		38
L1520	E	N	542482	6809359	1371	45	147.32	2.77	42		39
L1520	F	N	539581	6809324	1468	40	3.64	0.34	53		28
L1520	G	N	534797	6809273	1092	56	7.78	1.08	52		22
L1520	H	N	533787	6809260	958	112	25.49	1.65	67		26
L1520	I	K	531511	6809242	1069	60	361.81	2.99	34		44
L1520	J	N	530730	6809223	1077	52	60.35	1.92	40		32
L1530	A	N	530819	6809032	1090	60	47.23	1.72	39		31
L1530	B	K	531677	6809034	1052	58	426.82	3.04	32		44
L1530	C	N	533947	6809063	954	85	17.08	1.21	67		25
L1530	D	N	534858	6809083	1105	55	7.66	1.07	50		23
L1530	E	N	539706	6809132	1464	50	1.85	0.22	58		25
L1530	F	N	542559	6809158	1492	84	97.44	3.50	49		33
L1530	G	N	543612	6809172	1597	61	93.41	2.32	56		35
L1530	H	K	545004	6809197	1642	165	48.59	1.84	69		30
L1530	I	K	548628	6809225	1539	87	245.68	2.81	44		35
L1530	J	K	549403	6809232	1564	70	425.74	3.32	36		44
L1530	K	N	550540	6809257	1376	59	278.00	3.28	47		43
L1530	L	N	551520	6809259	1346	58	149.84	2.21	52		38
L1540	A	N	551666	6809059	1377	68	133.64	2.37	53		37
L1540	B	K	550611	6809055	1417	66	277.09	3.43	48		42
L1540	C	K	549533	6809045	1561	60	413.64	3.31	40		45

Line	Anom ID	Anom Type	X (m)	Y (m)	Z (m)	EMheight (m)	CondSFz (mS/m)	Tau_dB/dt (ms)	Estimated depth (m)	Cultural Affected	last Channel
L1540	D	K	548613	6809022	1521	68	319.21	2.58	40		42
L1540	E	K	545142	6808982	1531	58	57.89	1.77	61		35
L1540	F	N	543683	6808973	1576	53	77.09	2.40	55		34
L1540	G	N	542626	6808957	1472	40	109.52	3.04	53		36
L1540	H	N	542075	6808955	1313	83	43.99	2.21	69		30
L1540	I	N	539867	6808926	1433	57	1.46	0.16	60		22
L1540	J	N	534982	6808872	1134	41	10.61	1.26	51		24
L1540	K	N	534018	6808862	962	88	16.19	1.49	65		24
L1540	L	K	531783	6808843	1043	66	503.52	3.15	34		45
L1540	M	N	530903	6808831	1066	40	67.52	1.67	41		35
L1550	A	N	531031	6808633	1057	51	58.25	1.62	42		34
L1550	B	K	531865	6808638	1015	88	519.14	3.34	37		44
L1550	C	N	539943	6808734	1399	48	1.33	0.12	58		19
L1550	D	N	542807	6808757	1439	52	105.53	3.24	53		35
L1550	E	N	543860	6808770	1511	43	81.63	2.26	55		35
L1550	F	K	545231	6808789	1603	160	41.81	1.66	57		29
L1550	G	K	548668	6808825	1655	191	273.61	3.06	45		36
L1550	H	K	549700	6808835	1601	80	375.86	3.37	42		43
L1550	I	K	550965	6808855	1485	86	260.46	3.17	45		41
L1561	A	N	531089	6808430	1042	68	48.13	1.56	41		33
L1561	B	K	531938	6808437	952	57	614.04	3.51	31		46
L1561	C	N	540068	6808531	1358	46	0.94	0.11	60		21
L1561	D	N	542429	6808543	1288	72	105.42	3.27	55		31
L1561	E	N	543004	6808555	1382	60	78.86	2.88	54		34
L1561	F	N	543994	6808574	1481	73	64.00	2.02	58		33
L1561	G	K	545339	6808601	1612	117	35.43	1.68	56		29
L1561	H	K	548830	6808628	1632	123	395.13	3.22	44		42
L1561	I	K	549799	6808627	1594	95	338.09	3.37	43		41
L1561	J	K	550953	6808650	1508	92	256.96	3.19	46		40
L1571	A	K	550914	6808455	1487	85	244.62	3.42	48		39
L1571	B	K	550093	6808436	1498	92	306.26	3.65	44		41
L1571	C	K	548923	6808428	1614	51	515.69	3.31	36		45
L1571	D	K	545456	6808388	1628	67	31.59	1.36	53		30
L1571	E	N	543654	6808366	1380	47	58.90	2.22	55		31
L1571	F	N	543168	6808367	1312	67	55.48	2.29	57		32
L1571	G	N	542441	6808366	1219	61	118.38	3.25	55		37
L1571	H	N	540131	6808336	1331	43	1.64	0.13	58		22
L1572	A	N	531171	6808226	1017	69	52.39	1.53	40		33

Line	Anom ID	Anom Type	X (m)	Y (m)	Z (m)	EMheight (m)	CondSFz (mS/m)	Tau_dB/dt (ms)	Estimated depth (m)	Cultural Affected	last Channel
L1572	B	K	532053	6808240	931	49	554.30	3.36	34		46
L1580	A	N	531230	6808034	1010	68	49.10	1.58	39		33
L1580	B	K	532081	6808035	951	48	420.41	3.51	36		44
L1580	C	N	540226	6808132	1297	54	5.81	0.90	68		23
L1580	D	N	542523	6808157	1225	84	101.15	3.25	58		30
L1580	E	N	543403	6808152	1316	95	37.25	2.06	58		29
L1580	F	N	543865	6808163	1370	83	37.25	2.06	60		29
L1580	G	K	545665	6808192	1681	55	23.86	1.14	50		29
L1580	H	K	548991	6808227	1588	47	588.38	3.28	31		46
L1580	I	N	549774	6808240	1479	48	243.78	2.96	48		41
L1580	J	K	550173	6808248	1447	52	373.56	3.61	43		44
L1580	K	K	550970	6808258	1479	80	233.50	3.40	49		40
L1590	A	K	551224	6808060	1518	100	215.47	3.13	49		40
L1590	B	K	550266	6808044	1476	37	436.00	3.69	39		46
L1590	C	N	549855	6808032	1488	73	237.66	3.43	53		40
L1590	D	K	549182	6808035	1549	86	537.15	3.31	34		44
L1590	E	K	545390	6807989	1591	40	39.56	1.88	58		29
L1590	F	N	543567	6807971	1268	65	36.42	2.29	61		26
L1590	G	N	542530	6807960	1239	60	105.92	2.98	60		35
L1590	H	N	540361	6807930	1275	71	9.92	1.54	64		24
L1590	I	K	532208	6807838	958	72	369.12	3.46	38		42
L1600	A	K	532277	6807639	972	66	361.94	3.36	38		43
L1600	B	N	540468	6807731	1232	75	11.32	1.01	72		27
L1600	C	N	542628	6807754	1312	68	98.91	3.18	62		31
L1600	D	N	543779	6807777	1327	83	32.19	1.81	61		31
L1600	E	N	545583	6807794	1537	53	29.71	1.18	52		31
L1600	F	K	549238	6807839	1507	85	526.61	3.37	36		46
L1600	G	K	550386	6807842	1550	49	418.66	3.37	36		43
L1600	H	K	551350	6807860	1528	108	202.97	3.21	52		40
L1610	A	K	551588	6807658	1553	109	184.83	3.21	54		40
L1610	B	K	550365	6807640	1622	48	345.34	3.49	41		40
L1610	C	K	549243	6807626	1603	138	486.60	3.25	34		40
L1610	D	N	545722	6807591	1462	45	47.28	2.08	49		33
L1610	E	N	544624	6807584	1333	49	37.93	1.70	60		32
L1610	F	N	543951	6807575	1356	46	29.74	2.28	65		25
L1610	G	N	542698	6807561	1329	44	113.25	2.71	60		39
L1610	H	N	540573	6807534	1297	159	8.46	0.97	69		19
L1610	I	K	532295	6807448	993	84	340.11	3.33	38		42

Line	Anom ID	Anom Type	X (m)	Y (m)	Z (m)	EMheight (m)	CondSFz (mS/m)	Tau_dB/dt (ms)	Estimated depth (m)	Cultural Affected	last Channel
L1620	A	K	532374	6807250	977	96	285.33	3.50	46		41
L1620	B	N	540711	6807337	1173	77	4.18	0.55	74		26
L1620	C	N	542846	6807362	1388	52	86.85	2.94	59		35
L1620	D	N	544134	6807373	1435	79	33.29	1.78	61		28
L1620	E	N	544743	6807381	1472	175	37.42	1.79	60		27
L1620	F	K	549290	6807435	1558	46	552.49	3.21	30		46
L1620	G	N	550270	6807445	1647	49	316.28	3.45	43		43
L1630	A	N	550370	6807234	1679	53	423.85	3.38	43		45
L1630	B	K	549268	6807234	1614	58	527.86	3.14	29		44
L1630	C	N	545960	6807194	1674	79	33.89	1.70	58		29
L1630	D	N	544263	6807180	1437	56	29.07	1.65	66		31
L1630	E	N	542983	6807159	1433	54	81.69	3.30	65		35
L1630	F	N	540756	6807143	1231	166	4.51	0.68	78		17
L1630	G	N	536324	6807088	1211	54	5.29	0.82	53		22
L1630	H	K	532425	6807054	980	137	234.99	3.51	52		39
L1640	A	K	532518	6806852	967	143	191.17	3.52	57		36
L1640	B	N	536530	6806886	1222	66	4.39	0.75	52		22
L1640	C	N	543229	6806963	1490	69	76.78	3.28	65		30
L1640	D	N	544471	6806978	1543	138	30.68	1.74	68		25
L1640	E	N	546080	6807022	1774	72	29.82	1.75	61		26
L1640	F	K	549333	6807033	1639	48	545.29	3.09	30		44
L1640	G	N	550467	6807048	1717	59	398.65	3.15	40		43
L1650	A	K	550578	6806870	1730	47	525.94	3.13	30		44
L1650	B	K	549426	6806836	1669	55	613.95	3.21	30		45
L1650	C	N	546189	6806802	1842	54	25.38	1.73	63		26
L1650	D	N	545165	6806791	1535	61	37.84	1.70	60		32
L1650	E	N	544536	6806778	1517	103	27.24	2.02	71		22
L1650	F	N	543376	6806773	1526	54	91.99	3.03	70		37
L1650	G	N	536699	6806693	1196	51	2.72	0.45	51		22
L1650	H	K	532499	6806645	988	155	178.84	3.28	54		35
L1660	A	K	532563	6806448	916	95	172.71	3.39	54		38
L1660	B	N	536879	6806498	1202	55	3.87	0.70	48		23
L1660	C	N	543591	6806571	1604	102	77.22	3.25	67		32
L1660	D	N	545314	6806587	1707	150	34.09	1.55	59		25
L1660	E	N	546347	6806592	1825	78	22.53	1.25	63		28
L1660	F	K	549435	6806634	1698	47	675.28	3.17	29		46
L1660	G	K	550626	6806644	1736	42	737.44	2.72	26		46
L1660	H	K	551538	6806658	1593	52	202.13	3.28	52		41

Line	Anom ID	Anom Type	X (m)	Y (m)	Z (m)	EMheight (m)	CondSFz (mS/m)	Tau_dB/dt (ms)	Estimated depth (m)	Cultural Affected	last Channel
L1670	A	K	550603	6806462	1804	82	472.23	2.97	33		42
L1670	B	K	549501	6806442	1729	55	626.46	3.02	33		46
L1670	C	K	546624	6806405	1768	55	24.79	1.53	62		28
L1670	D	N	545416	6806399	1647	58	28.62	1.62	57		29
L1670	E	N	543730	6806367	1588	60	88.08	2.97	70		36
L1670	F	N	536956	6806298	1200	57	2.54	0.42	47		25
L1670	G	K	532619	6806246	982	144	154.65	3.28	53		32
L1680	A	K	532636	6806041	941	115	151.19	3.05	52		35
L1680	B	N	537193	6806099	1258	70	4.32	0.44	47		25
L1680	C	N	543847	6806168	1646	76	58.79	3.38	66		29
L1680	D	N	545629	6806184	1646	50	42.32	1.69	54		31
L1680	E	K	546822	6806203	1749	46	24.44	1.33	57		29
L1680	F	K	549760	6806226	1766	35	496.62	3.32	31		44
L1680	G	K	550676	6806241	1827	87	326.12	3.16	40		40
L1690	A	K	550908	6806087	1804	70	238.52	3.55	44		40
L1690	B	K	549777	6806037	1737	49	472.98	3.51	33		44
L1690	C	K	546895	6806006	1725	62	24.29	1.29	57		28
L1690	D	N	545666	6806011	1603	73	40.75	1.73	56		31
L1690	E	N	544015	6805972	1690	41	80.02	2.87	67		34
L1690	F	N	537324	6805895	1271	44	7.37	0.93	47		26
L1690	G	K	532633	6805851	965	122	150.90	2.83	50		34
L1700	A	K	532721	6805642	886	54	149.88	3.02	47		36
L1700	B	N	537491	6805702	1297	44	7.43	0.76	50		26
L1700	C	N	544155	6805774	1690	39	79.57	3.17	66		33
L1700	D	N	545170	6805790	1550	65	41.68	1.27	62		33
L1700	E	K	546990	6805802	1665	45	24.84	1.36	54		28
L1700	F	K	549832	6805836	1769	147	454.62	3.48	37		39
L1700	G	K	551201	6805848	1807	101	235.72	3.00	51		41
L1710	A	K	551664	6805646	1807	87	207.94	3.48	57		41
L1710	B	K	549792	6805642	1629	97	466.02	3.70	37		46
L1710	C	N	545269	6805594	1527	64	43.27	1.88	55		31
L1710	D	N	544253	6805577	1663	66	78.36	2.86	60		34
L1710	E	N	537598	6805509	1309	61	8.74	0.93	51		25
L1710	F	K	532768	6805453	931	86	143.27	3.18	47		33
L1720	A	K	532839	6805247	890	52	134.30	3.31	44		34
L1720	B	N	537721	6805302	1349	85	6.80	0.87	51		23
L1720	C	N	544402	6805379	1592	57	69.40	2.84	61		33
L1720	D	N	545453	6805389	1497	92	40.28	1.82	58		29

Line	Anom ID	Anom Type	X (m)	Y (m)	Z (m)	EMheight (m)	CondSFz (mS/m)	Tau_dB/dt (ms)	Estimated depth (m)	Cultural Affected	last Channel
L1720	E	K	549617	6805435	1799	266	518.66	3.02	30		25
L1720	F	K	551685	6805468	1867	121	178.80	3.22	55		37
L1730	A	K	549625	6805240	1571	44	733.25	2.88	23		46
L1730	B	N	547133	6805208	1562	84	22.96	1.27	59		27
L1730	C	N	545535	6805199	1450	119	42.63	2.47	63		27
L1730	D	N	544498	6805181	1555	102	46.10	2.16	64		26
L1730	E	N	537874	6805107	1347	64	2.67	0.43	54		23
L1730	F	N	536627	6805092	1380	68	4.59	0.82	56		20
L1730	G	K	532934	6805054	883	48	127.37	3.39	44		32
L1740	A	K	549742	6805041	1587	43	662.85	2.60	23		46
L1740	B	K	547248	6805011	1492	78	26.74	1.52	56		26
L1740	C	N	545674	6805001	1380	112	55.31	3.37	63		31
L1740	D	N	544580	6804979	1418	69	56.36	2.95	68		27
L1740	E	N	536858	6804885	1396	79	6.63	1.01	56		20
L1740	F	K	533017	6804845	884	48	128.60	3.56	45		31
L1750	A	K	549423	6804828	1513	41	383.36	2.82	30		43
L1750	B	N	547360	6804809	1406	64	31.89	1.57	59		30
L1750	C	N	545849	6804791	1299	61	52.70	3.73	61		33
L1750	D	N	544789	6804776	1301	75	84.22	3.23	61		29
L1750	E	K	538038	6804713	1398	49	7.13	0.95	53		23
L1750	F	N	536964	6804692	1396	54	11.47	1.19	56		23
L1750	G	K	533112	6804654	882	42	141.69	3.64	46		32
L1760	A	K	533221	6804454	881	40	171.50	3.59	47		34
L1760	B	N	537129	6804496	1434	68	14.46	1.21	56		25
L1760	C	K	538226	6804512	1443	69	6.39	0.93	55		23
L1760	D	N	545098	6804587	1197	54	135.20	3.12	62		40
L1760	E	N	546070	6804599	1305	84	56.22	3.51	52		32
L1760	F	K	549401	6804638	1774	311	240.93	2.94	40		18
L1770	A	K	532169	6804235	942	64	140.44	1.97	37		38
L1770	B	K	533391	6804253	913	68	222.24	3.48	47		36
L1770	C	N	537216	6804292	1467	72	24.19	1.28	57		29
L1770	D	K	538416	6804310	1482	93	8.29	0.98	59		23
L1770	E	K	543069	6804360	1119	58	2.20	0.56	65		18
L1770	F	N	545408	6804381	1170	57	66.92	2.53	66		31
L1770	G	N	546252	6804395	1223	62	102.53	3.62	50		39
L1770	H	K	549315	6804426	1599	198	163.63	2.99	51		33
L1780	A	K	532271	6804037	886	47	163.12	2.09	35		39
L1780	B	K	533663	6804058	944	91	427.04	3.41	38	1	41

Line	Anom ID	Anom Type	X (m)	Y (m)	Z (m)	EMheight (m)	CondSFz (mS/m)	Tau_dB/dt (ms)	Estimated depth (m)	Cultural Affected	last Channel
L1780	C	N	537306	6804099	1463	62	33.14	1.38	54		31
L1780	D	K	538525	6804111	1505	89	13.05	1.13	61		24
L1780	E	K	543148	6804162	1126	52	2.28	0.57	64		18
L1780	F	K	545358	6804191	1152	46	17.02	1.33	68		22
L1780	G	N	546458	6804204	1189	64	170.41	3.29	48		40
L1780	H	N	547850	6804217	1321	97	1.99	0.16	65		21
L1780	I	K	549275	6804225	1560	199	132.12	3.02	56		28
L1790	A	K	549134	6804031	1338	49	105.98	2.96	58		33
L1790	B	N	547838	6804017	1238	54	2.77	0.60	63		26
L1790	C	N	546652	6804004	1160	51	171.98	3.59	46		41
L1790	D	K	543490	6803966	1163	57	2.77	0.64	64		20
L1790	E	N	538778	6803914	1486	47	21.84	1.44	59		28
L1790	F	N	537300	6803898	1429	60	41.82	1.61	53		29
L1790	G	K	533740	6803860	900	41	629.27	3.44	31		46
L1790	H	K	532327	6803841	930	80	144.62	2.34	40		37
L1800	A	K	532361	6803646	896	47	134.47	2.48	40		37
L1800	B	K	533429	6803654	889	45	482.18	3.27	42	1	45
L1800	C	K	533808	6803657	913	47	706.59	3.51	32	1	46
L1800	D	N	537419	6803702	1401	44	49.98	1.71	50		30
L1800	E	N	538915	6803718	1555	68	21.66	1.19	59		29
L1800	F	K	544176	6803772	1198	45	5.93	1.02	65		17
L1800	G	N	546907	6803805	1200	74	153.53	3.25	47		38
L1800	H	N	547873	6803819	1267	103	16.60	1.03	64		28
L1800	I	K	549150	6803835	1466	214	95.37	2.98	54		23
L1810	A	K	549270	6803641	1282	76	104.22	3.00	56		30
L1810	B	N	547878	6803625	1190	62	6.09	0.82	63		27
L1810	C	N	547096	6803613	1197	56	185.40	3.82	46		41
L1810	D	N	545773	6803600	1231	55	2.51	0.22	66		28
L1810	E	K	544400	6803583	1251	67	9.93	1.12	70		23
L1810	F	N	538955	6803517	1582	74	26.07	1.55	64		29
L1810	G	N	537484	6803497	1429	58	38.93	1.81	51		27
L1810	H	K	533854	6803455	916	56	633.02	3.61	35	1	46
L1810	I	K	533458	6803456	897	50	595.16	3.32	37	1	46
L1810	J	K	532369	6803442	936	81	119.84	2.69	41		34
L1820	A	K	532393	6803249	903	52	107.30	2.79	42		35
L1820	B	K	533634	6803256	915	55	750.96	3.30	33	1	46
L1820	C	N	537655	6803302	1464	50	29.88	1.49	53		29
L1820	D	N	539012	6803325	1605	76	22.86	1.15	62		29

Line	Anom ID	Anom Type	X (m)	Y (m)	Z (m)	EMheight (m)	CondSFz (mS/m)	Tau_dB/dt (ms)	Estimated depth (m)	Cultural Affected	last Channel
L1820	E	N	544171	6803375	1300	69	8.28	1.07	68		21
L1820	F	K	545980	6803392	1285	59	6.03	0.68	66		15
L1820	G	N	547356	6803404	1224	59	147.00	3.16	45		38
L1820	H	N	547910	6803417	1211	57	3.80	0.61	58		24
L1820	I	K	549343	6803425	1352	157	105.66	3.07	58		26
L1830	A	K	549388	6803237	1242	66	119.99	3.12	56		35
L1830	B	N	547454	6803208	1265	56	100.33	3.27	45		36
L1830	C	K	546309	6803202	1340	69	12.97	1.18	69		18
L1830	D	K	543955	6803171	1327	55	5.72	1.04	71		15
L1830	E	N	539017	6803111	1609	72	22.32	1.40	65		25
L1830	F	N	537795	6803103	1501	60	35.44	1.56	57		31
L1830	G	K	533722	6803059	931	49	645.36	3.43	34		46
L1830	H	K	532415	6803038	921	66	96.01	2.84	42		33
L1840	A	K	532413	6802850	899	49	90.40	2.80	43		33
L1840	B	K	533773	6802867	954	55	590.54	3.48	34		45
L1840	C	N	537865	6802897	1524	73	34.08	1.44	60		30
L1840	D	N	539055	6802921	1606	87	19.43	1.28	67		25
L1840	E	K	544750	6803023	1509	88	20.35	1.79	77		23
L1840	F	N	547571	6803015	1315	61	80.73	3.12	51		30
L1840	G	K	549410	6803028	1516	331	133.27	2.87	52		10
L1840	H	K	551783	6803054	1676	51	166.87	3.18	52		37
L1850	A	K	550881	6802856	1481	59	186.48	3.74	57		40
L1850	B	K	549513	6802838	1206	46	190.18	2.83	53		41
L1850	C	K	547721	6802814	1388	69	32.67	1.73	52		28
L1850	D	K	545194	6802776	1675	54	38.95	1.76	79		25
L1850	E	N	539054	6802720	1571	79	18.18	1.18	67		26
L1850	F	N	537844	6802702	1513	56	21.11	1.22	60		27
L1850	G	K	535407	6802678	1205	65	7.04	0.66	73		26
L1850	H	K	533809	6802660	954	51	565.30	3.44	33		46
L1850	I	K	532410	6802646	914	61	88.46	2.81	44		33
L1860	A	K	532330	6802436	930	83	93.98	2.64	46		34
L1860	B	K	533830	6802454	988	79	511.27	3.40	36		43
L1861	A	K	535577	6802484	1291	103	16.84	0.96	75		30
L1861	B	N	537913	6802503	1539	60	13.33	1.02	64		22
L1861	C	N	539071	6802511	1557	92	17.49	1.17	67		27
L1861	D	K	544618	6802575	1624	52	8.21	1.45	79		14
L1861	E	K	545343	6802591	1737	64	31.33	1.71	75		31
L1861	F	K	547782	6802612	1456	91	20.41	1.47	56		27

Line	Anom ID	Anom Type	X (m)	Y (m)	Z (m)	EMheight (m)	CondSFz (mS/m)	Tau_dB/dt (ms)	Estimated depth (m)	Cultural Affected	last Channel
L1861	G	K	549621	6802629	1386	222	164.24	3.13	60		28
L1861	H	K	551020	6802644	1501	94	205.51	3.46	52		40
L1870	A	K	550541	6802452	1417	127	197.59	3.74	57		40
L1870	B	K	549834	6802454	1295	128	194.53	3.50	58		38
L1870	C	K	547833	6802426	1506	116	18.58	1.37	60		26
L1870	D	N	545301	6802371	1719	71	28.66	1.09	70		32
L1870	E	N	539035	6802304	1564	104	14.83	1.16	70		24
L1870	F	K	535566	6802282	1296	110	15.50	0.88	81		26
L1870	G	K	533868	6802264	986	70	467.78	3.43	37		43
L1870	H	K	532141	6802261	963	104	121.10	2.52	51		36
L1880	A	K	549993	6802248	1275	104	289.39	3.20	53		43
L1880	B	K	547886	6802220	1556	127	17.03	1.43	63		24
L1880	C	N	545653	6802195	1756	68	22.25	1.45	67		27
L1880	D	N	539061	6802125	1570	116	14.24	1.13	70		25
L1880	E	K	535632	6802084	1304	111	17.90	0.97	79		26
L1880	F	K	533901	6802067	993	67	419.03	3.46	37		43
L1880	G	K	532016	6802045	997	138	150.70	2.72	52		36
L1890	A	K	531967	6801847	932	81	178.13	2.79	50		40
L1890	B	K	534044	6801865	1034	91	386.75	3.28	38		41
L1890	C	K	535729	6801886	1246	129	35.22	1.31	71	1	32
L1890	D	K	538186	6801879	1629	51	5.31	0.50	63		27
L1890	E	N	539169	6801888	1560	129	11.35	0.88	70		24
L1890	F	N	545756	6801991	1810	60	8.86	0.92	73		18
L1890	G	N	548006	6802012	1568	111	17.26	1.27	69		24
L1890	H	K	550032	6802031	1278	102	248.49	3.10	48		40
L1890	I	K	551443	6802036	1387	85	198.53	3.09	47		37
L1900	A	K	531915	6801640	959	105	174.45	2.90	50		38
L1900	B	K	534080	6801659	1033	94	360.49	3.30	40		41
L1900	C	K	535778	6801693	1274	122	32.62	1.20	68		30
L1900	D	K	538218	6801686	1633	69	4.56	0.50	62		24
L1900	E	N	539230	6801707	1526	115	11.71	0.93	70		24
L1900	F	K	546080	6801800	1883	73	10.02	0.84	95		25
L1900	G	N	548038	6801821	1575	66	17.14	1.31	71		23
L1900	H	K	550752	6801845	1272	82	267.07	3.21	50		42
L1910	A	K	550695	6801651	1294	88	287.93	3.14	48		42
L1910	B	N	548026	6801628	1626	105	14.40	1.22	75		24
L1910	C	K	546245	6801599	1871	93	12.38	1.02	102		27
L1910	D	N	545156	6801588	1753	82	23.11	1.56	75		25

Line	Anom ID	Anom Type	X (m)	Y (m)	Z (m)	EMheight (m)	CondSFz (mS/m)	Tau_dB/dt (ms)	Estimated depth (m)	Cultural Affected	last Channel
L1910	E	N	539256	6801522	1545	140	12.18	0.98	67		24
L1910	F	K	538208	6801517	1626	86	3.21	0.56	63		22
L1910	G	K	535957	6801484	1324	123	19.69	0.89	64		31
L1910	H	K	534074	6801465	1001	83	363.34	3.38	45		42
L1910	I	K	531810	6801453	1006	140	166.72	2.93	50		36
L1920	A	K	531770	6801233	948	95	168.64	2.96	47		39
L1920	B	K	534108	6801269	979	98	346.54	3.56	47		43
L1920	C	K	536093	6801278	1347	75	21.77	0.96	59		32
L1920	D	N	539358	6801319	1462	85	12.05	1.03	64		27
L1920	E	N	545339	6801399	1821	84	35.85	1.27	69		33
L1920	F	K	546626	6801395	1902	155	11.01	1.26	91		21
L1920	G	K	548123	6801410	1644	136	10.68	1.24	60		25
L1920	H	K	550700	6801452	1318	102	295.35	3.09	48		42
L1930	A	K	531755	6801039	957	98	153.00	3.00	49		38
L1930	B	K	534057	6801059	1002	122	317.30	3.66	51		39
L1930	C	K	536163	6801097	1407	106	13.44	0.77	59		27
L1930	D	N	539435	6801119	1436	77	14.72	1.19	64		27
L1930	E	K	545481	6801195	1811	84	31.99	1.45	67		29
L1930	F	K	546936	6801193	1963	80	10.13	1.15	79		21
L1930	G	K	548157	6801223	1714	143	9.50	1.15	66		23
L1930	H	K	550647	6801247	1352	82	313.25	2.97	50		43
L1940	A	K	550582	6801044	1439	132	217.75	3.23	53		37
L1940	B	K	548234	6801033	1740	73	8.01	0.89	67		24
L1940	C	N	546989	6801008	1936	55	9.46	1.09	73		27
L1940	D	K	545567	6800994	1780	122	27.23	1.59	68		26
L1940	E	K	539210	6800920	1496	141	16.25	1.34	68		23
L1940	F	K	536463	6800890	1447	81	3.91	0.65	68		26
L1940	G	K	534009	6800866	962	91	334.57	3.68	52		42
L1940	H	K	531709	6800840	1060	183	132.32	3.06	52		32
L1950	A	K	550491	6800848	1505	163	189.39	3.22	55		34
L1950	B	K	548242	6800825	1780	84	4.97	0.58	67		24
L1950	C	N	547221	6800811	1928	55	10.09	1.00	64		28
L1950	D	N	545725	6800795	1724	92	25.13	1.41	68		29
L1950	E	K	539303	6800715	1449	132	18.25	1.35	67		24
L1950	F	K	536688	6800690	1417	138	10.80	1.03	71		25
L1950	G	K	534020	6800670	949	78	334.83	3.79	52		44
L1950	H	K	531616	6800639	1047	160	120.46	3.13	52		32
L1950	I	N	529146	6800609	1359	93	2.34	0.13	68		21

Line	Anom ID	Anom Type	X (m)	Y (m)	Z (m)	EMheight (m)	CondSFz (mS/m)	Tau_dB/dt (ms)	Estimated depth (m)	Cultural Affected	last Channel
L1960	A	N	529358	6800399	1339	120	0.13	0.11	69		19
L1960	B	K	531617	6800434	954	71	119.02	3.11	50		36
L1960	C	K	534150	6800462	1018	141	273.83	3.80	53		36
L1960	D	K	536766	6800491	1352	118	13.10	0.95	67		26
L1960	E	K	539347	6800521	1386	96	21.68	1.25	66		26
L1960	F	N	545855	6800596	1723	75	14.72	1.14	69		25
L1960	G	K	547166	6800616	1936	70	8.17	1.16	69		19
L1960	H	K	548330	6800634	1749	138	6.30	0.62	70		25
L1960	I	K	550562	6800655	1440	78	195.77	3.07	50		40
L1970	A	K	550780	6800442	1534	135	158.79	3.14	52		34
L1970	B	K	548309	6800427	1827	254	5.78	0.49	70		23
L1970	C	N	546178	6800394	1701	81	9.28	0.92	69		26
L1970	D	K	539360	6800326	1395	128	20.03	1.31	66		24
L1970	E	K	536785	6800293	1322	113	9.25	0.96	66		24
L1970	F	K	534219	6800266	967	95	269.76	3.71	54		42
L1970	G	K	531625	6800235	1053	173	114.81	3.09	51		30
L1970	H	N	529514	6800207	1282	113	0.13	0.13	69		21
L1980	A	N	529669	6800008	1272	117	0.79	0.16	71		21
L1980	B	K	531642	6800036	949	74	114.30	3.07	50		36
L1980	C	K	534352	6800074	1061	177	213.31	3.69	57		33
L1980	D	K	536795	6800083	1300	132	4.89	0.64	67		20
L1980	E	K	539413	6800110	1365	140	16.42	1.24	64		24
L1980	F	N	546566	6800199	1776	134	7.77	0.76	77		22
L1980	G	K	548336	6800222	1773	152	6.05	0.47	71		27
L1980	H	K	550927	6800252	1520	86	170.34	3.13	49		37
L1990	A	K	550900	6800050	1597	114	180.45	3.02	47		37
L1990	B	K	548303	6800020	1855	133	5.89	0.50	73		24
L1990	C	N	546825	6800009	1734	87	7.84	1.13	80		26
L1990	D	K	539488	6799924	1344	95	14.52	1.01	63		26
L1990	E	K	534409	6799865	964	89	217.17	3.61	57		41
L1990	F	K	532642	6799845	972	101	154.11	2.89	43		36
L1990	G	K	531036	6799833	1135	201	98.24	2.95	51		29
L1990	H	N	529736	6799818	1308	107	2.67	0.12	72		20
L2000	A	K	530895	6799635	1069	115	92.20	2.68	54		34
L2000	B	K	532723	6799649	935	74	170.56	2.89	41		38
L2000	C	K	534510	6799674	1061	175	181.87	3.72	60		33
L2000	D	K	539556	6799724	1398	127	17.18	0.99	61		25
L2000	E	K	547038	6799815	1858	184	6.55	0.88	81		14

Line	Anom ID	Anom Type	X (m)	Y (m)	Z (m)	EMheight (m)	CondSFz (mS/m)	Tau_dB/dt (ms)	Estimated depth (m)	Cultural Affected	last Channel
L2000	F	K	548333	6799828	1908	114	6.49	0.56	76		22
L2000	G	K	551009	6799853	1585	64	173.83	2.90	42		40
L2010	A	K	551205	6799655	1587	61	145.98	2.59	44		38
L2010	B	K	548334	6799619	1919	150	5.66	0.55	78		22
L2010	C	N	547435	6799613	1875	104	6.30	0.87	82		22
L2010	D	K	544299	6799591	1620	88	1.14	0.12	60		19
L2010	E	K	539578	6799525	1357	65	19.81	1.03	62		29
L2010	F	N	535380	6799478	1083	105	8.69	0.86	63		26
L2010	G	K	534581	6799472	997	120	181.09	3.81	61		39
L2010	H	K	532947	6799450	942	70	188.87	2.90	40		38
L2010	I	K	530854	6799443	1195	226	94.62	2.70	53		29
L2020	A	K	530901	6799228	1058	107	109.83	2.78	50		35
L2020	B	K	533077	6799252	938	66	201.56	2.89	39		39
L2020	C	K	534638	6799271	1037	150	170.00	3.69	61		36
L2020	D	N	535486	6799278	1131	152	11.25	0.93	61		25
L2020	E	K	539627	6799323	1449	139	16.12	0.96	62		25
L2020	F	K	544409	6799371	1641	96	1.43	0.13	62		20
L2020	G	K	548456	6799432	1807	150	6.52	0.57	80		26
L2020	H	K	551244	6799463	1614	82	102.71	2.70	49		28
L2030	A	K	548452	6799219	1867	246	6.23	0.58	83		23
L2030	B	K	544510	6799182	1636	73	1.43	0.13	65		21
L2030	C	K	539633	6799119	1356	69	12.44	0.88	64		28
L2030	D	N	535564	6799076	1099	129	13.06	0.99	60		26
L2030	E	K	534686	6799076	985	104	162.47	3.70	61		39
L2030	F	K	533263	6799066	940	62	207.74	2.70	38		39
L2030	G	K	530918	6799031	1124	177	124.65	2.85	50		33
L2040	A	K	532337	6798846	934	57	222.04	2.75	38		40
L2040	B	K	533467	6798859	941	57	209.61	2.49	38		40
L2040	C	K	534797	6798869	1018	126	129.75	3.49	61		34
L2040	D	K	539584	6798917	1412	151	10.76	0.98	66		24
L2040	E	K	544655	6798978	1761	129	1.14	0.13	68		19
L2040	F	K	548468	6799015	1851	250	5.86	0.64	92		21
L2040	G	K	551603	6799047	1629	82	63.28	2.99	59		21
L2050	A	K	532438	6798644	942	52	253.65	2.74	34		41
L2050	B	K	536483	6798691	1297	117	12.56	0.95	67		26
L2050	C	K	539527	6798715	1427	142	9.09	0.95	66		21
L2050	D	K	544803	6798775	1790	61	1.13	0.12	70		18
L2050	E	K	548402	6798829	1899	287	5.52	0.67	97		18

Line	Anom ID	Anom Type	X (m)	Y (m)	Z (m)	EMheight (m)	CondSFz (mS/m)	Tau_dB/dt (ms)	Estimated depth (m)	Cultural Affected	last Channel
L2050	F	K	551494	6798851	1650	94	58.25	2.68	62		19
L2060	A	K	551428	6798669	1690	108	52.80	2.69	65		16
L2060	B	K	548438	6798625	1967	298	5.50	0.74	95		16
L2060	C	K	546132	6798605	1856	114	2.95	0.72	86		18
L2060	D	K	539771	6798531	1401	102	2.02	0.19	62		21
L2060	E	K	536488	6798493	1300	131	15.03	1.00	73		27
L2060	F	K	532554	6798447	960	68	265.35	2.70	33		41
L2060	G	K	530676	6798428	1131	151	143.32	2.59	49		35
L2070	A	K	548408	6798424	2025	267	5.69	0.76	89		16
L2070	B	K	546227	6798396	1872	143	2.29	0.49	91		18
L2070	C	N	539733	6798333	1413	91	6.61	0.78	64		22
L2070	D	K	536484	6798297	1306	158	15.09	1.02	76		26
L2070	E	K	532673	6798249	968	68	253.12	2.64	34		41
L2070	F	K	530584	6798226	1134	157	142.85	2.44	48		36
L2080	A	K	530569	6798020	1045	81	149.84	2.43	46		39
L2080	B	K	532814	6798044	976	70	242.13	2.44	37		41
L2080	C	K	536476	6798099	1336	201	14.13	0.98	74		24
L2080	D	N	539739	6798126	1461	108	5.58	0.61	66		23
L2080	E	K	546353	6798200	1927	187	2.35	0.56	88		17
L2080	F	K	548437	6798214	2058	216	6.09	0.87	76		19
L2090	A	K	548436	6798026	2089	127	6.28	0.86	65		21
L2090	B	K	546287	6798016	1815	143	2.39	0.49	87		19
L2090	C	N	539712	6797931	1503	119	5.47	0.64	65		22
L2090	D	K	536452	6797890	1275	170	14.00	1.17	75		25
L2090	E	K	534040	6797865	1080	88	68.19	3.10	51		31
L2090	F	K	532864	6797851	994	77	209.36	2.33	39		39
L2090	G	K	531903	6797834	1001	78	172.49	2.86	42		37
L2101	A	K	548468	6797814	2069	72	7.97	0.78	58		24
L2101	B	K	546178	6797804	1762	83	2.38	0.22	78		18
L2101	C	N	539724	6797731	1509	95	4.72	0.54	67		23
L2101	D	K	536478	6797688	1251	136	16.26	1.25	72		24
L2101	E	K	534230	6797675	1096	91	60.01	2.80	52		30
L2101	F	K	532919	6797658	1022	89	176.21	2.27	40		38
L2101	G	K	531750	6797635	988	74	181.37	2.79	41		38
L2110	A	K	548510	6797624	2071	120	9.53	0.86	74		25
L2110	B	K	546011	6797607	1694	87	2.41	0.44	71		21
L2110	C	N	539818	6797532	1537	88	4.65	0.52	66		24
L2110	D	K	536559	6797494	1210	87	17.49	1.19	71		26

Line	Anom ID	Anom Type	X (m)	Y (m)	Z (m)	EMheight (m)	CondSFz (mS/m)	Tau_dB/dt (ms)	Estimated depth (m)	Cultural Affected	last Channel
L2110	E	K	534412	6797465	1092	86	48.99	2.99	55		29
L2110	F	K	533014	6797450	1046	81	142.00	2.23	41		37
L2110	G	K	531649	6797440	979	69	193.60	2.73	39		39
L2120	A	K	531317	6797231	977	60	202.39	2.68	37		40
L2120	B	K	533111	6797250	1073	68	110.91	2.22	41		35
L2120	C	K	536621	6797295	1264	151	21.17	1.41	72		24
L2120	D	K	539793	6797335	1524	71	4.36	0.46	67		24
L2120	E	K	546090	6797400	1737	118	2.29	0.17	68		20
L2120	F	K	548426	6797424	2066	90	9.72	0.80	74		26
L2130	A	K	548349	6797234	2094	184	10.32	0.78	75		25
L2130	B	K	546192	6797206	1687	62	2.22	0.19	72		21
L2130	C	N	540075	6797129	1472	74	5.53	0.52	72		25
L2130	D	K	536700	6797093	1192	109	27.90	1.41	71		29
L2130	E	K	533239	6797062	1114	66	84.43	2.14	42		32
L2130	F	K	531198	6797033	977	67	205.03	2.52	36		41
L2140	A	K	530961	6796834	1001	79	216.60	2.47	42		40
L2140	B	N	533211	6796850	1155	75	61.94	2.38	48		29
L2140	C	K	536774	6796890	1194	95	32.38	1.48	65		29
L2140	D	N	540257	6796922	1550	94	5.60	0.57	77		24
L2140	E	K	546299	6796990	1769	108	1.78	0.19	77		19
L2140	F	K	548233	6797022	2036	124	13.30	1.03	78		26
L2150	A	K	548305	6796822	1982	178	12.58	1.03	92		20
L2150	B	K	546408	6796804	1821	100	1.65	0.18	97		17
L2150	C	N	540302	6796731	1562	84	4.80	0.56	77		24
L2150	D	K	536821	6796701	1107	93	32.94	1.74	61		31
L2150	E	N	533217	6796653	1181	79	51.92	2.03	50		26
L2150	F	K	530855	6796626	1005	79	221.59	2.20	43		41
L2160	A	K	530826	6796431	1011	74	195.06	2.12	44		40
L2160	B	K	532148	6796446	1084	74	81.58	2.26	45		33
L2160	C	K	533056	6796451	1190	83	53.99	2.02	47		26
L2160	D	K	536898	6796504	1215	148	28.95	1.51	63		25
L2160	E	K	540128	6796529	1597	88	5.72	0.60	71		22
L2160	F	K	546504	6796596	1809	94	1.91	0.15	100		18
L2160	G	K	548521	6796620	1917	185	8.08	0.79	105		17
L2170	A	K	546600	6796401	1769	111	1.89	0.15	96		17
L2170	B	K	540198	6796333	1563	81	6.41	0.60	72		24
L2170	C	K	537039	6796299	1205	107	22.23	1.44	68		26
L2170	D	K	532989	6796251	1210	96	48.97	1.98	50		25

Line	Anom ID	Anom Type	X (m)	Y (m)	Z (m)	EMheight (m)	CondSFz (mS/m)	Tau_dB/dt (ms)	Estimated depth (m)	Cultural Affected	last Channel
L2170	E	K	530697	6796231	1007	81	131.16	2.07	46		37
L2180	A	K	530570	6796024	995	65	89.10	2.03	51		34
L2180	B	K	533025	6796055	1197	68	44.89	1.90	49		26
L2180	C	K	537218	6796088	1275	150	18.21	1.24	73		23
L2180	D	K	540212	6796118	1527	120	6.90	0.65	72		24
L2180	E	K	546749	6796207	1782	165	1.90	0.13	91		17
L2190	A	K	546793	6796008	1698	101	2.31	0.13	87		18
L2190	B	K	540220	6795936	1486	80	6.75	0.64	70		25
L2190	C	K	537260	6795901	1193	73	21.27	1.45	72		28
L2190	D	K	533203	6795853	1257	78	35.51	1.89	49		25
L2190	E	K	530517	6795823	1012	77	72.50	1.96	51		33
L2200	A	K	530535	6795631	1029	82	64.00	1.81	52		32
L2200	B	K	533364	6795659	1301	91	28.70	1.62	53		25
L2200	C	K	537459	6795706	1248	120	20.08	1.47	70		25
L2200	D	N	540194	6795733	1500	75	10.39	0.84	69		26
L2200	E	K	546846	6795806	1716	129	1.97	0.13	86		17
L2210	A	K	546790	6795604	1646	96	2.42	0.12	88		17
L2210	B	N	540308	6795530	1551	79	10.29	0.88	73		25
L2210	C	K	537543	6795502	1186	101	26.67	1.64	75		27
L2210	D	K	533511	6795461	1332	86	25.66	1.50	55		26
L2210	E	K	530548	6795420	1024	71	52.67	1.92	53		30
L2220	A	K	530714	6795222	1128	138	47.43	1.68	55		27
L2220	B	K	533675	6795257	1374	86	20.82	1.49	56		25
L2220	C	K	537488	6795305	1193	147	23.19	1.52	76		25
L2220	D	N	540418	6795327	1596	95	8.08	0.71	75		25
L2230	A	N	540517	6795142	1611	100	9.85	0.95	83		24
L2230	B	K	537469	6795104	1129	142	19.45	1.44	79		25
L2230	C	K	533740	6795069	1416	107	19.56	1.52	57		24
L2230	D	N	531293	6795027	1216	92	40.18	1.76	56		26
L2240	A	N	531530	6794834	1245	74	36.71	1.86	58		24
L2240	B	K	533952	6794864	1422	73	16.01	1.30	55		24
L2240	C	K	537612	6794904	1192	206	16.69	1.19	77		23
L2240	D	N	540729	6794932	1586	105	5.43	0.61	80		25
L2250	A	K	540982	6794740	1587	190	5.41	0.69	86		21
L2250	B	K	537690	6794706	1124	132	17.66	1.14	76		27
L2250	C	N	534138	6794673	1462	85	11.76	1.09	55		25
L2250	D	N	531617	6794632	1263	99	33.58	1.66	56		24
L2260	A	N	531826	6794441	1265	78	27.48	1.73	56		25

Line	Anom ID	Anom Type	X (m)	Y (m)	Z (m)	EMheight (m)	CondSFz (mS/m)	Tau_dB/dt (ms)	Estimated depth (m)	Cultural Affected	last Channel
L2260	B	N	534372	6794464	1469	79	11.04	0.95	56		25
L2260	C	K	537812	6794503	1169	170	17.78	1.11	71		27
L2260	D	N	541018	6794533	1577	183	9.65	1.02	98		21
L2271	A	K	541070	6794344	1594	183	9.68	1.43	97		19
L2271	B	K	537873	6794307	1118	123	15.63	1.03	70		27
L2271	C	N	534536	6794284	1483	72	12.55	1.21	56		25
L2271	D	N	531917	6794249	1278	66	25.34	1.47	59		25
L2280	A	N	532014	6794041	1302	92	23.44	1.47	62		23
L2280	B	N	534742	6794070	1476	74	11.47	1.07	60		25
L2280	C	K	535524	6794075	1300	100	9.68	0.91	68		25
L2280	D	K	537930	6794099	1124	139	14.56	0.98	70		24
L2280	E	K	541215	6794142	1591	184	17.20	1.56	98		20
L2280	F	K	545556	6794186	1553	120	2.40	0.61	98		7
L2290	A	K	548212	6794008	1335	113	3.55	0.80	88		15
L2290	B	K	545517	6793991	1436	124	3.36	0.65	95		17
L2290	C	K	541266	6793944	1517	147	24.01	1.82	98		21
L2290	D	K	537931	6793914	1083	123	16.13	1.12	70		25
L2290	E	K	535628	6793876	1320	120	9.56	0.85	66		26
L2300	A	K	530574	6793620	1267	129	14.68	1.39	67		21
L2300	B	K	535773	6793672	1290	105	9.34	0.94	67		26
L2300	C	K	537953	6793702	1083	138	17.35	1.11	66		25
L2300	D	K	541326	6793742	1460	113	22.90	1.63	95		20
L2300	E	K	545568	6793791	1347	108	2.74	0.60	86		21
L2300	F	K	548208	6793826	1266	84	3.49	0.83	80		18
L2310	A	K	548165	6793614	1267	108	3.55	0.74	80		18
L2310	B	K	545542	6793581	1274	92	2.60	0.65	82		19
L2310	C	K	541420	6793542	1410	145	15.06	1.24	85		18
L2310	D	K	537997	6793511	1052	124	17.35	1.01	61		29
L2310	E	K	535371	6793477	1396	126	11.70	1.04	63		24
L2310	F	K	530570	6793429	1250	89	13.54	1.23	65		21
L2320	A	K	530590	6793225	1255	66	12.78	1.31	63		21
L2320	B	K	535397	6793280	1330	76	11.83	1.02	60		26
L2320	C	K	538067	6793306	1028	69	16.82	0.98	58		30
L2320	D	N	541748	6793340	1303	107	5.66	0.62	86		23
L2320	E	K	545614	6793385	1228	76	2.10	0.57	78		19
L2330	A	K	545620	6793195	1217	79	1.64	0.14	75		17
L2330	B	N	541766	6793152	1273	128	6.75	0.89	77		19
L2330	C	K	538004	6793116	1068	107	14.88	0.90	57		26

Line	Anom ID	Anom Type	X (m)	Y (m)	Z (m)	EMheight (m)	CondSFz (mS/m)	Tau_dB/dt (ms)	Estimated depth (m)	Cultural Affected	last Channel
L2330	D	K	535410	6793073	1332	83	11.97	1.02	58		24
L2330	E	K	530642	6793023	1285	76	11.02	1.38	65		19
L2340	A	K	530674	6792823	1289	72	10.33	1.34	65		19
L2340	B	K	535518	6792886	1315	88	12.15	1.07	55		25
L2340	C	K	538007	6792905	1053	112	13.22	0.94	59		26
L2340	D	N	541894	6792953	1165	100	5.14	0.78	73		22
L2340	E	K	545686	6792993	1204	72	1.46	0.11	75		17
L2350	A	K	541856	6792748	1127	79	4.38	0.52	71		25
L2350	B	N	539096	6792732	1082	76	3.85	0.54	68		22
L2350	C	K	537954	6792693	1069	141	11.46	1.05	62		22
L2350	D	K	535639	6792680	1273	76	12.14	1.07	55		25
L2350	E	K	530738	6792630	1278	74	9.78	1.11	68		19
L2360	A	K	530804	6792438	1306	102	9.47	1.10	72		18
L2360	B	K	535761	6792478	1240	107	12.17	1.03	58		26
L2360	C	N	539135	6792520	1095	70	4.21	0.61	70		22
L2360	D	K	541949	6792541	1188	92	2.91	0.39	69		22
L2370	A	K	541972	6792361	1188	80	3.10	0.52	72		20
L2370	B	N	539153	6792324	1112	86	5.13	0.60	72		21
L2370	C	K	535781	6792284	1240	98	14.18	1.13	60		25
L2370	D	K	534177	6792253	1524	100	9.70	1.15	74		21
L2380	A	K	534269	6792066	1495	99	9.58	1.10	72		22
L2380	B	K	535840	6792085	1255	125	13.86	1.19	65		24
L2380	C	K	538902	6792124	1074	115	5.12	0.62	71		22
L2380	D	N	542414	6792151	1220	74	0.37	0.09	71		19
L2390	A	N	542567	6791961	1220	72	1.01	0.11	73		19
L2390	B	K	538705	6791917	1093	114	5.63	0.64	66		24
L2390	C	K	536028	6791886	1251	131	12.86	1.23	72		24
L2390	D	K	534482	6791864	1506	114	9.90	1.09	63		21
L2400	A	N	534297	6791671	1565	107	9.62	1.07	70		23
L2400	B	K	536167	6791684	1311	164	13.11	1.22	70		22
L2400	C	K	538703	6791713	1126	136	5.29	0.64	66		22
L2400	D	N	542761	6791757	1264	90	0.85	0.10	77		18
L2410	A	N	542969	6791563	1293	98	0.99	0.10	86		18
L2410	B	K	537675	6791502	1318	64	6.80	0.88	59		23
L2410	C	K	536309	6791498	1246	103	13.77	1.36	69		26
L2410	D	N	534528	6791469	1552	111	8.29	1.08	68		21
L2420	A	N	534686	6791271	1511	111	14.87	1.43	67		21
L2420	B	K	536442	6791294	1298	129	13.18	1.22	73		24

Line	Anom ID	Anom Type	X (m)	Y (m)	Z (m)	EMheight (m)	CondSFz (mS/m)	Tau_dB/dt (ms)	Estimated depth (m)	Cultural Affected	last Channel
L2420	C	K	537758	6791306	1346	87	7.97	0.82	58		22
L2420	D	N	543195	6791367	1432	166	1.48	0.05	90		15
L2430	A	N	543365	6791166	1474	97	2.24	0.59	92		18
L2430	B	K	537874	6791107	1334	77	8.38	0.89	55		24
L2430	C	K	536735	6791088	1291	87	13.13	1.21	71		24
L2430	D	N	534729	6791075	1491	108	14.41	1.39	67		23
L2440	A	N	534867	6790877	1448	147	14.11	1.37	64		26
L2440	B	K	536835	6790904	1300	126	13.60	1.39	69		23
L2440	C	K	538002	6790906	1321	65	7.49	0.71	48		25
L2440	D	N	543505	6790965	1585	84	1.97	0.56	90		16
L2450	A	N	543519	6790770	1640	90	2.26	0.64	91		13
L2450	B	N	538182	6790705	1329	73	9.44	0.79	49		25
L2450	C	K	537009	6790702	1268	102	13.82	1.34	69		24
L2450	D	N	535028	6790673	1404	98	18.43	1.20	64		28
L2460	A	N	543627	6790559	1673	99	2.68	0.76	95		14
L2460	B	N	538179	6790511	1318	57	10.49	0.95	48		26
L2460	C	N	535233	6790486	1475	144	14.70	1.40	66		22
L2470	A	N	535333	6790278	1498	145	12.74	1.29	64		21
L2470	B	N	538250	6790307	1307	53	10.60	0.79	47		27
L2470	C	N	543758	6790376	1731	146	2.75	0.88	96		12
L2480	A	N	543862	6790173	1726	133	4.75	0.91	97		15
L2480	B	N	538292	6790109	1332	69	10.96	0.76	46		27
L2480	C	N	535442	6790084	1518	127	10.14	1.24	64		20
L2490	A	N	544052	6789981	1774	157	4.59	1.17	99		16
L2491	A	N	535590	6789879	1495	67	11.37	1.29	57		22
L2491	B	N	538432	6789907	1301	44	10.14	0.56	44		28
T3001	A	K	551838	6799799	1572	91	142.74	3.63	53		35
T3001	B	K	551813	6802763	1770	234	69.39	3.25	106		26
T3002	A	K	551750	6807536	1602	155	149.29	3.52	77		35
T3002	B	K	551754	6808445	1549	133	82.74	2.67	73		32
T3010	A	K	550453	6816325	1550	139	11.13	0.79	95		25
T3010	B	K	550472	6814278	1608	229	22.41	1.81	92		23
T3010	C	K	550506	6811165	1552	113	247.01	3.79	60		39
T3010	D	K	550575	6806614	1736	62	738.84	2.91	31		45
T3010	E	K	550614	6802633	1589	250	53.46	3.96	109		18
T3010	F	K	550627	6799896	1836	338	27.87	2.20	109		15
T3020	A	K	549428	6800746	1505	86	99.07	2.58	55		34
T3020	B	K	549408	6802062	1341	122	139.82	2.48	60		36

Line	Anom ID	Anom Type	X (m)	Y (m)	Z (m)	EMheight (m)	CondSFz (mS/m)	Tau_dB/dt (ms)	Estimated depth (m)	Cultural Affected	last Channel
T3020	C	K	549374	6805416	1553	93	504.72	3.54	43		44
T3020	D	K	549364	6806547	1686	52	652.23	3.59	31		45
T3020	E	K	549333	6809395	1559	111	283.07	3.53	55		40
T3020	F	K	549292	6812898	1596	64	148.11	3.25	58		36
T3020	G	K	549287	6813893	1552	97	95.98	3.49	86		30
T3020	H	K	549238	6817959	1212	114	91.42	1.86	68		34
T3030	A	K	548038	6816779	1555	80	77.45	1.96	74		31
T3030	B	K	548068	6815491	1580	76	79.21	2.46	48		32
T3030	C	K	548134	6809520	1609	209	20.42	1.13	79		27
T3030	D	K	548224	6800426	1814	198	3.82	0.35	77		24
T3030	E	K	548276	6797172	2054	133	11.61	0.54	65		28
T3040	A	N	547037	6800964	1909	56	1.98	0.21	86		24
T3040	B	K	546972	6806028	1752	117	23.80	1.30	75		25
T3040	C	K	546864	6814624	1791	120	6.35	1.06	92		16
T3050	A	K	545629	6818362	1803	103	22.13	1.95	81		22
T3050	B	N	545636	6817119	1724	226	34.34	1.91	85		25
T3050	C	K	545748	6808125	1705	108	14.36	0.96	71		25
T3050	D	K	545754	6806925	1743	146	21.80	1.92	87		22
T3050	E	K	545764	6806172	1675	116	22.32	1.33	82		26
T3050	F	K	545771	6805467	1542	205	28.77	1.91	103		23
T3050	G	K	545797	6802344	1747	145	3.73	0.39	76		25
T3050	H	N	545823	6801572	1841	71	17.55	1.44	76		24
T3050	I	N	545837	6800573	1722	111	6.97	0.98	82		21
T3060	A	K	544581	6805605	1582	106	86.83	3.08	69		32
T3060	B	K	544547	6807206	1525	215	19.12	1.62	90		23
T3060	C	K	544545	6807974	1488	161	14.86	1.50	91		21
T3060	D	N	544546	6809603	1652	51	75.69	1.57	50		34
T3060	E	K	544466	6815867	1587	146	1.42	0.00	124		13
T3070	A	K	543292	6813453	1379	157	34.57	1.95	99		25
T3070	B	K	543317	6810266	1560	63	80.00	2.16	56		32
T3070	C	N	543329	6808811	1567	104	51.67	2.54	80		29
T3070	D	N	543373	6806743	1589	145	36.96	2.12	96		23
T3070	E	N	543540	6790757	1614	97	1.26	0.03	89		13
T3080	A	K	542133	6808725	1328	148	30.21	2.73	91		22
T3080	B	K	542143	6810261	1442	74	153.01	2.65	52		37
T3080	C	K	542090	6814017	1486	120	8.21	0.93	62		24
T3090	A	K	540824	6818516	1385	135	0.56	0.13	79		19
T3090	B	N	540885	6814029	1448	105	14.84	1.11	75		26

Line	Anom ID	Anom Type	X (m)	Y (m)	Z (m)	EMheight (m)	CondSFz (mS/m)	Tau_dB/dt (ms)	Estimated depth (m)	Cultural Affected	last Channel
T3090	C	N	540906	6811377	1232	101	16.58	1.34	102		20
T3090	D	K	540958	6807297	1167	119	6.40	0.86	114		17
T3090	E	N	541094	6794421	1493	110	30.12	2.01	85		25
T3100	A	K	539647	6816491	1264	101	6.78	0.67	70		23
T3100	B	N	539630	6815351	1452	54	0.63	0.15	55		27
T3100	C	K	539700	6812207	1181	200	0.41	0.04	97		13
T3100	D	N	539731	6809089	1482	73	4.72	0.49	67		25
T3100	E	K	539801	6802636	1565	80	1.03	0.16	63		22
T3100	F	K	539838	6799295	1418	76	2.92	0.37	48		25
T3100	G	N	539868	6797559	1525	85	3.37	0.40	67		24
T3100	H	K	539883	6795640	1491	125	11.09	1.01	77		23
T3110	A	K	538725	6791882	1072	98	5.97	0.57	61		25
T3110	B	K	538636	6801050	1580	79	4.86	0.95	70		19
T3110	C	K	538595	6803737	1523	62	32.27	1.51	64		29
T3110	D	K	538524	6810818	1392	119	5.36	0.58	90		23
T3110	E	K	538514	6812146	1087	116	5.31	0.79	98		14
T3110	F	K	538448	6817791	1046	73	0.18	0.13	43		23
T3120	A	N	537261	6816247	1150	78	8.53	0.54	58		27
T3120	B	N	537274	6814564	1174	71	7.52	0.69	66		23
T3120	C	N	537377	6805818	1342	106	2.11	0.35	67		23
T3120	D	N	537396	6803657	1432	83	40.81	1.82	58		27
T3120	E	N	537485	6795950	1215	102	41.21	1.95	64		28
T3120	F	N	537485	6794617	1035	100	19.46	0.99	64		28
T3130	A	K	536334	6791556	1294	158	10.40	1.01	75		23
T3130	B	K	536256	6798681	1202	105	17.48	1.08	61		27
T3130	C	N	536230	6801389	1390	78	28.02	0.86	60		31
T3130	D	K	536200	6805162	1454	88	1.83	0.59	86		16
T3130	E	K	536169	6806883	1245	142	2.40	0.45	73		20
T3130	F	K	536056	6816824	1331	72	17.06	0.97	77		27
T3130	G	K	536050	6817938	1357	112	0.28	0.12	70		18
T3140	A	N	534851	6817242	1364	75	7.77	0.51	61		25
T3140	B	K	534942	6809085	1164	107	3.96	0.69	56		21
T3140	C	K	535024	6800873	1037	119	36.74	1.85	52		29
T3140	D	N	535042	6799069	1032	66	115.44	3.21	43		34
T3140	E	K	535101	6793492	1399	81	8.97	0.77	51		25
T3140	F	N	535149	6790464	1397	79	35.37	1.91	57		28
T3150	A	N	533927	6792033	1613	109	2.48	0.55	78		19
T3150	B	K	533845	6799048	950	76	206.78	2.16	39		39

Line	Anom ID	Anom Type	X (m)	Y (m)	Z (m)	EMheight (m)	CondSFz (mS/m)	Tau_dB/dt (ms)	Estimated depth (m)	Cultural Affected	last Channel
T3150	C	K	533824	6800747	924	53	495.62	3.21	41		44
T3150	D	K	533795	6803730	925	59	626.93	3.63	36	1	45
T3150	E	N	533731	6809444	973	125	20.82	1.50	60		25
T3150	F	K	533676	6816011	1243	67	2.22	0.15	50		20
T3150	G	K	533610	6818678	1254	94	5.73	0.81	57		23
T3160	A	K	532647	6798328	964	65	323.95	2.66	31		41
T3160	B	K	532596	6803304	918	66	99.63	3.21	45		32
T3160	C	K	532555	6807002	877	67	442.84	3.63	43		43
T3170	A	N	531491	6794897	1243	79	5.20	0.58	64		24
T3170	B	K	531468	6797289	999	75	221.36	2.81	39		39
T3170	C	K	531421	6800752	965	78	203.84	3.06	39		38
T3170	D	K	531384	6804617	1047	70	26.77	1.10	45		29
T3172	A	K	531327	6809593	1073	67	463.49	2.93	32		43
T3180	A	N	530113	6811487	1062	87	127.32	3.24	54		34
T3180	B	K	530263	6797911	1086	74	132.72	1.93	37		37
T3180	C	K	530280	6795867	1019	79	39.93	1.39	49		31
T3190	A	N	529021	6800795	1486	177	1.35	0.08	97		16
T3190	B	K	528952	6806707	1258	113	5.96	0.64	66		24
T3190	C	K	528945	6808259	1239	102	6.67	0.68	58		24
T3190	D	K	528853	6817409	838	74	36.45	1.15	43		31
T3210	A	K	526517	6810799	1388	88	7.33	0.63	55		25
T3210	B	K	526492	6812490	1264	84	9.54	0.88	53		25
T3210	C	K	526458	6815625	1033	79	10.11	0.84	49		26
T3220	A	N	525243	6818204	1132	89	76.02	1.93	49		33